

Universitat de Lleida

Predicción de propiedades mecánicas en flexión de madera aserrada de *Pinus sylvestris L.* Mediante análisis multivariable basado en ensayos de vibración

Álvaro Fernández Serrano

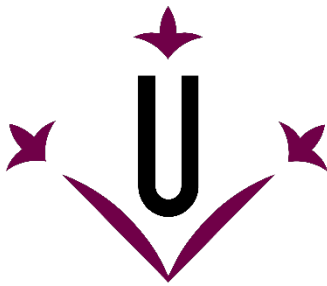
<http://hdl.handle.net/10803/675025>



*Predicción de propiedades mecánicas en flexión de madera aserrada de *Pinus sylvestris L.* mediante análisis multivariable basado en ensayos de vibración* i està subjecte a una llicència de [Reconeixement-NoComercial-SenseObraDerivada 4.0 No adaptada de Creative Commons](#)

Les publicacions incloses en la tesi no estan subjectes a aquesta llicència i es mantenen sota les condicions originals.

(c) 2022, Álvaro Fernández Serrano



Universitat de Lleida

TESIS DOCTORAL

Predicción de propiedades mecánicas en flexión de
madera aserrada de *Pinus sylvestris* L. mediante análisis
multivariable basado en ensayos de vibración

Álvaro Fernández Serrano

Memoria presentada para optar al grado de Doctor por la Universitat de Lleida

Programa de Doctorado en Gestión Forestal y Medio Natural

Director y Tutor

Antonio Villasante Plágaro

2022

Y el Cantábrico... siempre

AGRADECIMIENTOS

Acabado el trabajo, es momento de saldar las deudas de gratitud que uno ha contraído en su realización. Intentando hacer balance del proceso que concluye con la redacción de este documento, viene a mi mente el concepto de *energía de activación*, la energía que es necesario aportar a un sistema para que se produzca una reacción química. Muchas veces no es suficiente con disponer de los reactivos adecuados y mezclarlos en las proporciones requeridas. Sin esa energía de activación sencillamente no ocurrirá nada. Del mismo modo, yo no habría empezado nunca esta tesis sin la colaboración de mis compañeros en el departamento de Ingeniería Agroforestal, los doctores Antonio Villasante y Lluís Puigdomènec. A su amistad, con la que me honran, han sumado una colaboración profesional que ha sido condición *sine qua non* para que abandonara mis cavilaciones y comenzara este trabajo. Ellos me dieron el empujón que necesitaba.

Lluís estuvo en la fase inicial, su aportación fue clave para definir el diseño de los ensayos de resonancia. No obstante, siendo una mente inquieta, decidió después que su camino iría por otros derroteros.

Antonio, como director de tesis, ha puesto sobre la mesa su gran conocimiento sobre la madera, su tesón y ese punto de desconfianza tan necesario para acercarse a los resultados aparentemente prometedores que se van obteniendo. Su grado de implicación ha ido, objetivamente, más allá de lo que puede exigírsele a un director de tesis. Desde luego, sin su ayuda todo esto no habría llegado a buen puerto.

Siguiendo el paralelismo con la Química, también es necesario mencionar a los catalizadores. El doctor Jorge Lampurlánés, compañero de departamento, se ha ofrecido generosamente a impartir más docencia de la que le correspondía para liberarme de algunos créditos y hacerme así un poco más fácil el trabajo. La doctora Cristina Vega, directora del departamento, ha actuado como un paraguas eficaz en sus gestiones ante el rectorado para que, en estos momentos de crisis y ajustes, no me cayera encima demasiada carga docente.

RESUMEN	1
RESUM	3
ABSTRACT	5
CAPÍTULO 1	7
1. Introducción	9
1.1. Los ensayos no destructivos en madera	9
1.1.1. Una breve reflexión histórica	9
1.1.2. El estudio de la vibración de una barra	10
1.1.3. El estudio de la madera con técnicas de vibración	12
1.1.4. Equipos de ensayo disponibles en el mercado	13
1.2. Estado de la cuestión	15
1.2.1. Estudios previos	15
1.2.2. Análisis estadístico en los estudios previos	16
1.3. Objetivos	18
1.3.1. Predicción del MOE y del MOR	18
1.3.2. Predicción del MOE a partir de los armónicos	18
1.3.3. Influencia de la posición de los nudos y la dirección del ensayo de flexión en las propiedades mecánicas	18
1.4. Materiales y métodos	19
1.4.1. Muestras	19
1.4.2. Ensayos y singularidades de la madera	19
1.4.3. Equipamiento	19
1.4.4. Análisis estadístico	20
1.5. Resultados	21
1.5.1. Artículo 1	21
1.5.2. Artículo 2	21
1.5.3. Artículo 3	21
1.5.4. Artículo 4	22
1.5.5. Presentación de los artículos	22
1.6. Referencias	23
CAPÍTULO 2	31
2. Longitudinal, transverse and ultrasound vibration for the prediction of stiffness using models incorporating features in <i>Pinus sylvestris</i> timber	35
2.1. Abstract	35
2.2. Introduction	35
2.3. Materials and methods	38
2.3.1. Samples	38
2.3.2. Features and biological degradations	38
2.3.3. Ultrasounds	39
2.3.4. Vibration tests	39
2.3.5. Static bending test	40
2.3.6. Statistical analyses	41
2.4. Results and discussion	44
2.5. Conclusion	52
2.6. References	52

CAPÍTULO 3 **59**

3. Modulus of rupture prediction in <i>Pinus sylvestris</i> with multivariate models constructed with resonance, ultrasound, and wood heterogeneity variables	63
3.1. Abstract	63
3.2. Introduction	63
3.3. Experimental	64
3.3.1. Materials	64
3.3.2. Methods	65
3.4. Results and discussion	70
3.4.1. Simple linear regression	70
3.4.2. Multiple linear regression	73
3.4.3. Nonlinear multivariate models	75
3.5. Conclusions	76
3.6. References	76

CAPÍTULO 4 **83**

4. Dynamic modulus of elasticity in flexural vibration tests of <i>Pinus sylvestris</i> sawn timber obtained with fundamental resonant frequency and overtones	87
4.1. Abstract	87
4.2. Introduction	87
4.3. Materials and methods	89
4.3.1. Structural size samples	89
4.3.2. Vibration test and dynamic modulus of elasticity	90
4.3.3. Static modulus of elasticity calculation	91
4.3.4. Small size samples	92
4.3.5. Statistical analyses	92
4.4. Results and discussion	93
4.4.1. Structural size sample	93
4.4.2. Small size samples	98
4.5. Conclusions	99
4.6. References	100

CAPÍTULO 5 **105**

5. Alterations to the bending mechanical properties of <i>Pinus sylvestris</i> L. timber according to test direction and knot position in the cross-section	109
5.1. Abstract	109
5.2. Introduction	109
5.3. Materials and methods	111
5.3.1. Materials	111
5.3.2. Bending tests	112
5.3.3. Knottiness	113
5.3.4. Statistical analyses	114
5.4. Results and discussion	115
5.4.1. Comparison of MOE _{flat} and MOE _{edge}	117
5.4.2. Selection of knottiness variables for MOE and MOR prediction	118
5.4.3. Linear Regression to predict the MOE	120
5.4.4. Linear Regression to predict the MOR	121

5.5.	Conclusions	122
5.6.	References	123
	APPENDIX 1: Knottiness and MOE variables. Description	127
CAPÍTULO 6		131
6.	Discusión global de los resultados	133
6.1.	Análisis estadístico	133
6.2.	Propiedades mecánicas	133
6.3.	Predicción del MOEs	134
6.3.1.	Ensayos de vibración	134
6.3.2.	Ensayos de flexión estática	136
6.3.3.	Influencia de las singularidades de la madera en el MOEs	136
6.4.	Predicción del MOR	137
6.4.1.	Ensayos de vibración	137
6.4.2.	Influencia de las singularidades de la madera en el MOR	137
6.5.	Referencias	138
CAPÍTULO 7		145
7.	Conclusiones	147
7.1.	Procedimiento de ensayo y análisis estadístico	147
7.2.	Ensayos de vibración para predecir el MOR y el MOE	147
7.3.	Modelos univariable y multivariable para predecir el MOR y el MOE	148
7.4.	La influencia de las singularidades en la predicción del MOR y el MOE	148
7.5.	Efecto del cortante en el MOE	148

RESUMEN

Se utilizaron ensayos no destructivos basados en técnicas de vibración, así como información relativa a las singularidades y los defectos de la madera para predecir las propiedades mecánicas de un lote de 59 piezas de tamaño estructural de madera de *Pinus sylvestris* L. proveniente de la sierra del Montsec (Lleida). Se midieron las frecuencias de resonancia correspondientes a la vibración longitudinal, así como a la transversal de cara y a la transversal de canto. Además, se realizaron ensayos de ultrasonidos. Por último, las piezas se sometieron a un ensayo de flexión estática. Se construyeron modelos univariable y multivariable, tanto lineales como no lineales, para predecir el módulo de elasticidad (*modulus of elasticity*, MOE) y la resistencia a flexión (*modulus of rupture*, MOR). Se valoró la influencia del cortante tanto en los resultados de los ensayos de vibración como en los de flexión estática. También se identificaron las diferencias entre los resultados obtenidos en los ensayos de flexión dependiendo de la orientación de la pieza. La capacidad predictiva de los modelos se analizó a partir de la raíz error cuadrático medio (*root-mean-square error*, RMSE) obtenido mediante validación cruzada con 10 carpetas y 5 repeticiones. La existencia de diferencias estadísticamente significativas entre las capacidades predictivas de los diferentes modelos se analizó mediante el test no paramétrico de Kruskal–Wallis y la prueba *post hoc* de Dunn. El MOE dinámico estimado a partir de la frecuencia fundamental de resonancia en la vibración transversal de canto resultó la variable con el error más bajo en la predicción del MOE. Los modelos multivariable no consiguieron una reducción estadísticamente significativa del error de dicha predicción. El error más bajo en la predicción del MOR se consiguió con las variables que tienen en cuenta la posición de los nudos en la sección transversal. Se consiguió una reducción estadísticamente significativa de dicho error con modelos lineales multivariable que incluyeron variables relacionadas con los ultrasonidos y las vibraciones longitudinal y transversal. La influencia del cortante en el ensayo de flexión estática pudo ser eliminada tomando un valor del módulo de elasticidad transversal (G) igual a un diecisieteavo del MOE. En el caso de la vibración transversal, la influencia del cortante pudo ser cuantificada mediante una regresión potencial de las frecuencias de resonancia de diferentes armónicos.

RESUM

Es van realitzar assaigs no destructius basats en tècniques de vibració, això com informació relativa a les singularitats i els defectes de la fusta per a predir les propietats mecàniques d'un lot de 59 peces de mida estructural de fusta de *Pinus sylvestris* L. procedent de la serra del Montsec (Lleida). Es van mesurar les freqüències corresponents a la vibració longitudinal, així com a la transversal de cara i la transversal de cantell. A més es van fer assaigs d'ultrasons. Finalment, les mostres es van sotmetre a un assaig de flexió estàtica. Es van construir models univariable i multivariable, tant lineals com no lineals, per a predir el mòdul d'elasticitat (*modulus of elasticity*, MOE) i la resistència a flexió (*modulus of rupture*, MOR). Es va valorar la influència del tallant tant als resultats dels assaigs de vibració com als de flexió estàtica. També es van identificar les diferències entre els resultats obtinguts als assaigs de flexió dependent de l'orientació de la peça. La capacitat predictiva dels models es va analitzar a partir de l'arrel de l'error quadràtic mitjà (*root-mean-square error*, RMSE) obtingut mitjançant validació creuada amb 10 carpetes i 5 repeticions. L'existència de diferències estadísticament significatives entre les capacitats predictives dels diferents models es van analitzar mitjançant el test no paramètric de Kruskal–Waliis i la prova *post hoc* de Dunn. El MOE dinàmic estimat a partir de la freqüència fonamental de ressonància a la vibració transversal de cantell va resultar la variable amb l'error més baix a la predicción del MOE. Els models multivariable no van aconseguir una reducció estadísticament significativa del error d'aquesta predicción. L'error més baix a la predicción del MOR es va aconseguir amb les variables que tenen en compte la posició dels nusos a la secció transversal. Es va aconseguir una reducció estadísticament significativa d'aquest error amb models lineals multivariable que van incloure variables relacionades amb els ultrasons y las vibracions longitudinal i transversal. La influència del tallant a l'assaig de flexió estàtica es va poder eliminar prenent un valor del mòdul d'elasticitat transversal (G) igual a un dissetè del MOE. En el cas de la vibració transversal, la influencia del tallant es va poder quantificar mitjançant una regressió potencial de les freqüències de ressonància de diferents harmònics.

ABSTRACT

Non-destructive testing based on vibration techniques and information related to the timber features were used to predict the mechanical properties of a group of 59 structural size samples of *Pinus sylvestris* L. timber coming from Montsec mountains (Lleida, Spain). Fundamental resonant frequencies were obtained for different vibration directions: longitudinal, transverse in edgewise direction and transversal in flatwise direction. Ultrasounds tests were also carried out. Finally, all the samples were subjected to a static bending test. Univariate and multivariate models, both linear and non linear, were generated to predict the modulus of elasticity (MOE) and the modulus of rupture (MOR). The shear effect was analysed in both static and dynamic tests. Differences between results in edgewise and flatwise direction bending tests were also examined. The predictive capacity of the different models was analysed by comparing the root-mean-square error (RMSE) obtained using the 10-fold cross-validation method. The existence of statistically significant differences was examined with the non-parametric Kruskal-Wallis test and the post hoc Dunn test. The dynamic MOE obtained from the fundamental resonant frequency of the edgewise flexural vibration was the variable with the lowest error in the MOE prediction. Multivariate models did not achieve a statistically significant reduction in the error of that prediction. The variables that took into account the position of knots in the cross-section had the lowest error in the MOR prediction. A statistically significant reduction in that error was observed with multivariate linear models that included variables obtained by ultrasounds and both longitudinal and transverse vibration. The shear effect in the bending test was eliminated by taking a shear modulus (G) equal to the MOE divided by 17. The shear effect in the transverse vibration test was assessed with a power regression of the resonant frequencies corresponding to different overtones.

CAPÍTULO 1

Introducción

1. Introducción

1.1. Los ensayos no destructivos en madera

1.1.1. Una breve reflexión histórica

La madera es el material natural por excelencia para trabajar a flexión. Es fácil imaginarse al primer grupo de homínidos que intentó cruzar un río sin mojarse buscando un tronco de árbol para atravesarlo sobre el cauce. De madera fueron los primeros elementos estructurales, si no es exagerado el término, que se utilizaron para soportar las cubiertas de las construcciones temporales que realizaban aquellos homínidos para guarecerse. En el yacimiento de Terra Amata, en la actual Niza (Francia), se encuentran las evidencias de las estructuras artificiales más antiguas de las que se tiene noticia (Kostof 1988). Se trata de los restos de unas cabañas de madera construidas hace unos 400 000 años por homínidos, probablemente *Homo heidelbergensis*, que vivían allí mucho antes de que el *Homo sapiens* llegara a Europa.

A lo largo de la historia, la madera ha sido el material empleado sistemáticamente en aquellos elementos solicitados a flexión en estructuras comunes, como las cubiertas y los forjados. La explicación se antoja sencilla a partir de algunas de sus características. En primer lugar, se trata de un material abundante en prácticamente cualquier lugar habitado por seres humanos. Además, es ligera y relativamente blanda, al menos en las especies utilizadas en la construcción, lo que hace que sea fácil de obtener, transportar, trabajar y colocar en obra con medios sencillos y un esfuerzo reducido. A esas facilidades se les une un buen comportamiento a flexión debido a una elevada resistencia a tracción. La piedra o los materiales de origen pétreo tienen una resistencia a compresión muy superior a la de la madera, pero sufren cuando son sometidos a flexión por su escasa resistencia a los esfuerzos de tracción, lo que se ve agravado por su elevado peso propio. Desde luego, las grandes obras de la Historia de la Arquitectura se construyeron casi siempre con piedra u otros materiales de características parecidas, como el hormigón romano o el ladrillo. Probablemente el deseo de que la obra perdurara en el tiempo, junto a la prevención frente al fuego, que se usaba para iluminar y calentar, motivaron la elección, no sin asumir un elevado coste en recursos y tiempo y una enorme complejidad en la ejecución. Pero incluso en esos

edificios singulares la madera no pudo evitarse completamente, está presente, por ejemplo, en las cubiertas de los templos griegos o de las imponentes catedrales góticas. Todo ello sin olvidar que esas grandes obras no se hubieran podido construir sin la utilización de numerosos elementos auxiliares de madera como andamios, encofrados o cimbras. Remarcada la excepción, se puede afirmar, no sin cierta solemnidad, que la madera ha sido el material utilizado para los elementos estructurales que trabajan a flexión durante prácticamente toda la historia de la humanidad.

Su uso comenzó a decaer en la segunda mitad del siglo XIX, cuando las mejoras en los procesos de fundición del acero consiguieron poner en el mercado un material abundante, muy resistente, ligero y asequible, apto para la fabricación de todo tipo de elementos estructurales, que fue desplazando a la madera paulatinamente. A comienzos del siglo XX, el desarrollo de los hornos rotatorios para la fabricación del cemento Pórtland también facilitó la utilización del hormigón armado. Estos nuevos materiales de construcción se fabricaban en procesos industriales que permitían ofrecer elementos estructurales con una variabilidad controlada y unas características mecánicas garantizadas. Frente a esta nueva competencia, la madera tenía el inconveniente de presentar una alta variabilidad que depende de la especie, del origen e incluso de la posición dentro del árbol de la que se obtiene cada pieza. Por otra parte, el constante aumento de las exigencias a los materiales de construcción en las diferentes normativas nacionales e internacionales, obligaron a la industria de la madera a buscar métodos de ensayo rápidos y sencillos para poder poner en el mercado un producto certificado. Fue en ese contexto cuando en EE. UU., en la década de 1950, se comenzaron a sentar las bases de los ensayos no destructivos (*non destructive testing, NDT*) basados en técnicas de vibración.

1.1.2. El estudio de la vibración de una barra

El estudio de los fenómenos de vibración en barras no era algo nuevo, ya había sido abordado por Daniel Bernoulli a mediados del siglo XVIII, quien, a partir de la ecuación de la elástica planteada por su tío Jakob Bernoulli, formuló por primera vez las ecuaciones del movimiento de una barra en vibración. Sobre ese modelo también trabajó Leonhard Euler, por lo que se habla indistintamente del modelo de Bernoulli o de Euler–Bernoulli (Han *et al.* 1999). El modelo de Bernoulli describe bien las vibraciones en sentido longitudinal, no obstante, para las vibraciones en sentido transversal solo resulta válido bajo unas determinadas condiciones, la más

importante de las cuales es suponer que las secciones transversales que son planas y normales al eje de la pieza antes de la deformación permanecen planas y normales al eje después de la deformación. Este supuesto constituye uno de los denominados principios fundamentales de la Resistencia de Materiales, y se conoce como hipótesis de Navier–Bernoulli (Dias Da Silva 2006). En este caso, conviene aclararlo, se refiere a Jakob Bernoulli. Analizar la deformación de una viga considerando la hipótesis de Navier–Bernoulli supone asumir que las deformaciones provocadas por el esfuerzo cortante son de poca importancia en comparación con las provocadas por el momento flector y que, por lo tanto, pueden despreciarse, lo cual es aceptable para vigas en las que la longitud (L) sea sensiblemente mayor que el canto (h). Así, cuando la relación L/h es igual o superior a 20, el error cometido al despreciar la deformación provocada por el cortante es inferior al 1 %. En cambio, si L/h disminuye hasta un valor igual a 5, el error se dispara por encima del 10 % (Timoshenko 1938).

Trasladado este fenómeno al estudio de las vibraciones transversales, supone que, cuando no se puede considerar despreciable la deformación por cortante, el modelo de Bernoulli sobreestima las frecuencias de vibración de una barra, especialmente en los armónicos más altos (Han *et al.* 1999). De este modo, las frecuencias previstas por el modelo son mayores que las observadas. En consecuencia, el modelo de Bernoulli para explicar la vibración de una barra solo es válido en aquellos casos en los que la relación L/h sea elevada. Algunos autores han propuesto que esa relación debe ser mayor o igual que 20 (Arriaga *et al.* 2014).

En la década de 1920 Timoshenko propuso un modelo que explicaba el efecto de la vibración transversal en una viga teniendo en cuenta la influencia del cortante (Weaver *et al.* 1990). Una ventaja de la ecuación de Timoshenko es que permite encontrar el valor del módulo de elasticidad (*modulus of elasticity*, MOE) y del módulo de elasticidad transversal (G) a partir, exclusivamente, de las frecuencias de vibración transversal, lo que en la actualidad se puede conseguir con un equipamiento muy sencillo (Brancheriu 2014). Pero, a cambio, no se ha encontrado una solución exacta para dicha ecuación, aunque se han propuesto diferentes soluciones aproximadas, destacando la de Goens–Hearmon (Hearmon 1958). En general, con estas soluciones se consiguen mejores resultados que con el modelo de Bernoulli cuando la influencia del cortante no es despreciable, pero siguen teniendo un rango de validez limitado. El error es pequeño cuando la relación L/h es igual o mayor que 10 y solo para las frecuencias de los cinco primeros armónicos (Brancheriu 2006).

Algunos autores han propuesto modelos o procedimientos que mejoran los resultados de las soluciones descritas más arriba. Brancherieu (2014) propuso un método basado en un algoritmo de optimización para encontrar las soluciones a la ecuación de Timoshenko, evitando de este modo realizar las simplificaciones que son necesarias en los casos anteriores. No obstante, el método no es demasiado sencillo, requiere de un programa informático de cálculo numérico para ejecutar la optimización en un proceso que no es inmediato. Por otra parte, solo fue probado con una única pieza de madera tropical de 1 m de longitud, con elevada densidad y libre de defectos. Kubojima *et al.* (2020) propusieron un método basado en la solución de Goens–Hearmon que consistía en añadir masas concentradas a las piezas de madera para alterar la frecuencia de vibración, pero sin modificar el resto de sus propiedades. De este modo consiguieron reducir la influencia del cortante, pero a costa de seguir un procedimiento complejo, que solo fue comprobado en un número reducido de piezas de dimensiones reducidas (300 mm de longitud) y en tres piezas de tamaño estructural.

1.1.3. El estudio de la madera con técnicas de vibración

Siguiendo el resumen histórico realizado por Ross (2015), uno de los primeros estudios en los que se utilizó la vibración en sentido transversal fue llevado a cabo por Jayne (1959). En dicho estudio, realizado con *Picea sitchensis*, se demostró que los fenómenos de almacenamiento y disipación de energía estaban relacionados con las propiedades mecánicas de la madera. A lo largo de la década de 1960 otros trabajos realizados con diferentes coníferas fueron avanzando en el uso de ensayos de vibración (O'Halloran 1969; Pellerin 1965). Además de las técnicas basadas en la vibración transversal, otros autores también desarrollaron técnicas de ensayo para estimar las propiedades mecánicas de la madera a partir de la medición de la velocidad de propagación o la atenuación de una onda en sentido longitudinal, generada mediante un impacto mecánico o de ultrasonidos (Kolsky 1963; Bertholf 1965; Harris *et al.* 1972; Kaiserlik and Pellerin 1977). Posteriormente, trabajos como el de Ross *et al.* (1991) mostraron que la amplia disponibilidad de equipos informáticos y de un amplio abanico de equipamiento electrónico a precios asequibles, permitían que este tipo de ensayos pudieran alcanzar una difusión notable. A partir de entonces, y sobre todo en los últimos 15 años, se han generalizado en la literatura científica los estudios realizados con ensayos no destructivos basados en técnicas de vibración. En algunos países incluso se han aprobado normas al

respecto para establecer los procedimientos de ensayo, como es el caso de la norma ASTM E1876–15 (2015), cuya primera versión data de 1999.

1.1.4. Equipos de ensayo disponibles en el mercado

Como queda dicho anteriormente, en la actualidad se pueden encontrar diversos dispositivos comerciales diseñados para realizar ensayos no destructivos basados en técnicas de vibración. Se trata de aparatos pensados, sobre todo, para su uso en la industria, aunque también son muy utilizados en el ámbito de la investigación. A continuación, y sin ánimo de presentar una relación exhaustiva, se describen algunos de esos equipos, quizá los de uso más extendido.

Portable Lumber Grader

El Portable Lumber Grader (Fakkop, Ágfalva, Hungría) es un equipo que clasifica piezas de madera de acuerdo con European Standard EN 338 (2016). Se trata de un dispositivo sencillo que consta de un martillo para golpear en la testa de la pieza a clasificar, un micrófono para registrar la vibración longitudinal y una báscula y una cinta métrica para determinar la densidad. Un programa informático ofrece la clasificación de la pieza de madera a partir de los datos recogidos. El programa estima el MOE a partir de la frecuencia de resonancia en dirección longitudinal. En los artículos que componen la presente tesis se han citado diferentes estudios realizados en coníferas con este dispositivo (Arriaga *et al.* 2014; Dahlen *et al.* 2018; Görgün and Dündar 2018).

Hitman HM200

El equipo Hitman HM200 (Fibre-gen, Christchurch, Nueva Zelanda) integra la recogida de datos y el análisis en un solo aparato. A partir de la frecuencia de resonancia longitudinal, obtenida después de que la pieza haya sido golpeada con un martillo, ofrece las propiedades mecánicas en pantalla. En dos de los artículos citados se utilizó este aparato (Chauhan & Walker 2006; Dahlen *et al.* 2018).

MTG Timber Grader

Un funcionamiento similar tiene el equipo MTG Timber Grader (Brookhuis Applied Technologies, Enschede, Países Bajos), pero con la diferencia de que la excitación no debe realizarse con un objeto externo, es el propio aparato el que envía una señal sonora que genera una onda de sonido que se desplaza longitudinalmente

a través de la pieza que se está midiendo. Como resultado, ofrece la frecuencia fundamental y el MOE. Igual que en el caso anterior, varios estudios citados en la presente tesis se realizaron utilizando este equipo (Guntekin *et al.* 2013; Olsson *et al.* 2018; Simic *et al.* 2019).

BING

El sistema BING (CIRAD, Montpellier, Francia) también recoge a través de un micrófono las vibraciones en dirección longitudinal o transversal de una pieza de madera después de ser golpeada, para ofrecer las propiedades mecánicas de la misma. Dos de los estudios citados se llevaron a cabo con este sistema (Faydi *et al.* 2017; Olsson *et al.* 2018).

Sylvatest

Sylvatest (CBS–CBT, Lausanne, Switzerland) es un dispositivo que mide la velocidad de propagación de las ondas de ultrasonidos que atraviesan longitudinalmente una pieza de madera, sirviéndose de una sonda emisora y otra receptora. A partir de esta medida, el sistema ofrece una estimación del MOE y de la resistencia a flexión (*modulus of rupture*, MOR). También se han citado algunos estudios realizados con este aparato (Arriaga *et al.* 2014; Conde García *et al.* 2007; Sales *et al.* 2011).

Otros dispositivos

Los equipos reseñados, y otros de características similares que pueden encontrarse en el mercado, están pensados especialmente para la industria, no necesitan de cálculos, ni operaciones complementarias por parte de la persona que los maneja, son sistemas que podríamos denominar cerrados. Por otra parte, la amplia disponibilidad de equipamiento electrónico a precios asequibles ha permitido que muchos de los estudios consultados se realicen con equipos sencillos diseñados por los propios investigadores. Básicamente solo se necesitan tres elementos, un dispositivo para recoger la vibración, un ordenador y un programa para analizar la señal registrada. Para registrar las vibraciones en algunos casos se ha optado por un acelerómetro (Baar *et al.* 2015; How *et al.* 2014; Pommier *et al.* 2013) y en otras por un micrófono (Brancheriau 2014; Hassan *et al.* 2013; Kubojima *et al.* 2020), como es el caso de los ensayos realizados para la presente tesis.

1.2. Estado de la cuestión

1.2.1. Estudios previos

En las últimas décadas se han generalizado los ensayos no destructivos en madera basados en técnicas de vibración. Este tipo de ensayos han sido utilizados en diferentes estudios para estimar las propiedades mecánicas de la madera de *Pinus sylvestris* L. (Aira *et al.* 2019; Arriaga *et al.* 2012; Hassan *et al.* 2013). No obstante, la mayoría de los estudios realizados en madera de pino o de otras coníferas se basaron en único modo de vibración, ya fuera longitudinal, transversal de canto o transversal de cara. Son escasos los estudios que utilizaron más de un modo de vibración para estimar las propiedades mecánicas de la madera (Arriaga *et al.* 2014; Dahlen *et al.* 2018; Hassan *et al.* 2013). También son pocos los que combinaron diferentes técnicas, como los ultrasonidos y la frecuencia de resonancia (García-Iruela *et al.* 2016; Halabe *et al.* 1997; Hassan *et al.* 2013). Por último, algunos plantearon modelos multivariable que incluyeron singularidades o propiedades físicas, además de las frecuencias de resonancia (Arriaga *et al.* 2012; Martins *et al.* 2017; Villasante *et al.* 2019).

En la mayoría de los casos, el MOE de la madera se estimó a partir de la frecuencia fundamental, ya fuera de vibración longitudinal o transversal. Solo en algunos estudios se incluyeron los armónicos en los modelos predictivos, llegando hasta el cuarto o el quinto (Brancherieu 2006; Kubojima *et al.* 2006; Yoshihara 2012).

Valorar la influencia del cortante en la deformación representó un problema al que tuvieron que enfrentarse todos los autores (Olsson *et al.* 2012; Ouis 1999; Pantelić *et al.* 2020). En los armónicos más altos o en aquellos casos en que la relación entre la longitud y el canto no es muy elevada, resulta imposible despreciar el efecto del cortante y es difícil encontrar un modelo que prediga correctamente el MOE. Tan solo Brancherieu (2014) propuso un método que podía salvar esa dificultad, pero fue comprobado únicamente con una pieza libre de defectos de 1 m de longitud.

Es de sobra conocido que los nudos tienen una gran influencia en el MOE y, muy especialmente, en el MOR. Son numerosos los estudios realizados para conocer las propiedades mecánicas de la madera de *Pinus sylvestris* L. y también los que valoraron la influencia de los nudos en dichas características (Arriaga *et al.* 2012; Hautamäki *et al.* 2014; Wright *et al.* 2019). No obstante, solo unos pocos analizaron

la influencia en el MOE o en el MOR de la posición de los nudos en la sección transversal (Algin 2019; Lam *et al.* 2005; Lukacevic *et al.* 2015).

Normalmente, los ensayos de flexión suelen hacerse de canto porque es la posición en la que se supone que trabajará la pieza cuando se coloque en una estructura y, por lo tanto, es el comportamiento en esa posición el que interesa conocer. Sin embargo, la mayoría de las maquinas que clasifican madera de forma continua lo hacen a partir de la flexión de cara, por lo que también es interesante conocer el MOE de cara. Algunos estudios compararon el MOE obtenido en ensayos de flexión de cara con el obtenido de canto (Kim *et al.* 2010; Pošta *et al.* 2016; Yang *et al.* 2015). Debido al carácter destructivo del ensayo, es imposible realizar en una misma pieza el ensayo de rotura de canto y de cara para conocer el MOR en ambas direcciones. Para salvar esta dificultad, es posible encontrar algún estudio que relacionó el MOE de cara con el MOR de canto (Baillères *et al.* 2012).

1.2.2. Análisis estadístico en los estudios previos

Raíz del error cuadrático medio

En general, la mayoría de los estudios consultados realizaron la validación de los diferentes modelos propuestos mediante el coeficiente de determinación (R^2), una medida de la proporción de la variabilidad que puede ser explicada por cada modelo. No obstante, para validar un modelo puede ser más interesante utilizar la raíz del error cuadrático medio (*root-mean-square error*, RMSE) que ofrece una medida de la exactitud de la predicción a través de la diferencia entre los valores predichos y los observados (Alexander *et al.* 2015). En algunos casos, dependiendo del problema estudiado, un modelo con un valor elevado de R^2 puede predecir valores que se alejan de los observados con una diferencia inaceptable para esa situación concreta. Solo algunos de los estudios consultados utilizaron el RMSE (Pommier *et al.* 2013; Villasante *et al.* 2019).

Modelos multivariable

En cuanto a los modelos multivariable, lo más habitual es que se construyan mediante regresión lineal múltiple, aunque algunos estudios (García-Iruela *et al.* 2016; García Esteban *et al.* 2009; Villasante *et al.* 2019) utilizaron redes neuronales (*artificial neural network*, ANN) con resultados dispares. Algunos algoritmos permiten realizar una clasificación mediante un método no paramétrico, como es el

caso del método de los k vecinos más cercanos (k -nearest neighbors, KNN), utilizado por Villasante *et al.* (2019)

Sobreajuste

Los modelos multivariable pueden explicar mejor la variabilidad de un conjunto de datos, pero, a cambio, corren el riesgo de adaptarse incluso al ruido de la muestra, confundiéndolo con la estructura interna de los datos y provocando un sobreajuste (Lever *et al.* 2016). De este modo, provocan errores elevados cuando se aplican a conjuntos de datos diferentes de aquellos a partir de los que se han generado. Algunos de los estudios consultados utilizaron procedimientos para evitar el sobreajuste, como el *early stopping*, dividiendo el conjunto de datos en tres subgrupos, utilizando el primero para el entrenamiento del modelo, el segundo para la validación y el tercero para valorar el ajuste del modelo (García–Iruela *et al.* 2016; García Esteban *et al.* 2009). También puede utilizarse algún método de validación cruzada, que mediante diferentes procedimientos divide los datos en varios grupos para generar el modelo y para validarla (Lever *et al.* 2016; Tetko *et al.* 1995). Villasante *et al.* (2019) utilizaron el procedimiento de validación cruzada con 10 carpetas y 10 repeticiones. Después de dividir los datos en 10 grupos, se utilizó cada uno de ellos para validar el modelo creado por los otros nueve. Además, este proceso se repitió 10 veces. Este tipo de validación cruzada con carpetas (k -fold cross-validation) es el más adecuado para analizar conjuntos pequeños de datos (Lever *et al.* 2016).

Diferencias significativas entre modelos

La utilización del valor de R^2 para comparar los diferentes modelos propuestos normalmente no se acompaña de la comprobación de la existencia de diferencias significativas entre los errores de predicción de dichos modelos. Solo algunos de los estudios previos realizaron esta comprobación (Hodousek *et al.* 2017; Larsson *et al.* 1998; Villasante *et al.* 2019).

1.3. Objetivos

Teniendo en cuenta los estudios realizados hasta el momento en el ámbito de los ensayos no destructivos en madera de *Pinus sylvestris* L. y otras coníferas, así como el tratamiento estadístico realizado en la mayoría de los trabajos previos consultados, es posible definir unos objetivos para el presente estudio que vengan a cubrir algunos ámbitos del problema no suficientemente estudiados.

1.3.1. Predicción del MOE y del MOR

El objetivo de los dos primeros artículos fue predecir el MOE (artículo 1) y el MOR (artículo 2), en un grupo de piezas de tamaño estructural de madera de *Pinus sylvestris* L., mediante modelos multivariable lineales y complejos (ANN, KNN) que incluyeran datos procedentes de los ensayos no destructivos, así como singularidades y propiedades físicas de la madera. Dentro de los ensayos no destructivos se incluyeron los de ultrasonidos y los de vibración para obtener las frecuencias de resonancia en diferentes direcciones (transversal de cara, transversal de canto y longitudinal).

1.3.2. Predicción del MOE a partir de los armónicos

El objetivo del tercer artículo fue predecir el MOE de un grupo de piezas de tamaño estructural de madera de *Pinus sylvestris* L., a partir de los diferentes armónicos obtenidos mediante vibración transversal. También se valoró la influencia del cortante en los diferentes armónicos mediante la comparación de los resultados anteriores con los obtenidos en piezas de la misma madera, de tamaño reducido (1 m de longitud) y con una relación L/h elevada (115).

1.3.3. Influencia de la posición de los nudos y la dirección del ensayo de flexión en las propiedades mecánicas

El objetivo del cuarto artículo fue analizar las diferencias entre las propiedades mecánicas obtenidas mediante ensayos de flexión de canto y las obtenidas de cara en un grupo de piezas de tamaño estructural de madera de *Pinus sylvestris* L. También se buscó analizar si las variables que tienen en cuenta la posición de los nudos dentro de la sección transversal podían mejorar la predicción de las propiedades mecánicas calculadas en ambas direcciones (cara y canto).

1.4. Materiales y métodos

1.4.1. Muestras

Se obtuvieron 69 piezas de madera de *Pinus sylvestris* L. procedentes de la sierra del Montsec (Lleida) en un aserradero local, con dimensiones nominales de 70 mm × 100 mm × 2000 mm. Después de una inspección visual, se rechazaron 12 piezas que presentaban entrecasco o evidencias de pudrición. Las muestras se almacenaron en el laboratorio hasta que alcanzaron masa constante, momento en el que se realizaron los ensayos.

1.4.2. Ensayos y singularidades de la madera

Se midieron diferentes singularidades de acuerdo con European Standard EN 1309–3 (2018): desviación de la fibra, coeficiente de crecimiento, azulado, gemas y nudos. Los nudos también se valoraron con diferentes medidas basadas en el *knot area ratio* (KAR), de acuerdo con British Standard 4978 (2017). Se llevaron a cabo ensayos de vibración, en las direcciones longitudinal y transversal (de cara y de canto), para conocer las frecuencias de resonancia y los armónicos, de acuerdo con la norma ASTM E1875–15 (2015), así como ensayos de ultrasonidos. Se realizaron ensayos de flexión para conocer el MOE (de cara y de canto) y el MOR (de canto) siguiendo la European Standard EN 408:2010 + A1 (2012), que también se siguió para determinar la densidad. Después del ensayo de rotura se midió el contenido en humedad de cada pieza mediante secado en estufa, de acuerdo con European Standard EN 13183–1 (2002).

1.4.3. Equipamiento

Para registrar la vibración se utilizó un micrófono de condensador Rode NT–USB (Rode Microphones, Sidney, Australia), con patrón polar cardioide y un rango de frecuencias de 20 Hz a 20 kHz. La señal se registró y analizó con el programa Audacity (Audacity Team, Pittsburg, PA, EE. UU.), que mediante una transformada de Fourier y una ventana Hann, realizaba el cambio del dominio del tiempo al dominio de frecuencias.

Los ensayos de ultrasonidos se hicieron con un dispositivo Sylvatest Duo (CBS–CBT, Lausana, Suiza). El equipo ofrece como resultados de la medición la velocidad de transmisión de la onda, la atenuación de la onda, el MOE y el MOR.

Para los ensayos de flexión se utilizó una máquina universal con una capacidad de carga máxima de 50 kN (Cohiner, Lleida, España). La adquisición de datos (fuerza y desplazamiento) se llevó a cabo con el programa LabVIEW v7.1 (National Instruments, Austin, TX, EE. UU.).

El cálculo del RMSE mediante validación cruzada de los diferentes modelos se llevó a cabo con el programa WEKA v3.6 (Waikato University, Hamilton, Nueva Zelanda). Para el análisis de las diferencias significativas existentes entre los diferentes modelos se utilizó el programa R v3.6.1 (The R Foundation, Viena, Austria).

1.4.4. Análisis estadístico

Se crearon modelos de predicción univariable y multivariable mediante regresiones lineales, y también mediante algoritmos no lineales como ANN y KNN.

La capacidad predictiva de los modelos fue evaluada a partir del RMSE obtenido mediante validación cruzada con 10 carpetas. De este modo, el resultado fue un conjunto de valores no independientes, por lo que no fue posible realizar un análisis de varianza o un T-test (Refaeilzadeh *et al.* 2009). En su lugar se analizaron las diferencias significativas entre modelos mediante el test no paramétrico de Kruskal–Wallis y la prueba *post hoc* de Dunn.

En algunos casos, para poder comparar los resultados obtenidos con los publicados en otros estudios, se calculó el coeficiente de determinación, R^2 , sin utilizar la validación cruzada.

1.5. Resultados

La presente tesis doctoral está compuesta por cuatro artículos, dos de ellos publicados, un tercero aceptado y un cuarto remitido a una revista, tal y como se detalla a continuación.

1.5.1. Artículo 1

Fernández-Serrano, Á., Villasante, A. (2021) Longitudinal, transverse and ultrasound vibration for the prediction of stiffness using models incorporating features in *Pinus sylvestris* timber. European Journal of Wood and Wood Products 79(6):1541–1550. DOI: 10.1007/s00107-021-01707-0.

European Journal of Wood and Wood Products (JCR, 2020)

Factor de impacto (JIF): 2,014

Clasificación (JIF): Q2 (7/22), categoría Materials Science, Paper and Wood

1.5.2. Artículo 2

Fernández-Serrano, Á., Villasante, A. (2022) Modulus of Rupture Prediction in *Pinus sylvestris* with Multivariate Models Constructed with Resonance, Ultrasound, and Wood Heterogeneity Variables. BioResources 17(1):1106–1119. DOI: 10.15376/biores.17.1.1106-1119.

BioResources (JCR, 2020)

Factor de impacto (JIF): 1,614

Clasificación (JIF): Q2 (8/22), categoría Materials Science, Paper and Wood

1.5.3. Artículo 3

Villasante, A., Fernández-Serrano, Á., (2022) Dynamic modulus of elasticity in flexural vibration tests of *Pinus sylvestris* sawn timber obtained with fundamental resonant frequency and overtones. Holzforschung 76(6):485–492. DOI: 10.1515/hf-2021-0190.

Holzforschung (JCR, 2020)

Factor de impacto (JIF): 2,393

Clasificación (JIF): Q1 (5/22), categoría Materials Science, Paper and Wood

1.5.4. Artículo 4

Fernández-Serrano, Á., Villasante, A. Alterations to the bending mechanical properties of *Pinus sylvestris* L. timber according to test direction and knot position in the cross-section.

Enviado a Maderas–Ciencia y Tecnología

Maderas–Ciencia y Tecnología (JCR, 2020)

Factor de impacto (JIF): 1,576

Clasificación (JIF): Q2 (9/22), categoría Materials Science, Paper and Wood

1.5.5. Presentación de los artículos

Los cuatro artículos se incluyen en los capítulos del 2 al 5. Se ha optado por no respetar el formato original de cada revista y uniformizar los aspectos formales para dar continuidad al presente documento. También se ha añadido color a alguna figura que en la publicación original aparece en blanco y negro. No se ha realizado ninguna alteración del texto, el contenido de los tres artículos publicados que aquí se presentan se corresponde exactamente con el contenido que puede consultarse en las revistas referenciadas.

1.6. Referencias

- Aira, J.R., Villanueva, J.L., Lafuente, E. (2019) Visual and machine grading of small diameter machined round *Pinus sylvestris* and *Pinus nigra* subsp. *salzmannii* wood from mature Spanish forests. Mater. Struct. 52(2):1–12.
- Alexander, D.L.J., Tropsha, A., Winkler, D.A. (2015) Beware of R₂: Simple, Unambiguous Assessment of the Prediction Accuracy of QSAR and QSPR Models. J. Chem. Inf. Model. 55(7):1316–1322.
- Algin, Z. (2019) Multivariate performance optimisation of scaffold boards with selected softwood defects. Constr. Build. Mater. 220:667–678.
- Arriaga, F., Íñiguez-Gonzalez, G., Esteban, M., Divos, F. (2012) Vibration method for grading of large cross-section coniferous timber species. Holzforschung 66(3):381–387.
- Arriaga, F., Monton, J., Segues, E., Íñiguez-Gonzalez, G. (2014) Determination of the mechanical properties of radiata pine timber by means of longitudinal and transverse vibration methods. Holzforschung 68(3):299–305.
- ASTM (2015) E1876–15. Standard Test Method for Dynamic Young's Modulus, Shear Modulus, and Poisson's Ratio by Impulse Excitation of Vibration. ASTM: West Conshohocken, PA, EE. UU.
- Baar, J., Tippner, J., Rademacher, P. (2015) Prediction of mechanical properties – modulus of rupture and modulus of elasticity – of five tropical species by nondestructive methods. Maderas. Cienc. y Tecnol. 17(2):239–252.
- Baillères, H., Hopewell, G., Boughton, G., Brancherieu, L. (2012) Strength and stiffness assessment technologies for improving grading effectiveness of radiata pine wood. BioResources 7(1):1264–1282.
- Bertholf, L.D. (1965) Use of elementary stress wave theory for prediction of dynamic strain in wood. Bull. 291. Washington State University, College of Engineering: Pullman, WA, EE. UU.
- Brancherieu, L. (2006) Influence of cross section dimensions on Timoshenko's shear factor – Application to wooden beams in free-free flexural vibration. Ann. For. Sci. 63(3):319–321.
- Brancherieu, L. (2014) An alternative solution for the determination of elastic parameters in free-free flexural vibration of a Timoshenko beam. Wood Sci. Technol. 48(6):1269–1279.
- British Standard (2017) BS 4978:2017. Visual strength grading of softwood. Specification. British Standards Institution: Londres, Reino Unido.
- Chauhan, S.S., Walker, J.C.F. (2006) Variations in acoustic velocity and density with age, and their interrelationships in radiata pine. For. Ecol. Manage. 229(1–3):388–394.

- Conde García, M., Fernández–Golfín Seco, J.I., Hermoso Prieto, E. (2007) Mejora de la predicción de la resistencia y rigidez de la madera estructural con el método de ultrasonidos combinado con parámetros de clasificación visual. *Mater. Constr.* 57(288):49–59.
- Dahlen, J., Montes, C., Eberhardt, T.L., Auty, D. (2018) Probability models that relate nondestructive test methods to lumber design values of plantation loblolly pine. *Forestry* 91(3):295–306.
- Dias Da Silva, V. (2006) Mechanics and strength of materials. Springer: Berlín, Alemania.
- European Standard (2002) EN 13183–1:2002. Moisture content of a piece of sawn timber. Part 1: Determination by oven dry method European Committee for Standardization (CEN): Bruselas, Bélgica.
- European Standard (2012) EN 408:2011+A1:2012. Timber structures. Structural timber and glued laminated timber. Determination of some physical and mechanical properties. European Committee for Standardization (CEN) : Bruselas, Bélgica.
- European Standard (2016) EN 338:2016. Structural timber. Strength classes European Committee for Standardization (CEN): Bruselas, Bélgica.
- European Standard (2018) EN 1309–3:2018. Round and sawn timber – Methods of measurements – Part 3: Features and biological degradations European Committee for Standardization (CEN): Bruselas, Bélgica.
- Faydi, Y., Brancherieu, L., Pot, G., Collet, R. (2017) Prediction of oak wood mechanical properties based on the statistical exploitation of vibrational response. *BioResources* 12(3):5913–5927.
- García-Iruela, A., Fernández, F.G., Esteban, L.G., De Palacios, P., Simón, C., Arriaga, F. (2016) Comparison of modelling using regression techniques and an artificial neural network for obtaining the static modulus of elasticity of *Pinus radiata* D. Don. timber by ultrasound. *Compos. Part B–Eng.* 96:112–118.
- García Esteban, L., García Fernández, F., de Palacios, P. (2009) MOE prediction in *Abies pinsapo* Boiss. timber: Application of an artificial neural network using non-destructive testing. *Comput. Struct.* 87(21–22):1360–1365.
- Görgün, H.V., Dündar, T. (2018) Strength grading of Turkish Black Pine structural timber by visual evaluation and nondestructive testing. *Maderas Cienc. y Tecnol.* 20(1):57–66.
- Guntekin, E., Emiroglu, Z., Yilmaz, T. (2013) Prediction of Bending properties for Turkish Red Pine (*Pinus brutia* Ten.) Lumber using stress wave method. *BioResources* 8(1):231–237.
- Halabe, U.B., Bidigal, G.M., GangaRao, H.V.S., Ross, R.J. (1997) Nondestructive evaluation of green wood using stress wave and transverse vibration techniques. *Mater. Eval.* 55(9):1013–1018.

- Han, S.M., Benaroya, H., Wei, T. (1999) Dynamics of transversely vibrating beams. *J. Sound Vib.* 225(5):935–988.
- Harris, D.O., Telleman, A.S., Darwish, F.A.I. (1972) Detection of fiber cracking by acoustic emission. Acoustic emission. ASTM 505. ASTM: West Conshohocken, PA, EE. UU.
- Hassan, K.T.S., Horacek, P., Tippner, J. (2013) Evaluation of stiffness and strength of Scots pine wood using resonance frequency and ultrasonic techniques. *BioResources* 8(2):1634–1645.
- Hautamäki, S., Kilpeläinen, H., Verkasalo, E. (2014) Factors and models for the bending properties of sawn timber from Finland and north-western Russia. Part II: Scots pine. *Balt. For.* 20(1):142–156.
- Hearmon, R.F.S. (1958) The influence of shear and rotatory inertia on the free flexural vibration of wooden beams. *Br. J. Appl. Phys.* 9(10):381–388.
- Hodousek, M., Dias, M., Martins, C., Marques, A., Böhm, M. (2017) Comparison of non-destructive methods based on natural frequency for determining the modulus of elasticity of *Cupressus lusitanica* and *Populus x canadiensis*. *Bioresources* 12(1):270–282.
- How, S.S., Williamson, C.J., Carradine, D., Tan, Y.E., Cambridge, J., Pang, S. (2014) Predicting the young's modulus of defect free radiata pine shooks in finger-jointing using resonance frequency. *Maderas Cienc. y Tecnol.* 16(4):435–444.
- Jayne, B.A. (1959) Vibrational properties of wood as indices of quality. *For. Prod. J.* 9(11):413–416.
- Kaiserlik, J.H., Pellerin, R.F. (1977) Stress wave attenuation as an indicator of lumber strength. *For. Prod. J.* 27(6):39–43.
- Kim, K.-M., Shim, K.-B., Lum, C. (2010) Predicting tensile and compressive moduli of structural lumber. *Wood Fiber* 43(1):83–89.
- Kolsky, P. (1963) Stress waves in solids. Dover Publications, Inc.: Nueva York, EE. UU.
- Kostof, S. (1988) Historia de la arquitectura. Alianza: Madrid, España.
- Kubojima, Y., Sonoda, S., Kato, H., Harada, M. (2020) Effect of shear and rotatory inertia on the bending vibration method without weighing specimens. *J. Wood Sci.* 66(1):51.
- Kubojima, Y., Tonosaki, M., Yoshihara, H. (2006) Young's modulus obtained by flexural vibration test of a wooden beam with inhomogeneity of density. *J. Wood Sci.* 52(1):20–24.
- Lam, F., Barrett, J.D., Nakajima, S. (2005) Influence of knot area ratio on the bending strength of Canadian Douglas fir timber used in Japanese post and beam housing. *J. Wood Sci.* 51(1):18–25.

- Larsson, D., Ohlsson, S., Perstorper, M., Brundin, J. (1998) Mechanical properties of sawn timber from Norway spruce. *Holz Als Roh–Und Werkst.* 56(5):331–338.
- Lever, J., Krzywinski, M., Altman, N. (2016) Model selection and overfitting. *Nat. Methods* 13(9):703–704.
- Lukacevic, M., Füssl, J., Eberhardsteiner, J. (2015) Discussion of common and new indicating properties for the strength grading of wooden boards. *Wood Sci. Technol.* 49(3):551–576.
- Martins, C.E.J., Dias, A.M.P.G., Marques, A.F.S., Dias, A.M.A. (2017) Non-destructive methodologies for assessment of the mechanical properties of new utility poles. *BioResources* 12(2):2269–2283.
- O'Halloran, M.R. (1969) Nondestructive parameters for lodgepole pine dimension lumber. M. S. Thesis. Colorado State University: Fort Collins, CO, EE. UU.
- Olsson, A., Oscarsson, J., Johansson, M., Källsner, B. (2012) Prediction of timber bending strength on basis of bending stiffness and material homogeneity assessed from dynamic excitation. *Wood Sci. Technol.* 46(4):667–683.
- Olsson, A., Pot, G., Viguier, J., Faydi, Y., Oscarsson, J. (2018) Performance of strength grading methods based on fibre orientation and axial resonance frequency applied to Norway spruce (*Picea abies* L.), Douglas fir (*Pseudotsuga menziesii* (Mirb.) Franco) and European oak (*Quercus petraea* (Matt.) Liebl./*Quercus robur* L.). *Ann. For. Sci.* 75(4):102.
- Ouis, D. (1999) Vibrational and acoustical experiments on logs of spruce. *Wood Sci. Technol.* 33(2):151–184.
- Pantelić, F., Mijić, M., Šumarac Pavlović, D., Ridley–Ellis, D., Dudeš, D. (2020) Analysis of a wooden specimen's mechanical properties through acoustic measurements in the very near field. *J. Acoust. Soc. Am.* 147(4):EL320–EL325.
- Pellerin, R.F. (1965) Correlation of Strength properties of 1-inch lumber. Washington State University, Division of Industrial Research. Potlatch Forests, Inc.: Lewiston, ID, EE. UU.
- Pommier, R., Breysse, D., Dumail, J.F. (2013) Non-destructive grading of green Maritime pine using the vibration method. *Eur. J. Wood Wood Prod.* 71(5):663–673.
- Pošta, J., Ptáček, P., Jára, R., Terebesyová, M., Kuklík, P., Dolejš, J. (2016) Correlations and differences between methods for non-destructive evaluation of timber elements. *Wood Res.* 61(1):129–140.
- Refaeilzadeh, P., Tang, L., Liu, H. (2009) Cross–Validation. In Liu L and Özsü MT (Eds.), *Encyclopedia of Database Systems*. Springer US: Boston, USA.
- Ross, R.J. (2015) Nondestructive evaluation of wood. General Technical Report FPL–GTR–238. Department of Agriculture, Forest Service, Forest Products Laboratory: Madison, WI, EE. UU.

- Ross, R.J., Geske, E.A., Larson, G.L., Murphy, J.F. (1991) Transverse vibration nondestructive testing using a personal computer. Res. Pap. FPL-RP-502. Department of Agriculture, Forest Service, Forest Products Laboratory: Madison, WI, EE. UU.
- Sales, A., Candian, M., De Salles Cardin, V. (2011) Evaluation of the mechanical properties of Brazilian lumber (*Goupia glabra*) by nondestructive techniques. Constr. Build. Mater. 25(3):1450–1454.
- Simic, K., Gendvilas, V., O'Reilly, C., Harte, A.M. (2019) Predicting structural timber grade—determining properties using acoustic and density measurements on young Sitka spruce trees and logs. Holzforschung 73(2):139–149.
- Tetko, I. V., Livingstone, D.J., Luik, A.I. (1995) Neural Network Studies. 1. Comparison of Overfitting and Overtraining. J. Chem. Inf. Comput. Sci. 35(5):826–833.
- Timoshenko, S. (1938) Strength of materials D. Van Mostrand Company, Inc.: Nueva York, EE. UU.
- Villasante, A., Íñiguez-Gonzalez, G., Puigdomenech, L. (2019) Comparison of various multivariate models to estimate structural properties by means of non-destructive techniques (NDTs) in *Pinus sylvestris* L. timber. Holzforschung 73(4):331–338.
- Weaver, W., Timoshenko, S., Young, D.H. (1990) Vibration problems in engineering. Wiley: New York, USA.
- Wright, S., Dahlen, J., Montes, C., Eberhardt, T.L. (2019) Quantifying knots by image analysis and modeling their effects on the mechanical properties of loblolly pine lumber. Eur. J. Wood Wood Prod. 77(5):903–917.
- Yang, B.Z., Seale, R.D., Shmulsky, R., Dahlen, J., Wang, X. (2015) Comparison of nondestructive testing methods for evaluating no. 2 southern pine lumber: Part B, modulus of rupture. Wood Fiber Sci. 47(4):375–384.
- Yoshihara, H. (2012) Examination of the specimen configuration and analysis method in the flexural and longitudinal vibration tests of solid wood and wood-based materials. For. Prod. J. 62(3):191–200.

CAPÍTULO 2

MOE prediction

Fernández-Serrano, A., Villasante, A. (2021) Longitudinal, transverse and ultrasound vibration for the prediction of stiffness using models incorporating features in *Pinus sylvestris* timber. Eur. J. Wood Wood Prod. 79(6):1541–1550.

2. Longitudinal, transverse and ultrasound vibration for the prediction of stiffness using models incorporating features in *Pinus sylvestris* timber

2.1. Abstract

Non-destructive testing was used to predict the static modulus of elasticity (MOEs) of Scots pine (*Pinus sylvestris*) timber from the northeast of Spain. Three vibration tests were performed, longitudinal, flatwise and edgewise, to obtain the dynamic modulus of elasticity (MOE_{dyn}) based on the fundamental resonant frequencies. The MOE_{dyn} was additionally obtained from ultrasound tests. Measurements of different features were performed of the various samples, which were also subjected to a bending test to find the MOEs. Different types of models, simple linear regression (SLR), multiple linear regression (MLR) and artificial neural network (ANN), were generated to predict the MOEs based on the study variables. The predictive capacity of the different models was analysed by comparing the root mean square error (RMSE) obtained using the 10-fold cross-validation method. The vibration techniques showed a better MOEs prediction than the ultrasound techniques. The MOE_{dyn} obtained from the fundamental resonant frequency of the edgewise flexural vibration (MOE_{EV}) was the variable that best predicted the MOEs. The error of the SLR with MOE_{EV} was not significantly improved by any other model, whether univariate or multivariate. The ANN-based models did not significantly improve the error of the MLR-based models.

2.2. Introduction

In recent years, the use of non-destructive testing (NDT) to determine the mechanical properties of wood has reached a high level of development (Arriaga *et al.* 2012), especially for techniques based on ultrasound (Sandoz 1989) and vibration (Brancherieu and Bailleres 2002). In some countries, technical standards have been established in reference to vibration tests (ASTM Standard E1876–15 2015) with the aim of determining the correlation between the dynamic modulus of elasticity (MOE_{dyn}), calculated using vibration or ultrasound techniques, and the static modulus of elasticity (MOEs). Knowledge of this relationship can be useful to make simple and rapid estimations of the MOEs.

Several authors (Arriaga *et al.* 2012; Hassan *et al.* 2013; Villasante *et al.* 2019) have carried out vibration tests with Scots pine timber (*Pinus sylvestris* L.). Scots pine is a very common species in mountainous areas in the north of Spain (Pardos *et al.* 1990) and is extensively used in timber structures throughout Europe. Other authors have carried out similar tests with other pine species, including *Pinus pinaster* (Pommier *et al.* 2013), *Pinus nigra* (Arriaga *et al.* 2012; Íñiguez González *et al.* 2007), *Pinus brutia* (Guntekin *et al.* 2013), *Pinus radiata* (Arriaga *et al.* 2012; García-Iruela *et al.* 2016; How *et al.* 2014) and southern pine (Wang *et al.* 2008). Tests have also commonly been performed to determine the MOE_{dyn} of the wood of Asian conifers (Cho 2007; Wang *et al.* 2008), American conifers (Barrett and Hong 2010; Wang *et al.* 2008) and European conifers (Hodousek *et al.* 2016; Larsson *et al.* 1998). Similar studies have also been published on temperate hardwood species (Cho 2007; Ilic 2001; Nocetti *et al.* 2016), and tropical hardwood species (Baar *et al.* 2015; Chauhan and Sethy 2016; Sales *et al.* 2011). Some of the studies involving pine combined vibration tests with ultrasound tests (García-Iruela *et al.* 2016; Hassan *et al.* 2013; Villasante *et al.* 2019).

Most of these studies establish the correlation through the coefficient of determination (R^2) of linear regressions. However, recent studies (Pommier *et al.* 2013; Villasante *et al.* 2019) have indicated that the root-mean-square error (RMSE) is a better reflection of the prediction error of the model.

Some authors have proposed the use of artificial neural network (ANN) to establish the MOEs prediction models. García Esteban *et al.* (2009) found that ANN improved the MOEs prediction compared to MLR in *Abies pinsapo* timber. García-Iruela *et al.* (2016) observed the same tendency in *Pinus radiata*. However, Villasante *et al.* (2019) did not detect any statistically significant differences between the predictive capacity of ANN and MLR in *Pinus sylvestris*.

Although MOEs prediction models have usually been developed without testing for the existence of significant differences between them and have been limited to a comparison of mean values, some studies have analysed the significant differences. Larsson *et al.* (1998) observed that the longitudinal vibration MOE (MOE_{LV}) value was significantly higher than that of the edgewise MOE (MOE_{EV}) in *Picea abies*. However, no comparisons were made between these MOE_{dyn} values and the MOEs. Larsson *et al.* (1998) also observed that the MOEs value in samples without pith was significantly higher than in those with pith, although this effect was not observed in all the sample types. Hodousek *et al.* (2016) obtained the MOE_{dyn} using the MTG Timber Grader and an accelerometer.

For *Cupressus lusitanica*, they found statistically significant differences between both MOE_{dyn} values and the MOEs. For *Populus canadiensis*, these differences disappeared. Villasante *et al.* (2019) analysed the capacity of different algorithms to predict the MOEs based on NDT of *Pinus sylvestris* timber. They found that none of the algorithms significantly improved the MLR–obtained errors.

Some authors have tested the effect of including features of sawn timber in MOEs prediction based on the MOE_{dyn}. However, Arriaga *et al.* (2014) and Villasante *et al.* (2019) found no improvement in the MOEs prediction model when incorporating the concentrated knot diameter ratio (CKDR). Density showed a low correlation with stiffness in studies carried out with both conifers (Larsson *et al.* 1998; Simic *et al.* 2019) and hardwoods (Baar *et al.* 2015; Chauhan and Sethy 2016; Faydi *et al.* 2017). Other works found that the annual ring width explained only a small proportion of the variability in stiffness (Guntekin *et al.* 2013; Larsson *et al.* 1998). Mania *et al.* (2020) found that in five temperate hardwood species the increment in the slope of grain produced a statistically significant decrease in MOEs.

Whereas predictions were initially made using linear regressions of a single variable, some studies today are using multivariate models based on MLR or machine learning techniques. Complex models allow a more precise fit of the data of the tested samples, but there is a risk of losing predictive capacity when applied to an independent dataset, an effect known as overfitting. An overfitted model only responds to the particular case it has been trained for, and the bigger the fit the further it will be from the general behaviour prediction, especially in small datasets. As it uses a specific dataset for the training, an overfitted model even fits the noise of the sample, confusing the noise with the underlying structure of the model (Lever *et al.* 2016). In this way, overfitting will generate models that will provoke high errors when applied to datasets with noise different to that of the training set. The researcher may erroneously suppose that the model has a high predictive capacity, but this only occurs if it is applied to the samples that have been analysed, not with the rest.

Most of the studies consulted do not take into consideration the effect of overfitting on MOEs prediction, and only a few authors have incorporated measures to avoid its occurrence. García Esteban *et al.* (2009) and García–Iruela *et al.* (2016) used the so-called early–stopping method, dividing the set of samples into three groups: a training set (60% of the samples), a validation set (20%) and a testing set (20%). For small datasets the assumption that each set was representative of the full dataset might not be true and K–

fold cross-validation is the most appropriate procedure (Lever *et al.* 2016). Villasante *et al.* (2019) used the 10-fold cross-validation method, randomly dividing the samples into 10 groups or folds and applying the training and validation process 10 times, once for each group. The cross-validation method avoids overfitting in complex predictive models like ANN (Tetko *et al.* 1995).

The aim of this work was to compare prediction models of the MOEs of *Pinus sylvestris* wood based on features of sawn timber and the MOE_{dyn} obtained from vibration and ultrasound tests. Both univariate simple linear regression (SLR) models and multivariate MLR and ANN models are used for this purpose. The fit of the model was evaluated using the RMSE.

2.3. Materials and methods

2.3.1. Samples

Analyses were undertaken with samples of *Pinus sylvestris* from the same forest in the Pyrenees obtained from a local sawmill (Lleida, Spain) in two visits within one month. A total of 69 samples were obtained by random sampling of sawn timber stored at the sawmill. At the laboratory, twelve samples with bark pockets or rot were rejected, leaving a final total of 57 samples. Due to the sampling procedure and the small number of samples, the reported values are not necessarily representative of the resource. The average age of the trees was 60 years and the nominal sample size was 70 mm x 100 mm x 2000 mm. The samples were stored in the test laboratory. Initially, a periodic moisture testing was performed using the oven dry method (European Standard EN 13183–1 2002a) with 20 mm thick slices cut from the central part of the samples included in a moisture control group, until a moisture content (MC) below 14% was observed. The samples from this moisture control group were different from the 57 samples used for the analyses. Finally, testing was conducted when the 57 samples used for the analyses had reached a constant weight ($\pm 0.1\%$ in 6 hours), in accordance with European Standard EN 408:2010+A1 (2012).

2.3.2. Features and biological degradations

The dimensions of each sample were measured in accordance with European Standard EN 408+A1 (2012). The samples were also weighed to obtain the density (ρ). Subsequently, the following features and biological degradations were measured in accordance with the

procedure outlined in European Standard 1309–3 (2018): slope of grain (SLG), rate of growth (RG), blue stain (BS), and wanes (WN). It was decided to include the numerical values of these features and biological degradation instead of using a visual classification of the samples, as the latter would offer few nominal values with less predictive potential. The influence of knots was studied using the knot area ratio (KAR), which is the proportion of the cross-section occupied by the knots (Walker 1993). The highest KAR value in the central third of the sample was the value used. Pre-test MC was measured in the central area of each sample using a wood moisture meter (Hydromette HB 30, Gann, Germany), in accordance with European Standard EN 13183–2 (2002b).

2.3.3. Ultrasounds

A Sylvatest Duo ultrasound device with a frequency of 22 kHz (CBS–CBT, Lausanne, Switzerland) was used, placing the transducers at opposite ends of the sample to obtain the velocity of ultrasound waves propagation (V_U) and the modulus of elasticity by ultrasound (MOE_U) provided by the device.

2.3.4. Vibration tests

The samples were subjected to a longitudinal vibration (LV) test and two transverse (or flexural) vibration tests: flatwise (FV) and edgewise (EV). Following the procedure set out in ASTM Standard E1876–15 (2015), the samples were suspended with elastic cords situated on the nodes of the fundamental transverse mode of vibration. In the transverse vibration with free ends, the two nodal points were located at a distance of 0.224 times the length (L) of the sample from each end (Figure 2.1). This type of support allows isolation of the sample from external vibrations with no restriction of the desired vibration. To generate the vibration, the samples were tapped in the centre of the face and edge (transverse modes) and at one of the ends (longitudinal mode) with a special 22.7 g impulser consisting of a 230 mm long x 4 mm diameter wooden handle with a 26 mm diameter glass marble at the tip. The vibrations were recorded using a microphone with cardioid polar pattern and frequency range of 20 Hz to 20 kHz (Rode NT–USB, Rode Microphones, Australia). The microphone was placed at the opposite end to the end that was tapped in the longitudinal mode (Figure 2.1). The signal picked by the microphone was recorded and analysed using the Audacity® software (Audacity Team 2015). A project sampling rate of 384 kHz and resolution of 24 bits were used for the recording in order to

obtain a time domain with sufficient data for spectrum analysis. The frequency spectrum analysis was performed with the Hann function. For each sample, the fundamental resonant frequency was obtained for each type of tested vibration: longitudinal (f_{LV}), flexural flatwise (f_{FV}) and flexural edgewise (f_{EV}). Based on the frequencies, the MOE_{dyn}

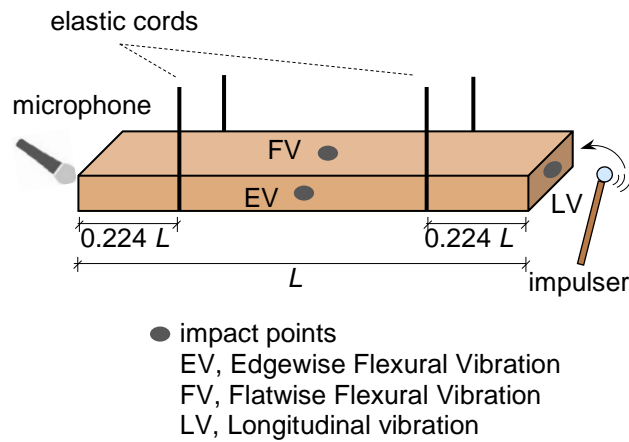


Figure 2.1. Scheme of the vibration tests

was calculated for each sample in accordance with the following equations (Weaver *et al.* 1990):

$$MOE_{LV} = 4f_{LV}^2 L^2 \rho \quad (2.1)$$

$$MOE_{FV} = \frac{48\pi^2 \rho f_{FV}^2 L^4}{4.73^4 b^2} \quad (2.2)$$

$$MOE_{EV} = \frac{48\pi^2 \rho f_{EV}^2 L^4}{4.73^4 h^2} \quad (2.3)$$

where f_{LV} , f_{FV} and f_{EV} are the fundamental resonant frequencies for each type of vibration, ρ is the density of the sample, and L , b and h are the actual length, width and thickness of each sample, respectively. The effect of shear was not taken into account because it had little influence, as the ratios L/b and L/h were equal to or greater than 20 (Arriaga *et al.* 2014).

2.3.5. Static bending test

To obtain the global MOEs, the four point bending test in edgewise direction was performed using a 50-kN universal testing machine (Cohiner, Spain), in accordance with European Standard EN 408:2010+A1 (2012). Data acquisition was done with

LabVIEW 7.1 (National Instruments, USA). The supports were placed at a distance equal to 18 times the width, and the two load points were placed at a distance from each support equal to 6 times the width. The position of the critical defect with respect to the load points was not considered. A displacement transducer was placed at the midpoint between the two supports. The MOEs was derived using the stress–strain curve in the loading area between 10% and 40% of ultimate bending strength. The linear regression in this loading area presented an R^2 value above 0.99 for all the samples. After the bending test had been concluded, a 20 mm thick slice was cut as close as possible to the failure point to determine MC using the oven dry method (European Standard EN 13183–1 2002a). No adjustment of density and stiffness was made for MC, because all the samples had very close MC values. Destructive and non–destructive tests for every sample were carried out within one hour.

2.3.6. Statistical analyses

A prior analysis was performed to obtain the R^2 from the SLR between the MOEs and all the study variables (MOE_U , MOE_{LV} , MOE_{FV} , MOE_{EV}). WEKA software (Waikato University, version 3.6, Hamilton, New Zealand) was employed, using the simple linear regression algorithm, including all the data of the samples without cross-validation, as is usually implicitly done in the studies that were consulted. This prior analysis was carried out to enable a comparison of the results obtained with those of other authors. In this first stage of the analysis, the comparison of errors was undertaken using the mean absolute error (MAE) as it is an intuitive measure and easy to interpret. The RMSE was not used during the first stage in order to avoid any potential confusion; it was reserved for carrying out the subsequent statistical analysis of the models.

After the comparison was made with other studies, the RMSE was obtained to evaluate the model fit of the MOEs using SLR. Although R^2 is an adequate metric to describe the proportion of variation in the response that can be explained by the model, the RMSE provides better information about the goodness-of-fit of the model based on the difference between the values obtained by the prediction and the actual observed values. Alexander *et al.* (2015) observed that the value of a model depends on its overall accuracy and precision (RMSE) and not on how successfully it explains the variation in a particular data set (R^2). They recommended using RMSE because it is a more helpful indicator of a model's usefulness than is R^2 .

Prediction models obtained from the whole dataset can cause overfitting, overestimating the goodness-of-fit. To avoid model overfitting, a 10-fold cross-validation method was used (Faydi *et al.* 2017; Hashim *et al.* 2016; Villasante *et al.* 2019). The samples were randomly split into ten groups or folds. Each fold was used to validate the model generated from the remaining 9 folds (Refaeilzadeh *et al.* 2009). In other words, this method allows ten validation values to be obtained. The 10-fold cross-validation method was repeated 5 times, randomly distributing the samples each time. In this way, 50 RMSE values were obtained for each of the models. This process was carried out with WEKA 3.6 software (Waikato University 2014, Hamilton, New Zealand).

The dataset with 50 RMSE values of each model was analysed with R-software (The R Foundation, version 3.6.1, Vienna, Austria). The cross-validation method generated RMSE values that were not independent, and for this reason it was not possible to carry out an ANOVA or a paired t-test (Refaeilzadeh *et al.* 2009). Instead, the non-parametric Kruskal-Wallis test was used to compare the models. If statistically significant differences between the RMSE were found, post hoc analysis was carried out using Dunn's test with Bonferroni adjustment. In all cases, the level of significance was 0.05.

Firstly, the MOEs prediction was analysed on the basis of simple variables: SLG, RG, BS, WN, KAR, V_U , density, f_{LV} , f_{FV} and f_{EV} . Subsequently, the MOEs prediction was analysed on the basis of the four MOE_{dyn} (MOE_U , MOE_{LV} , MOE_{FV} , MOE_{EV}). This analysis was considered different to the previous analysis as the MOE_{dyn} is a compound variable which includes various simple variables (Equations. 2.1, 2.2 and 2.3).

Finally, multivariate models were used. The analysis was first performed with MLR, generating a model which included all the study variables. Following this, a greedy selection using the Akaike information metric was used with WEKA 3.6 software (Waikato University, Hamilton, New Zealand) as a variable selection method to obtain the model with the lowest RMSE. This model was then simplified, eliminating one by one the variables which caused the least variation in the RMSE. A Kruskal-Wallis test was applied, using Dunn's test with Bonferroni adjustment, when necessary to verify whether there were any statistically significant differences between the RMSE of the models.

A prediction model was also generated using an ANN. A multilayer perceptron was used with sigmoid nodes and learning by backpropagation. The ANN parameters were adjusted in a prior test. The parameters were tested with a minimum of five values, corresponding to the default value proposed by WEKA 3.6 software (Waikato University, Hamilton, New Zealand), two values above and two values below. For each parameter, the

value which offered the lowest RMSE was chosen. The values chosen were 0.1 for the learning rate, 500 for the training time and 0.1 for momentum applied to the weights. It was found that the models with a lower number of variables gave a lower error when using fewer neurons, the same that found Tetko *et al.* (1995). The best predictions were obtained with an ANN based on a single hidden layer of 3 to 5 neurons.

For each of the models obtained with MLR and ANN, 50 RMSE values were obtained using the 10-fold cross-validation method with five repetitions, with WEKA 3.6 software (Waikato University, Hamilton, New Zealand). The dataset with 50 RMSE values of each model was compared with the non-parametric Kruskal-Wallis test and Dunn's test with Bonferroni adjustment. The level of significance was 0.05.

Table 2.1. Summary of the study variables

Variable	units	Mean value	CV (%)
SLG	%	5.2	66.7
RG	mm	3.2	23.8
BS	%	10.4	147.0
WN	%	1.2	282.8
KAR	$\text{mm}^2 \cdot \text{mm}^{-2}$	0.25	70.1
MC	%	11.3	5.9
ρ	$\text{kg} \cdot \text{m}^{-3}$	549.5	7.1
V_U	$\text{m} \cdot \text{s}^{-1}$	4672	11.9
f_{LV}	Hz	999.9	13.0
f_{FV}	Hz	69.6	12.8
f_{EV}	Hz	99.0	11.6
MOE _U	MPa	7683	32.6
MOE _{LV}	MPa	8887	25.3
MOE _{FV}	MPa	8810	25.3
MOE _{EV}	MPa	8739	23.6
MOEs	MPa	7701	23.9

SLG: slope of grain, RG: rate of growth, BS: blue stain, WN: wanes, KAR: knot area ratio, MC: moisture content, ρ : density, V_U : velocity of ultrasounds, f_{LV} , f_{FV} , f_{EV} : longitudinal, flatwise and edgewise frequency respectively, MOE_U: modulus of elasticity by ultrasound, MOE_{LV}, MOE_{FV}, MOE_{EV}: modulus of elasticity by longitudinal, flatwise and edgewise vibration respectively, MOEs: static modulus of elasticity

2.4. Results and discussion

The values obtained for the different variables are shown in Table 2.1. In general, the MOEs values were lower than those obtained in previous studies with *Pinus sylvestris* (Arriaga *et al.* 2012; Hassan *et al.* 2013; Ranta–Maunus *et al.* 2011) or with other species of pine, including *Pinus pinaster* (Pommier *et al.* 2013), *Pinus nigra* (Arriaga *et al.* 2012; Íñiguez González *et al.* 2007), *Pinus brutia* (Guntekin *et al.* 2013), *Pinus radiata* (Arriaga *et al.* 2012 2014; García–Iruela *et al.* 2016; How *et al.* 2014) and southern pine (Wang *et al.* 2008). The values are also lower than those obtained in previous studies with different conifer species, including *Picea abies* (Larsson *et al.* 1998; Spycher *et al.* 2008), *Cryptomeria japonica*, *Taiwania cryptomerioides* and *Pseudotsuga menziesii* (Wang *et al.* 2008). In all these studies, the MOE_{dyn} and MOEs values were between 8900 MPa and 12700 MPa, except for the study on southern pine (Wang *et al.* 2008) which gave values between 14900 MPa and 16200 MPa. However, other authors obtained values with conifer species lower than those obtained in the present study, including *Picea sitchensis* (Simic *et al.* 2019), *Abies pinsapo* (García Esteban *et al.* 2009) and *Cupressus lusitanica* (Hodousek *et al.* 2016). In these cases, the MOE_{dyn} and MOEs values were between 5800 MPa and 8000 MPa. The MOEs values obtained were lower than the values found in most previous studies, though they cannot be considered atypical. The mean MOEs value obtained (7701 MPa) lies within the range of values included in the European classification system (European Standard EN 338 2016).

The mean values of the different MOE_{dyn} were similar (MOE_{U}) or slightly higher (between 13% and 15% for MOE_{LV} , MOE_{FV} and MOE_{EV}) than the mean MOEs values (Table 2.1). In general, the same trend was observed in studies by other authors, with the mean MOE_{dyn} value higher than that of the mean MOEs. In some cases, the difference was smaller, between 3% and 5% (Arriaga *et al.* 2012; Guntekin *et al.* 2013; Íñiguez González *et al.* 2007). While Wang *et al.* (2008) found differences of up to 9%, those recorded in another group of studies were as high as 19% (Arriaga *et al.* 2014; Hassan *et al.* 2013; Larsson *et al.* 1998; Pommier *et al.* 2013; Simic *et al.* 2019). Only Hodousek *et al.* (2016) obtained a mean MOE_{dyn} value lower than that of the MOEs (-11%).

The MOE_{EV} overestimated the MOEs by 13.5%, the MOE_{FV} by 14.4% and the MOE_{LV} by 15.4%, a trend also observed in the studies consulted. Arriaga *et al.* (2014) found in *Pinus radiata* that both the MOE_{EV} and the MOE_{LV} overestimated the MOEs by 14%. Ilic (2001) also observed in *Eucalyptus delegatensis* that the MOE_{EV} and MOE_{LV} overestimated the MOEs. Overestimation of the MOE_{LV} was higher than that of the

MOE_{EV}. Cho (2007) found in five Asian species that the MOE_{EV} and MOE_{LV} overestimated the MOEs, with overestimation of the MOE_{LV} (20%) higher in all cases than that of the MOE_{EV} (8%). Cheng and Hu (2011) found in *Populus tomentosa* that the MOE_{EV} overestimated the MOEs by 9% and the MOE_{LV} by 12%. Hassan *et al.* (2013) found in *Pinus sylvestris* that the MOE_{EV} overestimated the MOEs by 4%, the MOE_{LV} by 12% and the MOE_U by 19%. Baar *et al.* (2015) found in 5 African hardwood species that the MOE_{EV} overestimated the MOEs by 13%, the MOE_{LV} by 24% and the MOE_U by 41%. Chauhan and Sethy (2016) found in 8 hardwood species that both the MOE_{EV} and MOE_{LV} overestimated the MOEs. Hassan *et al.* (2013) explained the difference between the values of the MOE_{dyn} and the MOEs as being due to the influence of shear deflection in the bending test. To calculate the MOEs, they took into account this effect, significantly reducing the difference between the two MOE values. This correction was important because Hassan *et al.* (2013) performed the three point bending test. Ilic (2001) also performed the three point bending test and corrected the MOE_{EV} value taking into account shear deflection. In the present study, the four point bending test was carried out, in which the influence of shear deflection is lower. Another explanation for the difference between the MOEs and MOE_{dyn} values is based on the viscoelastic behaviour of the timber. When forces with a short duration are applied, timber exhibits an elastic behaviour, whereas with a long duration, the behaviour is like that of a viscous liquid. As the vibration tests had a very short duration compared to the static bending tests, the timber exhibited different types of behaviour in the two tests and, in consequence, different results were observed (Cho 2007; Halabe *et al.* 1997).

The R² values that were obtained for the relationship of the MOEs with the different MOE_{dyn} (Table 2.2) are similar to those found in previous studies with *Pinus sylvestris* (Arriaga *et al.* 2012; Hassan *et al.* 2013; Ranta–Maunus *et al.* 2011). Similar values are also found in studies with other pine species (Arriaga *et al.* 2012 2014; Guntekin *et al.* 2013; How *et al.* 2014; Íñiguez González *et al.* 2007), and with different conifer species, including Asian (Cho 2007; Wang *et al.* 2008), American (Barrett and Hong 2010; Wang *et al.* 2008) and European (Hodousek *et al.* 2016; Larsson *et al.* 1998) species. Likewise, studies made with different hardwood species have given similar values, for both temperate (Cho 2007; Ilic 2001; Nocetti *et al.* 2016), and tropical (Baar *et al.* 2015; Chauhan and Sethy 2016; Sales *et al.* 2011) species. The R² values were between 0.68 and 0.99 in the studies cited above. Only Liu *et al.* (2014) obtained noticeably lower R² values (of between 0.31 and 0.41) in tests performed with *Betula alleghaniensis* and *Acer saccharum*.

Table 2.2. Simple linear regression to predict the MOEs

Variable	Linear Regression Model (MPa)	R ²	RMSE (MPa) [CI] ⁽¹⁾	RMSE increase with respect to the lowest value (MOE _{EV})
SLG	MOEs = - 235.8 SLG + 8930	0.20	1632 [1508–1755]	390%
RG	MOEs = -1498 RG + 12567	0.40	1389 [1250–1529]	317%
BS	MOEs = 9.730 BS + 7600	0.01	1797 [1643–1952]	440%
WN	MOEs = 275.7 WN + 7379	0.25	1546 [1395–1697]	364%
KAR	MOEs = -4260.4 KAR + 8753	0.16	1649 [1500–1797]	395%
ρ	MOEs = 10.03 ρ + 2192	0.04	1788 [1647–1930]	437%
V_U	MOEs = 2.660 V_U - 4731	0.65	1051 [957–1144]	216%
f_{LV}	MOEs = 12.54 f_{LV} - 4834 ⁽²⁾	0.78	851 [781–920]	155%
f_{FV}	MOEs = 185.4 f_{FV} - 5201 ⁽²⁾	0.81	795 [741–848]	139%
f_{EV}	MOEs = 147.4 f_{EV} - 6897 ⁽²⁾	0.85	694 [639–749]	108%
MOE _U	MOEs = 0.563 MOE _U + 3371	0.59	1158 ^c [1057–1259]	248%
MOE _{LV}	MOEs = 0.782 MOE _{LV} + 757	0.91	544 ^b [504–585]	63%
MOE _{FV}	MOEs = 0.796 MOE _{FV} + 693	0.93	477 ^b [439–514]	43%
MOE _{EV}	MOEs = 0.876 MOE _{EV} + 45	0.97	333 ^a [307–359]	0%

a, b, c = values matched by the same letter do not differ significantly ($p = 0.05$)

⁽¹⁾confident interval at 95% confidence level

⁽²⁾equations only valid for samples with the same dimensions as the study

SLG: slope of grain, RG: rate of growth, BS: blue stain, WN: wanes, KAR: knot area ratio, ρ : density, V_U : velocity of ultrasounds, f_{LV} , f_{FV} , f_{EV} : longitudinal, flatwise and edgewise frequency respectively, MOE_U: modulus of elasticity by ultrasound, MOE_{LV}, MOE_{FV}, MOE_{EV}: modulus of elasticity by longitudinal, flatwise and edgewise vibration respectively, MOEs: static modulus of elasticity

The highest coefficient of determination in the SLR between the MOEs and MOE_{dyn} obtained by vibration was attained with the MOE_{EV} ($R^2 = 0.97$). In the case of the MOE_{FV} and the MOE_{LV}, the R^2 values worsened, decreasing by 4% and 6%, respectively (Table 2.2). Ilic (2001) found in *Eucalyptus delegatensis* that prediction of the MOEs on the basis of the MOE_{EV} had an 8% higher R^2 value than prediction on the basis of the MOE_{LV}, similar to the increase in the present study. Faydi *et al.* (2017) found in oak that prediction of the MOEs on the basis of the MOE_{EV} had a 9% higher R^2 value than prediction on the basis of the MOE_{LV} and a 12% higher value than with the MOE_{FV}. Hassan *et al.* (2013) found in *Pinus sylvestris* that prediction of the MOEs on the basis of the MOE_{EV} had an 18% higher R^2 value than prediction on the basis of the MOE_{LV}. In contrast, other studies have found smaller differences, Baar *et al.* (2015), Chauhan and Sethy (2016) and Larsson *et al.* (1998) found that prediction of the MOEs on the basis of the MOE_{EV} and the MOE_{LV} had similar

R^2 values, with differences of below 3%. Finally, Arriaga *et al.* (2014) found in *Pinus radiata* that prediction of the MOEs on the basis of the MOE_{EV} had a similar R^2 value to that made on the basis of the MOE_{LV} .

Table 2.3. Mean absolute error (MAE) of simple linear regression with dynamic MOE to predict the MOEs (MPa)

Variable	MAE observed MOE	MAE estimated MOE	MAE reduction
MOE_U	1390	906	35%
MOE_{LV}	1208	425	65%
MOE_{FV}	1110	387	65%
MOE_{EV}	1037	262	75%

MOE_U : modulus of elasticity by ultrasound, MOE_{LV} , MOE_{FV} , MOE_{EV} : modulus of elasticity by longitudinal, flatwise and edgewise vibration respectively

One of the advantages of knowing the MOE_{dyn} values is that they can be used for simple and rapid *in situ* prediction of the MOEs. To obtain any of the MOE_{dyn} , a mean time of 1.5 minutes (data collection and calculations) was required, while the mean time for the MOEs was 7 minutes. However, the results show clear overestimation. Despite a very high correlation, the MOE_{dyn} values obtained with vibration (Equations 2.1, 2.2 and 2.3) overestimated the MOEs value, with a MAE of above 1000 MPa (Table 2.3). This overestimation can easily be adjusted using a linear equation (Figure 2.2 for MOE_{EV}). The values estimated in this way show a clear decrease in the prediction error of the MOEs, with a noticeably lower MAE (75% for MOE_{EV}). If the estimated values are used rather than the corrected ones, the prediction errors that are made increase with the value of the MOEs that is being predicted.

With respect to the ultrasound technique, the R^2 value for the V_U used to predict the MOEs (0.65) was higher than the R^2 value for the MOE_U (0.59). That difference could have been an abnormal result, but the values in question were very similar and there were not statistically significant differences between them. The mean value of the MOE_U was similar to that of the MOEs. However, as a consequence of the high variability of the values, the MAE of the MOE_U were 34% larger than that of the MOE_{EV} (Table 2.3). Variability of the MOE_U was higher than that of the MOE_{EV} , as can be seen in the 38% difference in R^2 values (Table 2.2). Hassan *et al.* (2013) found similar values in *Pinus sylvestris*, with the variability of MOEs on the basis of the MOE_U presenting a 39% lower R^2 value than that of the prediction on the basis of the MOE_{EV} . Other authors have found

the same trend, though with smaller differences. Ranta–Maunus *et al.* (2011) found that in *Pinus sylvestris*, the MOEs prediction based on the MOE_U had a 10% lower R^2 value than that of the prediction based on the MOE_{EV} . Wang *et al.* (2008) found in four conifer species that variability of the MOEs on the basis of the MOE_U presented an 11% lower R^2 value than that of the prediction on the basis of the MOE_{EV} . Baar *et al.* (2015) found that variability of the MOEs on the basis of the MOE_U presented a 7% lower R^2 value than that of the prediction on the basis of the MOE_{EV} . Sales *et al.* (2011) also found in *Gouphia glabra* higher variability in the MOE_U than in the MOE_{EV} in the SLR to predict the MOEs, although the difference between the R^2 values was very low (1%). A further consequence of this variability is that there is only a very slight reduction of the MAE with the corrected MOE_U .

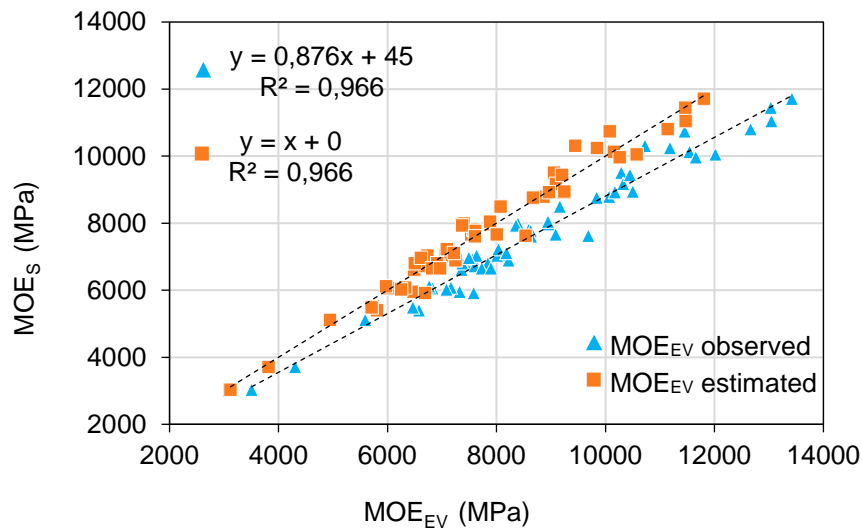


Figure 2.2. Correlation of the MOEs with the observed MOE_{EV} and with the MOE_{EV} estimated by linear regression to adjust overestimation.

A low correlation with the MOEs was found in the present study for the features (SLG, RG, BS, WN, KAR) and the density, as can be seen in the R^2 values (Table 2.2). For this reason, it is unadvisable to use either the features or the density to predict the MOEs using SLR. However, RG had a clearly higher R^2 value (0.40) than the rest, and could thus be useful in multivariate models. In the studies that have been consulted, the capacity of RG to predict the MOEs is dubious. Guntekin *et al.* (2013) found that annual ring width had a significant impact on their model to predict the MOEs in *Pinus brutia*. In contrast, Larsson *et al.* (1998) found in *Picea abies* that RG was not a good measure for stiffness.

SLG showed a weak correlation with MOEs (0.20); similar results were found to those reported by Mania *et al.* (2020) with slopes of grain between 0% and 9%. In the present study, a weak correlation ($R^2 = 0.04$) between density and the MOEs was found. Similar results have been observed in other studies: in Faydi *et al.* (2017) with oak ($R^2 = 0.09$), Simic *et al.* (2019) with *Picea sitchensis* ($R^2 = 0.18$) and Baar *et al.* (2015) with five African hardwood species ($R^2 = 0.23$). Other studies have shown higher R^2 values, but always with weak correlations: in Ranta–Maunus *et al.* (2011) with *Pinus sylvestris* ($R^2 = 0.50$), in Larsson *et al.* (1998) with *Picea abies* ($R^2 = 0.50$) and in Chauhan and Sethy (2016) with eight hardwood species ($R^2 = 0.45$). In the present study, the correlation between density and the MOEs was lower than in the other studies consulted. This may be due to the low variability in the density of the samples, with the lowest CV of all the study variables (7.1%). A low correlation was also found in the present study between the KAR and the MOEs, ($R^2 = 0.16$), although it was similar to that reported in Ranta–Maunus *et al.* (2011) with *Pinus sylvestris* ($R^2 = 0.25$). This result is in agreement with Arriaga *et al.* (2014) who found for *Pinus radiata* that the addition of knottiness to the prediction model of the MOEs on the basis of the MOE_{dyn} did not improve the R^2 value. Villasante *et al.* (2019) also observed that the inclusion of knottiness in the prediction model of the MOEs in *Pinus sylvestris* did not significantly decrease the RMSE.

The R^2 values were only used in the present study to allow a comparison with other studies made by different authors. We preferred to use the RMSE to assess the capacity of the different variables to predict the MOEs. In addition, the 10-fold cross-validation method was used with 5 repetitions to avoid overfitting.

Firstly, an analysis was made of the simple variables (V_U , f_{LV} , f_{FV} , f_{EV}). The results obtained (Table 2.2) showed statistically significant differences between their MOEs predictive capacities. The V_U variable had the highest mean RMSE value, higher than any of the vibration frequencies, and was therefore the variable with the weakest prediction capacity. With respect to the frequencies, f_{EV} and f_{FV} had the lowest mean RMSE values and with no statistically significant differences between them.

As for the compound variables (MOE_U , MOE_{LV} , MOE_{FV} , MOE_{EV}), the results show statistically significant differences between some of them (Table 2.2). The MOE_U had a significantly higher RMSE mean value than any of the other compound variables. As in the case of the simple variables, the edgewise flexural vibration test was the most suitable for MOEs prediction, as the MOE_{EV} variable had the significantly lowest RMSE mean value. The MOE_{LV} and the MOE_{FV} , had RMSE values somewhere in between (increase of

63% and 43% respectively with respect to the MOE_{EV} , with no statistically significant differences between them. Faydi *et al.* (2017) found a similar trend in oak, with the RMSE for the MOE_{LV} 24% higher than for the MOE_{EV} .

Table 2.4. Multiple linear regression to predict the MOEs, mean value and confident interval at 95% confidence level [in square brackets] of the RMSE

Regression Model	RMSE (MPa)
all variables	396 ^b [372–421]
$-33.793 \cdot \text{SLG} - 134.7937 \cdot \text{RG} + 0.823 \cdot \text{MOE}_{\text{EV}} + 1123.6$	323 ^a [301–343]
$-141.1613 \cdot \text{RG} + 0.8441 \cdot \text{MOE}_{\text{EV}} + 783.4$	333 ^a [310–356]
$0.8761 \cdot \text{MOE}_{\text{EV}} + 45.8$	333 ^a [307–359]

a, b = values matched by the same letter do not differ significantly ($p = 0.05$)

SLG: slope of grain, RG: rate of growth, MOE_{EV} : modulus of elasticity by edgewise vibration, MOEs: static modulus of elasticity

The MOE_{dyn} values obtained through the vibration tests (MOE_{EV} , MOE_{FV} , MOE_{LV}) predicted the MOEs better than the resonance frequencies (f_{EV} , f_{FV} , f_{LV}). The RMSE values of any of the vibration MOE_{dyn} were significantly lower than the RMSE values of any of the frequencies. This is because the MOE_{dyn} are compound variables which include the resonance frequency and other variables of the sample (Equations 2.1, 2.2 and 2.3).

The multivariate analysis was performed using MLR and ANN. The analysis with MLR (Table 2.4) showed that the inclusion of different variables in the model did not improve the result obtained with the MOE_{EV} . The RMSE values obtained with the models that included MOE_{EV} , RG and SLG did not show statistically significant differences to those obtained only with MOE_{EV} . In contrast, when all the variables were used, the RMSE value was significantly worse. The results obtained are in agreement with Faydi *et al.* (2017), who found that the multivariate models slightly improved (2%) the RMSE of an SLR based on the MOE_{EV} . Although they did not analyse the existence of significant differences, they did not find utility for the use of multivariate models. Villasante *et al.* (2019) found that the MLR model with two variables significantly improved the SLR model based on the longitudinal vibration velocity. The difference with the results of the present study may be due to the fact that the velocity offers less information than the MOE_{EV} and that only longitudinal vibration was considered, with lower predictive capacity than edgewise vibration. This difference can be seen in the RMSE values of the SLR models, 1206 MPa in Villasante *et al.* (2019) and 333 MPa in the present study. The analysis with

ANN (Figure 2.3) gave the same results, with no combination of variables offering an improvement over the RMSE value obtained with MOE_{EV} .

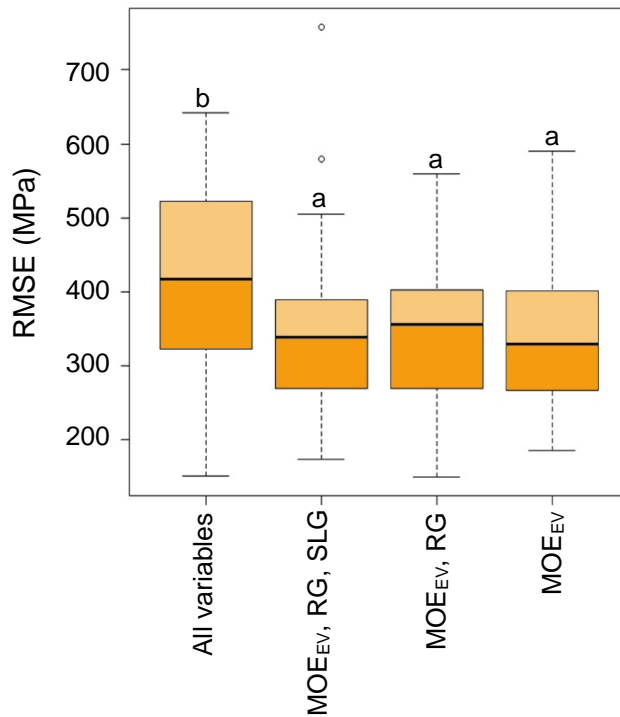


Figure 2.3. RMSE of the artificial neural network. a, b = values matched by the same letter do not differ significantly ($p = 0.05$)

Finally, it was verified that there were no statistically significant differences between the MLR and ANN results when using the same variables. Other authors have obtained a similar result. Villasante *et al.* (2019) found that the ANN-constructed model did not significantly improve the prediction of the MOEs made with the MLR-based model in *Pinus sylvestris*. Tanaka *et al.* (1996) found that the ANN-constructed model did not contribute to improving the prediction of the MOR made through linear regression in *Cryptomeria japonica*. Other authors, in contrast, have found improvements in ANN-constructed models. García-Iruela *et al.* (2016), working with ultrasound in *Pinus radiata*, found that the models made with ANN improved by 10% the R^2 of the SLR-based models, although they did not consider whether this difference was statistically significant. García Esteban *et al.* (2009), working with ultrasound in *Abies pinsapo* found that ANN-based models notably improved the R^2 of the MLR-based models (from 0.12 to 0.75). Although the R^2 value of the ANN was similar to that of the present study, the R^2 value of the MLR

was unusually low. Authors attributed this low value to the large amount of knots in the studied samples.

2.5. Conclusion

The results of the present study show the MOE_{dyn} obtained in the vibration tests (edgewise, flatwise and longitudinal) to be a good MOEs predictor, better than the timber features (slope of grain, rate of growth, blue stain, wanes and knot area ratio), the density and the ultrasound technique, as seen in the R^2 and RMSE values with a low error and high fit of data. Although all the MOE_{dyn} obtained in the vibration tests overestimate the MOEs value, this is easy to correct with a linear equation. The edgewise flexural vibration mode is a better MOEs predictor than the flatwise and longitudinal modes. The MOE_{EV} variable had the significantly lowest RMSE in the MOEs prediction. None of the multivariate models developed with MLR significantly reduced the RMSE obtained with the SLR model based on the MOE_{EV} . This model is the most suitable for its accuracy and simplicity.

The ANN-based models did not significantly improve the models generated using linear regressions.

Conflict of interest

On behalf of all authors, the corresponding author states that there is no conflict of interest.

2.6. References

- Alexander, D.L.J., Tropsha, A., Winkler, D.A. (2015) Beware of R^2 : Simple, Unambiguous Assessment of the Prediction Accuracy of QSAR and QSPR Models. *J. Chem. Inf. Model.* 55(7):1316–1322.
- Arriaga, F., Iñiguez-Gonzalez, G., Esteban, M., Divos, F. (2012) Vibration method for grading of large cross-section coniferous timber species. *Holzforschung* 66(3):381–387.
- Arriaga, F., Monton, J., Segues, E., Iñiguez-Gonzalez, G. (2014) Determination of the mechanical properties of radiata pine timber by means of longitudinal and transverse vibration methods. *Holzforschung* 68(3):299–305.
- ASTM Standard (2015) E1876–15 Standard Test Method for Dynamic Young's Modulus, Shear Modulus, and Poisson's Ratio by Impulse Excitation of Vibration. ASTM: West Conshohocken, PA, USA.
- Audacity Team (2015) Audacity®. Version 2.1.12. Audio editor and recorder. <http://audacityteam.org/>.

- Baar, J., Tippner, J., Rademacher, P. (2015) Prediction of mechanical properties – modulus of rupture and modulus of elasticity – of five tropical species by nondestructive methods. *Maderas–Cienc. Tecnol.* 17(2):239–252.
- Barrett, J.D., Hong, J.P. (2010) Moisture content adjustments for dynamic modulus of elasticity of wood members. *Wood Sci. Technol.* 44(3):485–495.
- Brancherieu, L., Bailleres, H. (2002) Natural vibration analysis of clear wooden beams: A theoretical review. *Wood Sci. Technol.* 36(4):347–365.
- Chauhan, S., Sethy, A. (2016) Differences in dynamic modulus of elasticity determined by three vibration methods and their relationship with static modulus of elasticity. *Maderas–Cienc. Tecnol.* 18(2):373–382.
- Cheng, F., Hu, Y. (2011) Reliability analysis of timber structure design of poplar lumber with nondestructive testing methods. *BioResources* 6(3):3188–3198.
- Cho, C.L. (2007) Comparison of three methods for determining Young's modulus of wood. *Taiwan Journal of Forest Science* 22(3):297–306.
- European Standard (2002a) EN 13183–1:2002. Moisture content of a piece of sawn timber. Part 1: Determination by oven dry method. European Committee for Standardization (CEN): Brussels, Belgium.
- European Standard (2002b) EN 13183–2:2002. Moisture content of a piece of sawn timber – Part 2: Estimation by electrical resistance method. European Committee for Standardization (CEN): Brussels, Belgium.
- European Standard (2012) EN 408:2010+A1:2012. Timber structures. Structural timber and glued laminated timber. Determination of some physical and mechanical properties. European Committee for Standardization (CEN): Brussels, Belgium.
- European Standard (2016) EN 338:2016. Structural timber. Strength classes. European Committee for Standardization (CEN): Brussels, Belgium.
- European Standard (2018) EN 1309–3:2018. Round and sawn timber – Methods of measurements – Part 3: Features and biological degradations. European Committee for Standardization (CEN): Brussels, Belgium.
- Faydi, Y., Brancherieu, L., Pot, G., Collet, R. (2017) Prediction of oak wood mechanical properties based on the statistical exploitation of vibrational response. *BioResources* 12(3):5913–5927.
- García Esteban, L., Fernández, F.G., De Palacios, P. (2009) MOE prediction in *Abies pinsapo* Boiss. timber: Application of an artificial neural network using non-destructive testing. *Comput. Struct.* 87(21–22):1360–1365.
- García-Iruela, A., Fernández, F.G., García Esteban, L., De Palacios, P., Simón, C., Arriaga, F. (2016) Comparison of modelling using regression techniques and an artificial neural network for obtaining the static modulus of elasticity of *Pinus radiata* D. Don. timber by ultrasound. *Compos. Part B–Eng.* 96:112–118.

- Guntekin, E., Emiroglu, Z., Yilmaz, T. (2013) Prediction of bending properties for Turkish Red Pine (*Pinus brutia* Ten.) Lumber using stress wave method. *BioResources* 8(1):231–237.
- Halabe, U.B., Bidigalu, G.M., GangaRao, H.V.S., Ross, R.J. (1997) Nondestructive evaluation of green wood using stress wave and transverse vibration techniques. *Mater. Eval.* 55(9):1013–1018.
- Hashim, U.R., Hashim, S.Z.M., Muda, A.K. (2016) Performance evaluation of multivariate texture descriptor for classification of timber defect. *Optik* 127(15):6071–6080.
- Hassan, K.T.S., Horacek, P., Tippnera, J. (2013) Evaluation of stiffness and strength of Scots pine wood using resonance frequency and ultrasonic techniques. *BioResources* 8(2):1634–1645.
- Hodousek, M., Dias, M., Martins, C., Marques, A., Böhm, M. (2016) Comparison of non-destructive methods based on natural frequency for determining the modulus of elasticity of *Cupressus lusitanica* and *Populus x canadiensis*. *BioResources* 12(1):270–282.
- How, S.S., Williamson, C.J., Carradine, D., Tan, Y.E., Cambridge, J., Pang, S. (2014) Predicting the young's modulus of defect free radiata pine shooks in finger-jointing using resonance frequency. *Maderas–Cienc. Tecnol.* 16(4):435–444.
- Ilic, J. (2001) Relationship among the dynamic and static elastic properties of air-dry *Eucalyptus delegatensis* R. Baker. *Holz Als Roh–und Werkst.* 59(3):169–175.
- Íñiguez González, G., Arriaga Martítegui, F., Esteban Herrero, M., Argüelles Alvarez, R. (2007) Los métodos de vibración como herramienta no destructiva para la estimación de las propiedades resistentes de la madera aserrada estructural [Vibration methods as non-destructive tool for structural properties assessment of sawn timber]. *Inf. Constr.* 59(506):97–105.
- Larsson, D., Ohlsson, S., Perstorper, M., Brundin, J. (1998) Mechanical properties of sawn timber from Norway spruce. *Holz Als Roh–Und Werkst.* 56(5):331–338.
- Lever, J., Krzywinski, M., Altman, N. (2016) Model selection and overfitting. *Nat. Methods*. 13(9):703–704.
- Liu, Y., Gong, M., Li, L., Chui, Y.H. (2014) Width effect on the modulus of elasticity of hardwood lumber measured by non-destructive evaluation techniques. *Constr. Build. Mater.* 50:276–280.
- Mania, P., Siuda, F., Roszyk, E. (2020) Effect of slope grain on mechanical properties of different wood species. *Materials* 13:1503.
- Nocetti, M., Brunetti, M., Bacher, M. (2016) Efficiency of the machine grading of chestnut structural timber: prediction of strength classes by dry and wet measurements. *Mater. Struct.* 49(11):4439–4450.
- Pardos, J.A., Werner, L., Günter, W. (1990) Morphological and Chemical Aspects of *Pinus sylvestris* L. from Spain. *Holzforschung* 44(2):143–146.

- Pommier, R., Breysse, D., Dumail, J.F. (2013) Non-destructive grading of green Maritime pine using the vibration method. *Eur. J. Wood Prod.* 71(5):663–673.
- R Core Team (2019) R: A language and environment for statistical computing. Version 3.6.1. R Foundation for Statistical Computing, Vienna, Austria. <http://www.R-project.org/>.
- Ranta-Maunus, A., Denzler, J.K., Stapel, P. (2011) Strength of European timber. Part 2. Properties of spruce and pine tested in Gradewood project. VTT Technical Research Centre of Finland. VTT Working Papers, No. 179. <http://www.vtt.fi/inf/pdf/workingpapers/2011/W179.pdf>.
- Refaeilzadeh, P., Tang, L., Liu, H. (2009) Cross-Validation. In Liu L and Özsü MT (Eds.), *Encyclopedia of Database Systems*. Springer US: Boston, USA.
- Sales, A., Candian, M., De Salles Cardin, V. (2011) Evaluation of the mechanical properties of Brazilian lumber (*Gouania glabra*) by nondestructive techniques. *Constr. Build. Mater.* 25(3):1450–1454.
- Sandoz, J.L. (1989) Grading of construction timber by ultrasound. *Wood Sci. Technol.* 23(1):95–108.
- Simic, K., Gendvilas, V., O'Reilly, C., Harte, A.M. (2019) Predicting structural timber grade—determining properties using acoustic and density measurements on young Sitka spruce trees and logs. *Holzforschung* 73(2):139–149.
- Spycher, M., Schwarze F.W.M.R., Steiger, R. (2008) Assessment of resonance wood quality by comparing its physical and histological properties. *Wood Sci. Technol.* 42(4):325–342.
- Tanaka, T., Tanaka, T., Nagao, H., Kato, H. (1996) A preliminary investigation on evaluation of strength of soft wood timbers by neural network. Proceeding of the 10th International Symposium on Nondestructive Testing of Wood, Lausanne, Switzerland.
- Tetko, I.V., Livingstone, D.J., Luik, A.I. (1995) Neural Network Studies. 1. Comparison of Overfitting and Overtraining. *J. Chem. Inf. Comput. Sci.* 35(5):826–833.
- Villasante, A., Iñiguez-Gonzalez, G., Puigdomenech, L. (2019) Comparison of various multivariate models to estimate structural properties by means of non-destructive techniques (NDTs) in *Pinus sylvestris* L. timber. *Holzforschung* 73(4):331–338.
- Waikato University (2014) WEKA software. Version 3.6.12. Waikato University, Hamilton, New Zealand. <https://www.cs.waikato.ac.nz/ml/weka/>.
- Walker, J. (1993) Primary Wood Processing: Principles and Practice. Chapman & Hall: London, UK.
- Wang, S.Y., Chen, J.H., Tsai, M.J., Lin, C.J., Yang, T.H. (2008) Grading of softwood lumber using non-destructive techniques. *J. Mater. Process. Tech.* 208(1–3):149–158.
- Weaver, W., Timoshenko, S., Young, D.H. (1990) Vibration problems in engineering. Wiley: New York, USA.

CAPÍTULO 3

MOR prediction

Fernández-Serrano, Á., Villasante, A. (2022) Modulus of Rupture Prediction in *Pinus sylvestris* with Multivariate Models Constructed with Resonance, Ultrasound, and Wood Heterogeneity Variables. BioResources 17(1):1106–1119.
DOI: 10.15376/biores.17.1.1106-1119.

3. Modulus of rupture prediction in *Pinus sylvestris* with multivariate models constructed with resonance, ultrasound, and wood heterogeneity variables

3.1. Abstract

Multivariate models with multiple linear regression (MLR), artificial neural network (ANN), and k–nearest neighbors (KNN) were developed to predict the modulus of rupture of *Pinus sylvestris* structural timber. The aim of this study was to develop and compare these models obtained from resonance and ultrasound tests, static modulus of elasticity tests, and different measured wood feature. Resonance tests were performed in the three vibration modes (edgewise, flatwise, and longitudinal) to obtain the fundamental resonant frequencies. To compare the goodness-of-fit of the different models, the 10-fold cross-validation method was used, which proved to be an adequate strategy to avoid overfitting. The variable with the best predictive capacity of the modulus of rupture was knottiness. The error was notably lower in the multivariate than the univariate models. The ANN and KNN algorithms showed no improvement over the MLR. The most suitable MLR for prediction of the modulus of rupture was the model with four variables: knottiness, edgewise dynamic modulus of elasticity, velocity of ultrasounds, and longitudinal resonant frequency.

Keywords: cross-validation; k–Nearest neighbors; neural network; non-destructive testing; resonant frequency

3.2. Introduction

Resonant frequencies have been employed to determine bending strength with *Pinus sylvestris*. Most of the works (Arriaga *et al.* 2012; Hassan *et al.* 2013; Aira *et al.* 2019) only used one vibration mode (edgewise, flatwise, or longitudinal) to predict the modulus of rupture (MOR). Only a few used more than one vibration mode (Hassan *et al.* 2013; Arriaga *et al.* 2014; Dahlen *et al.* 2018). Likewise, few studies have used a combination of vibration and ultrasound techniques (Halabe *et al.* 1997; Hassan *et al.* 2013). Some authors have analysed the effect on the MOR of features of sawn timber such as knots (Arriaga *et al.* 2014; França *et al.* 2019; Villasante *et al.* 2019), the slope of grain (Arriaga *et al.* 2014), or the rate of growth (Martins *et al.* 2017; França *et al.* 2019).

Some studies have taken into account the combined effect of different variables, while using multiple linear regression (MLR) for MOR prediction, with different pine species (Arriaga *et al.* 2012; Martins *et al.* 2017; Villasante *et al.* 2019). Usually, the coefficient of determination (R^2) is used to compare the model's capacity to predict MOR. However, some authors proposed use of the root-mean-square error (RMSE) as a more suitable measure of the fit of the model (Pommier *et al.* 2013; Yang *et al.* 2017; Villasante *et al.* 2019).

Most of the works consulted employed linear regressions, though some authors proposed nonlinear regressions based on artificial neural networks (ANNs). In some cases, prediction of the mechanical properties of wood through ANN has given good results (Mansfield *et al.* 2007; García Esteban *et al.* 2009; Fathi *et al.* 2020); however, in others no improvements over MLR-based models were found when using ANN-based models (Tanaka *et al.* 1996; Villasante *et al.* 2019)

Multivariate analysis can be affected by overfitting, producing misleading models valid only for the used dataset. To avoid overfitting (Lever *et al.* 2016), a few authors employed the cross-validation method in studies on pine (Villasante *et al.* 2019), chestnut (Vega *et al.* 2012), poplar (Fathi *et al.* 2020), and oak (Faydi *et al.* 2017).

The aim of this study was to develop and compare multivariate (linear, and non-linear) models for MOR prediction of a batch of *Pinus sylvestris* timber. These models were developed based on the values of different variables obtained in resonance and ultrasound tests and different measured features (blue stain, rate of growth, slope of grain, resin pockets, knottiness, and wanes). Models were compared using RMSE values obtained with the cross-validation method. This study also aimed to find the variables that best explained the MOR. Grading of *Pinus sylvestris* timber from Montsec mountains (Spain) was not an objective of this work.

3.3. Experimental

3.3.1. Materials

Analyses were undertaken with samples of *Pinus sylvestris* from Montsec Range (NE of Spain) obtained from a local sawmill (Lleida, Spain). A total of 69 sawn wood samples were obtained by random sampling of timber stored at the sawmill. The nominal sample size was 70 mm × 100 mm × 2000 mm with different growth rings orientations. At the laboratory, 12 samples with bark pockets or rot were rejected, leaving a final total of 57

samples. The samples were stored in the test laboratory and subjected to periodic moisture content (MC) analyses using a wood moisture meter (Hydromette HB 30, GANN, Gerlingen, Germany) following European Standard EN 13183–2 (2002b). The samples were removed from the drying process when they reached a constant weight ($\pm 0.1\%$ in 6 h), in accordance with European Standard EN 408:2011+A1 (2012). Final moisture was calculated using the oven dry method following European Standard EN 13183–1 (2002a), with 20-mm-thick slices obtained from similar specimens that were not included in the test batch.

3.3.2. Methods

Resonance tests

The resonance tests were conducted following ASTM Standard E1876 15 (2015). The specimens were suspended using elastic cords situated in the nodes corresponding to the fundamental flexural resonance (Figure 3.1) and were tapped in the centre of the edge, face, and end to obtain the three vibration modes: edgewise, flatwise, and longitudinal, respectively. A 22.7 g impulser was used, consisting of a 230 mm long \times 4 mm diameter wooden handle with a 26-mm diameter glass marble at the tip. The vibration was registered using a microphone with cardioid polar pattern and frequency range of 20 Hz to 20 kHz (Rode NT-USB, Rode Microphones, Silverwater, Australia). The signal obtained was recorded and analysed with Audacity® (2015) (Audacity Team, Pittsburgh, PA, USA). A project sampling rate of 384 kHz and resolution of 24 bits were used for the recording. The frequency spectrum was analysed with the Hann function to obtain the fundamental resonant frequencies for the longitudinal (f_{LV}), flatwise (f_{FV}), and edgewise (f_{EV}) vibration modes.

On the basis of the frequencies, the corresponding MOE_{dyn} were obtained through the following Equations 3.1 through 3.3 (Weaver *et al.* 1990),

$$MOE_{LV} = 4 \times (f_{LV})^2 \times L^2 \times \rho \quad (3.1)$$

$$MOE_{FV} = [48 \times \pi^2 \times \rho \times (f_{FV})^2 \times L^4] / [4.73^4 \times b^2] \quad (3.2)$$

$$MOE_{EV} = [48 \times \pi^2 \times \rho \times (f_{EV})^2 \times L^4] / [4.73^4 \times h^2] \quad (3.3)$$

where MOE_{LV} , MOE_{FV} , and MOE_{EV} are the dynamic modulus of elasticity (all expressed in MPa) for each type of vibration (longitudinal, flatwise, and edgewise, respectively), f_{LV} , f_{FV} , and f_{EV} are the fundamental resonant frequencies (kHz) for each type of vibration, ρ is the density (g mm^{-3}) of the sample; L , h , and b are the actual length,

width, and thickness (all expressed in mm) of each sample, respectively. The effect of shear in the MOE_{dyn} calculation was not taken into account because it had a reduced influence, as the ratios L/b and L/h were equal to or greater than 20 (Arriaga *et al.* 2014).

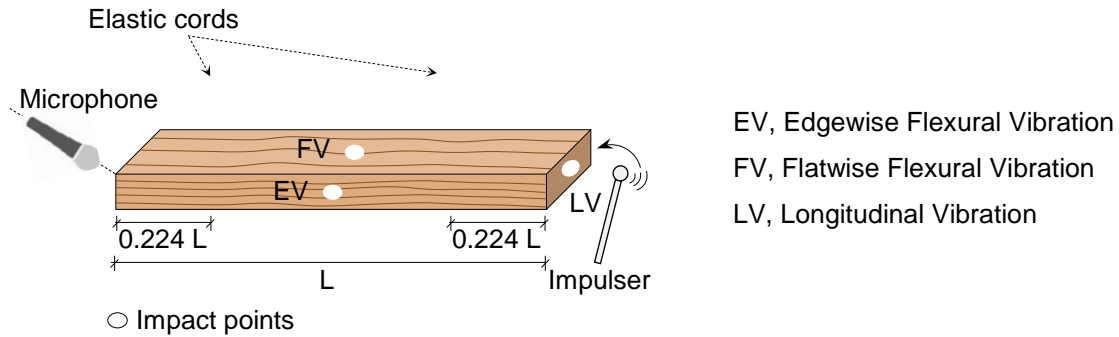


Figure 3.1. Scheme of the resonant frequencies tests

Ultrasounds tests

The ultrasounds tests were performed with a Sylvatest Duo ultrasound device with a frequency of 22 kHz (Concept Bois Structure, Montandon, France). The transducers were placed at the ends of the samples. Information about species, length, and MC of each sample had to be introduced in the ultrasounds device. After the test, the device's screen showed the velocity of ultrasound waves (V_U), the attenuation of the ultrasonic wave (peak_U), the modulus of elasticity by ultrasound (MOE_U), and the modulus of rupture by ultrasound (MOR_U).

Features and biological degradations

The samples were measured and weighed to obtain their dimensions and density following European Standard EN 408:2011+A1 (2012). The blue stain (BS), rate of growth (RG), slope of grain (SLG), and resin pockets were also measured in accordance with the procedure outlined in European Standard EN 1309–3 (2018).

Two different procedures were used for knot measurement. The first procedure (Figure 3.2a) was based on the knot area ratio (KAR). The second one (Figure 3.2b) was based on Annex A of European Standard EN 1309–3 (2018). The KAR indicates the proportion of the cross-section occupied by knots (Walker 1993), while MKAR (Figure 3.2a) indicates the proportion of the margin cross-section (outer quarters) occupied by knots (Lam *et al.* 2005). The MKAR in compression (MKARc) refers to the outer quarter

subjected to compression, and the MKAR in tension (MKAR_T) denotes to the outer quarter subjected to tension. The KAR-based measurements were made in the centre third of the length of the sample, in the section where the KAR values were higher.

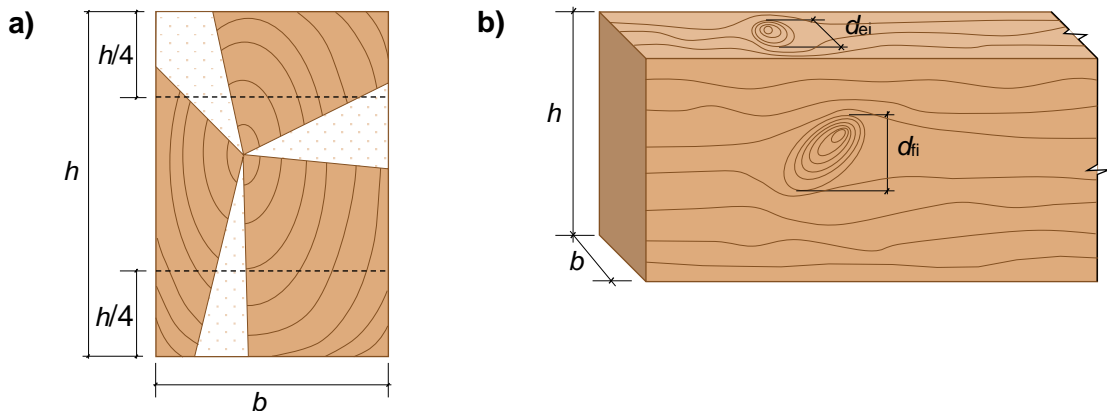


Figure 3.2. Scheme for the measurement of knottiness: a) Cross-section, KAR, MKAR, MKARc, and MKAR_T). The dotted areas represent knots; b) Measure of knots following Annex A of European Standard EN 1309–3 (2018)

The knottiness was also measured following the procedure set out in Annex A of European Standard EN 1309–3 (2018), measuring each knot in the direction perpendicular to the length of the sample (Figure 3.2b). For the variable knot_r, the sum of the measurements of knots in the four faces was calculated. For the variable knot_{1/3}, only the knots situated in the centre third of length of the sample were included.

Two procedures were also followed to measure the waness. The procedure described in European Standard EN 1309–3 (2018) was performed first (see Figure 3.3). The wane was evaluated as the highest ratio of the dimension of the wane on the face with respect to the complete dimension of the face (WN_F). The same procedure was performed with respect to the edge (WN_E). The mean of these two values was also calculated (WN_M). These same measurements were also taken exclusively in the centre third of the length of the sample (WN_{F1/3}, WN_{E1/3}, and WN_{M1/3}). The second procedure was to measure the waness with the loss of volume with respect to the theoretical volume without waness (WN_{VOL}).

Static bending test

The samples were subjected to a four point static bending test following European Standard EN 408:2011+A1 (2012). This test was performed to obtain the global static

modulus of elasticity (MOEs) and the MOR. The tests were completed with a 50-kN universal testing machine (Cohiner, Lleida, Spain) and data acquisition with LabVIEW 7.1 (National Instruments, Austin, TX, USA). The distance between supports was 1.8 m and the distance between load points was 0.6 m. A displacement transducer was placed at the midpoint between the two supports. After the bending test, a 20-mm-thick slice was obtained close to the area of rupture to determine moisture content using the oven dry method following European Standard EN 13183–1 (2002).

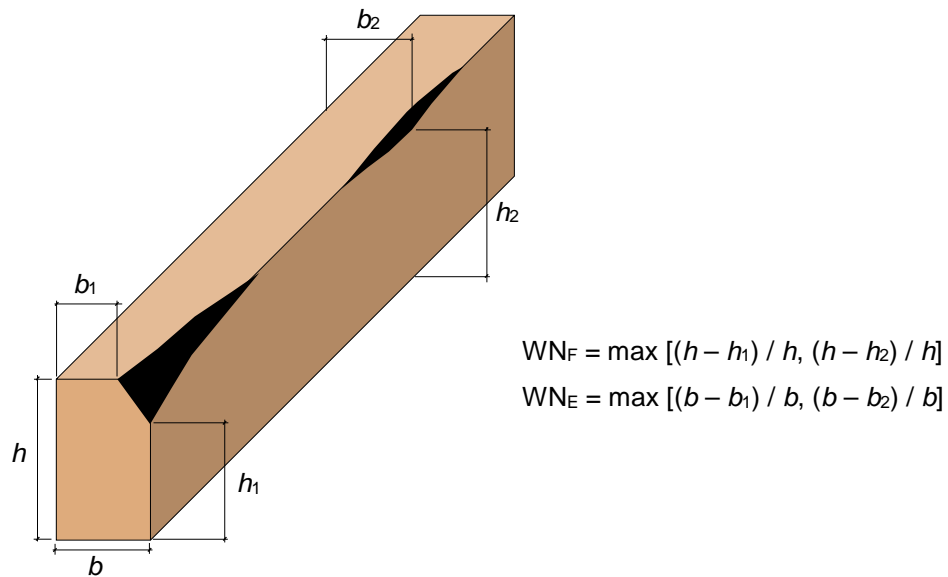


Figure 3.3. Measure of wanes following EN 1309–3 (2018)

Statistical analyses

Simple linear regressions (SLR) were developed to predict the MOR from each of the studied variables. The significance level for each variable was calculated with F-test. In the present work, the RMSE (Equation 3.4) was used to compare the fit of the MOR prediction models.

$$RMSE = \sqrt{\frac{\sum_{i=1}^n (\widehat{MOR}_i - MOR_i)^2}{n}} \quad (3.4)$$

where \widehat{MOR}_i is the predicted value from non-destructive testing (NDT), MOR_i is the observed value with European Standard EN 408:2011+A1 (2012), and n the number of observations.

To evaluate the usefulness of a prediction model, it is more important to know the precision of the values that it generates (RMSE) than to quantify the variability (R^2) of the predicted values (Mansfield *et al.* 2007; Alexander *et al.* 2015). The R^2 value obtained with the whole dataset was used exclusively to compare the results with those of other authors. The MOR prediction was also carried out using multivariate models with different algorithms: multiple linear regression (MLR), artificial neural network (ANN), and k-nearest neighbors (KNN). For the multivariate algorithms, the variables that did not present a statistically significant SLR were discarded. Similarly, only one knottiness and one wane variable were selected.

For the MLR, a greedy selection method was applied using the Akaike information metric to reduce the number of variables (Frank *et al.* 2016). A stepwise regression method was then applied, removing one-by-one the variables that caused the lowest increase in the RMSE until a univariate model was obtained. The predictive capacity of the three multivariate algorithms was compared for each group of variables.

The ANN prediction model was generated with the WEKA software (Waikato University, version 3.6, Hamilton, New Zealand). A multilayer perceptron was used with sigmoid nodes and learning by backpropagation (Frank *et al.* 2016). The ANN parameters were adjusted in a prior test (learning rate, training time, momentum applied to the weights, and number of neurons).

Finally, a prediction model was also generated using a KNN model with the IBk algorithm in WEKA software. The KNN model is a non-parametric classification method that constructs a regression from the weighted average of the values of KNN (Frank *et al.* 2016). The KNN parameters were adjusted in a prior test (number of neighbor values and distance weighting method).

The prediction models generated for a dataset can be affected by overfitting. This effect appears when the model is fitted even to the noise of the sample, confusing the noise with the internal structure of the model (Lever *et al.* 2016). For small datasets, the K-fold cross-validation can help avoid overfitting (Lever *et al.* 2016). In this respect, according to Tetko *et al.* (1995), the cross-validation method avoids overfitting in complex predictive models.

The 10-fold cross-validation method (Hashim *et al.* 2016; Faydi *et al.* 2017; Villasante *et al.* 2019) was used to calculate the RMSE of the models. The samples were randomly distributed into ten groups or folds, using each group to validate the model generated with the remaining nine. Using the WEKA software, this procedure was repeated 5 times to

obtain 50 RMSE values of each model (MLR, ANN, and KNN). The nonparametric Kruskal–Wallis test was used to detect significant differences between the RMSEs of the models. In those cases in which significant differences were detected, a post hoc analysis was performed with Dunn’s test and Bonferroni adjustment (Brunetti *et al.* 2016). A significance level of 0.05 was applied. The analysis of significant differences was performed using R–software (The R Foundation, version 3.6.1, Vienna, Austria).

3.4. Results and discussion

The values obtained for the measured variables are shown in Table 3.1. The mean MOR value (40.0 MPa) was similar to those obtained in previous studies (between 35 and 45 MPa) for *Pinus sylvestris* (Arriaga *et al.* 2012; Villasante *et al.* 2019) and other pine species, including *Pinus radiata* (Arriaga *et al.* 2014), *Pinus nigra* (Íñiguez González *et al.* 2007; Arriaga *et al.* 2012), and southern pine (Yang *et al.* 2017).

3.4.1. Simple linear regression

For most of the variables in this study, a statistically significant correlation, though weak, was found for the MOR prediction while using a SLR (Table 3.1). In this work, the R^2 value was used only to facilitate a comparison with results obtained by other authors in previous studies. The R^2 values for the variables of knottiness were similar or slightly higher than those observed in previous studies with different pine species (Conde García *et al.* 2007; Arriaga *et al.* 2014; França *et al.* 2019). In addition, the R^2 values for the different MOE_{dyn} were similar to those found by other authors in different pine species (Pommier *et al.* 2013; Arriaga *et al.* 2014; França *et al.* 2019).

Table 3.2 contains the RMSE results obtained through the 10–fold cross-validation method with 5 repetitions. The variables that did not present a statistically significant SLR were excluded. In this sense, the 29 initial variables were reduced to 15.

For knot–based MOR prediction, no significant differences were observed between the RMSE of the different measurement methods employed (KAR based or European Standard EN 1309–3 (2018)–based), except for MKARc that gave a worse predictive capacity than the rest (Table 3.1). Conde Garcia *et al.* (2007) in *Pinus sylvestris* and *Pinus nigra* and França *et al.* (2019) in southern pine also found small differences in the R^2 values between different knottiness variables and MOR. In the present study, the variable knott was chosen because it is easier to measure than any of the KAR–based variables.

Table 3.1. Summary of the Study Variables (Regression with the Whole Dataset)

Variable	Units	Mean Value	CV (%)	Linear Regression Model (MPa)	R ²	SSD ⁽¹⁾
Features						
SLG	%	5.2	66.6	MOR = - 1.702 · SLG + 48.90	0.14**	
RG	mm	3.2	23.8	MOR = - 11.29 · RG + 76.70	0.31***	
BS	%	10.4	147.0	MOR = - 0.085 · BS + 40.920	0.01ns	
WN _E	mm · mm ⁻¹	0.08	179.1	MOR = 44.42 · WN _E + 36.629	0.15**	w-a
WN _{E1/3}	mm · mm ⁻¹	0.04	236.5	MOR = 48.15 · WN _{E1/3} + 37.978	0.10*	w-a
WN _F	mm · mm ⁻¹	0.05	181.3	MOR = 61.56 · WN _F + 37.200	0.11*	w-a
WN _{F1/3}	mm · mm ⁻¹	0.03	242.4	MOR = 74.17 · WN _{F1/3} + 38.054	0.09*	w-a
WN _M	mm · mm ⁻¹	0.06	176.1	MOR = 54.24 · WN _M + 36.706	0.14**	w-a
WN _{M1/3}	mm · mm ⁻¹	0.03	235.9	MOR = 59.81 · WN _{M1/3} + 37.958	0.10*	w-a
WN _{VOL}	%	1.17	282.8	MOR = 2.068 · WN _{VOL} + 37.615	0.19***	w-a
resin	mm	21.7	225.3	MOR = - 0.072 · RES + 41.592	0.05ns	
knot _T	mm	283.4	59.1	MOR = - 0.066 · knot _T + 58.826	0.51***	k-a
knot _{1/3}	mm	77.9	79.1	MOR = - 0.169 · knot _{1/3} + 53.219	0.45***	k-a
KAR	mm ² · mm ⁻²	0.25	70.1	MOR = - 64.00 · KAR + 56.090	0.52***	k-a
MKAR	mm ² · mm ⁻²	0.25	80.1	MOR = - 56.61 · MKAR + 54.177	0.53***	k-a
MKAR _C	mm ² · mm ⁻²	0.23	114.5	MOR = - 26.25 · MKAR _C + 46.115	0.20***	k-b
MKAR _T	mm ² · mm ⁻²	0.27	95.2	MOR = - 41.34 · MKAR _T + 51.070	0.45***	k-a
ρ	kg · m ⁻³	549.5	7.1	MOR = 0.120 · ρ - 25.758	0.09*	
Simple Vibration Variables						
V_U	m · s ⁻¹	4672	11.9	MOR = 0.010 · V_U - 4.390	0.12**	
peak _U	mV	406.8	25.2	MOR = 0.010 · peak _U + 35.974	0.004 ns	
f_{LV}	Hz	999.9	13.0	MOR = 0.063 · f_{LV} - 22.712	0.27***	
f_{FV}	Hz	69.6	12.8	MOR = 0.941 · f_{FV} - 25.431	0.29***	
f_{EV}	Hz	99.0	11.6	MOR = 0.749 · f_{EV} - 34.080	0.30***	
Compound Variables						
MOE _U	MPa	7683	32.6	MOR = 0.002 · MOE _U + 24.252	0.11*	
MOR _U	MPa	15.0	50.7	MOR = 0.708 · MOR _U + 29.415	0.12**	
MOE _{LV}	MPa	8887	25.3	MOR = 0.004 · MOE _{LV} + 0.799	0.40***	
MOE _{FV}	MPa	8810	25.3	MOR = 0.004 · MOE _{FV} + 1.139	0.40***	
MOE _{EV}	MPa	8739	23.6	MOR = 0.005 · MOE _{EV} - 3.844	0.44***	
MOEs	MPa	7701	23.9	MOR = 0.006 · MOEs - 3.216	0.44***	
MOR	MPa	40.0	39.0			

⁽¹⁾Statistical Significant Differences. The same letter (a or b) indicates there are no statistically significant differences between the RMSE values in MOR prediction based on wanes (w) or knots (k)

*** significant at 0.001 level, ** significant at 0.01 level, * significant at 0.05 level, ns not significant (F-test)

SLG: slope of grain; RG: rate of growth; BS: blue stain; WN: wanes; KAR: knot area ratio; MKAR: margin knot area ratio; ρ : density; V_U : velocity of the ultrasounds; peak_U: attenuation of the ultrasounds; f : frequency

With respect to the different methods used to measure the influence of wanes, no statistically significant differences were observed between the RMSE values in MOR prediction (Table 3.1). The variable WN_M was chosen because it was easier to measure than the loss of volume.

Table 3.2. RMSE of the Simple Linear Regressions for MOR Prediction (10-fold cross-validation, 5 repetitions)

Variable	RMSE (MPa)
Features Group	
SLG	14.07 ^b
RG	12.78 ^{ab}
WN_M	14.54 ^b
knott	10.59 ^a
ρ	14.86 ^b
Simple Vibration Variables Group	
V_U	14.40 ^a
f_{LV}	13.18 ^a
f_{FV}	13.10 ^a
f_{EV}	12.97 ^a
Compound Variables Group	
MOE_U	14.54 ^c
MOR_U	14.44 ^{bc}
MOE_{LV}	11.95 ^{ab}
MOE_{FV}	12.11 ^{ab}
MOE_{EV}	11.66 ^a
$MOEs$	11.71 ^a

Within each group of variables, the same letter indicates there are no statistically significant differences (Kruskal–Wallis test, Dunn's test and Bonferroni adjustment).

SLG: slope of grain; RG: rate of growth; WN: wanes; ρ : density; V_U : velocity of the ultrasounds; f : frequency

With respect to the variables included in the group of features and biological degradations, it was found that knott and RG provided the lower RMSE values in MOR prediction (Table 3.2). Various authors have also found in different conifers that knottiness is a good MOR predictor, better than density (Conde García *et al.* 2007) and better than SLG (Zhou & Smith 1991). According to Zhou and Smith (1991), RG was also a good MOR predictor. However, other studies conducted with different pine species found that density was a better MOR predictor than other characteristics such as knottiness and

RG (Carballo *et al.* 2009; França *et al.* 2019). The RMSE values obtained for RG (12.8 MPa) and for density (14.9 MPa) are higher than those obtained by Hautamäki *et al.* (2014) in *Pinus sylvestris* (9.8 MPa and 10.2 MPa, respectively). These differences may be due to the heterogeneity of timber from such distant sources. It is notable, however, that the RMSE of knot_T (10.6 MPa) was practically the same as that obtained by Hautamäki *et al.* (2014) for KAR (10.4 MPa).

In the simple vibration variables for MOR prediction, no statistically significant differences were found between the RMSE values obtained from V_U and the three resonance frequencies (f_{LV} , f_{FV} , and f_{EV}). In the compound variables, it was found that the ultrasound-based variables (MOE_U and MOR_U) had the highest errors, while MOEs and MOE_{EV} gave the best MOR predictions. The RMSE value obtained for MOR prediction with MOEs (11.71 MPa) was similar to those obtained by Pommier *et al.* (2013) in *Pinus pinaster* (13.9 MPa), Yang *et al.* (2017) in southern pine (14.65 MPa), and Hautamäki *et al.* (2014) in *Pinus sylvestris* (8.20 MPa). The RMSE values for MOE_{dyn} calculated on the basis of SLR with the resonance tests (MOE_{LV}, MOE_{FV}, and MOE_{EV}) were between 11.66 MPa and 12.11 MPa, which were similar to those obtained by Pommier *et al.* (2013) and by Yang *et al.* (2017) in different pine species (12.5 MPa and 14.65 MPa, respectively).

3.4.2. Multiple linear regression

Including different variables should improve the fit of the model. A comparison of the RMSE values obtained in the univariate and multivariate linear regressions is shown in Table 3.3. To show overfitting, the RMSE calculated with the whole dataset, without cross-validation, is also provided in the table. It can be seen that this overfitted RMSE decreases constantly as the number of variables increases. However, this decrease is the result of the model being fitted to the noise of the dataset and therefore becoming an overfitted model. This can be verified in the fact that the RMSE calculated with 10-fold cross-validation initially decreases as variables are added to the model, but then subsequently increases. These results confirm that the cross-validation method is a good strategy to avoid overfitting.

Starting with a SLR with knot_T, the inclusion of a new variable in the model resulted in important RMSE decrease in MOR prediction, reaching 17.9% in the model with 4 variables. However, the models with 5 or 6 variables added small decreases in the RMSE that were below 1% (with no statistically significant differences). With 7 or more variables the RMSE values began to increase indicating that these new variables added to the model

were redundant. The model that obtained the lowest RMSE value was the MLR with 6 variables (8.56 MPa). However, the MLR model with 4 variables (*knot_T*, *V_U*, *f_{LV}*, and *MOE_{EV}*) was the simplest model that presented an RMSE (8.69 MPa) significantly lower than the SLR.

Table 3.3. RMSE for MOR Prediction through MLR and SLR with 10-fold cross-validation and 5 Repetitions

Number of Variables	Variables in the model	RMSE Overfitted (MPa)	RMSE (MPa)	ΔRMSE ⁽¹⁾ (%)
15	All 15 variables shown in Table 3.2	(7.07)	10.29 ^a	-2.8
7	-0.581 SLG -5.92 RG -20.0 WN_m -0.0249 knot_T -0.033 · V_U +0.0923 · f_{LV} +0.0047 MOE_{EV} +91.07	(7.52)	8.77 ^b	-17.2
6	-5.19 RG -21.9 WN_m -0.031 knot_T -0.0306 · V_U +0.0852 · f_{LV} +0.0049 MOE_{EV} +81.58	(7.70)	8.56 ^b	-19.2
5	-4.33 RG -0.0301 knot_T -0.0289 · V_U +0.0892 · f_{LV} +0.004 MOE_{EV} +73.28	(7.92)	8.60 ^b	-18.8
4	-0.0405 knot_T -0.0242 · V_U +0.0725 · f_{LV} +0.0045 MOE_{EV} +53.11	(8.20)	8.69 ^b	-17.9
3	-0.0414 knot_T -0.014 · V_U +0.0063 MOE_{EV} +62.29	(8.55)	9.04 ^{ab}	-14.6
2	-0.0464 knot_T +0.003 MOE_{EV} +27.24	(9.63)	9.96 ^{ab}	-5.9
1	-0.0663 knot_T +58.83	(10.88)	10.59 ^a	-

⁽¹⁾RMSE increase with respect to the SLR model; the RMSE obtained with the whole dataset (RMSE overfitted) is shown in brackets

SLG: slope of grain; RG: rate of growth; WN: wanes; *V_U*: velocity of the ultrasounds; *f*: frequency

Other authors have also found improvements in MLR compared to SLR models in MOR prediction in pine. Arriaga *et al.* (2012, 2014) found that MOR prediction on the basis of *MOELV* or *MOEV* improved when including in the model a knottiness variable. The results obtained by Grazide *et al.* (2015) showed that multivariate models based on knot variables and the MOEs increased the R² value 27% compared to the SLR based only on the MOEs. Similarly, while working with RG, *MOELV*, and knottiness, França *et al.* (2019) found that the univariate MOR prediction models obtained lower R² values than the MLR models that included two of these variables. The best result was obtained with those three variables for the MLR. Villasante *et al.* (2019) found that the lowest RMSE value in MOR prediction was obtained with a MLR that included 5 variables (velocity of resonant

frequency, concentrated knot diameter ratio, attenuation of the ultrasonic wave, penetration depth, and withdrawal force of a screw).

3.4.3. Nonlinear multivariate models

It was found that the ANN models with a lower number of variables gave a lower error when using fewer neurons. The same was found by Tetko *et al.* (1995). The best predictions were obtained with an ANN based on a single hidden layer of 3 to 5 neurons. No statistically significant differences were found in MOR prediction between the MLR– and ANN–based models for any of the eight groups of variables studied (Figure 3.4). These results concur with those of Villasante *et al.* (2019) with *Pinus sylvestris* and Tanaka *et al.* (1996) with *Cryptomeria japonica*. However, other studies have reported better predictions with ANN than MLR, including Mansfield *et al.* (2007) with *Tsuga heterophyla* and Fathi *et al.* (2020) with poplar. These discrepancies may be attributable to the fact that both these studies worked with small clear samples whereas the present study was conducted using structural size samples.

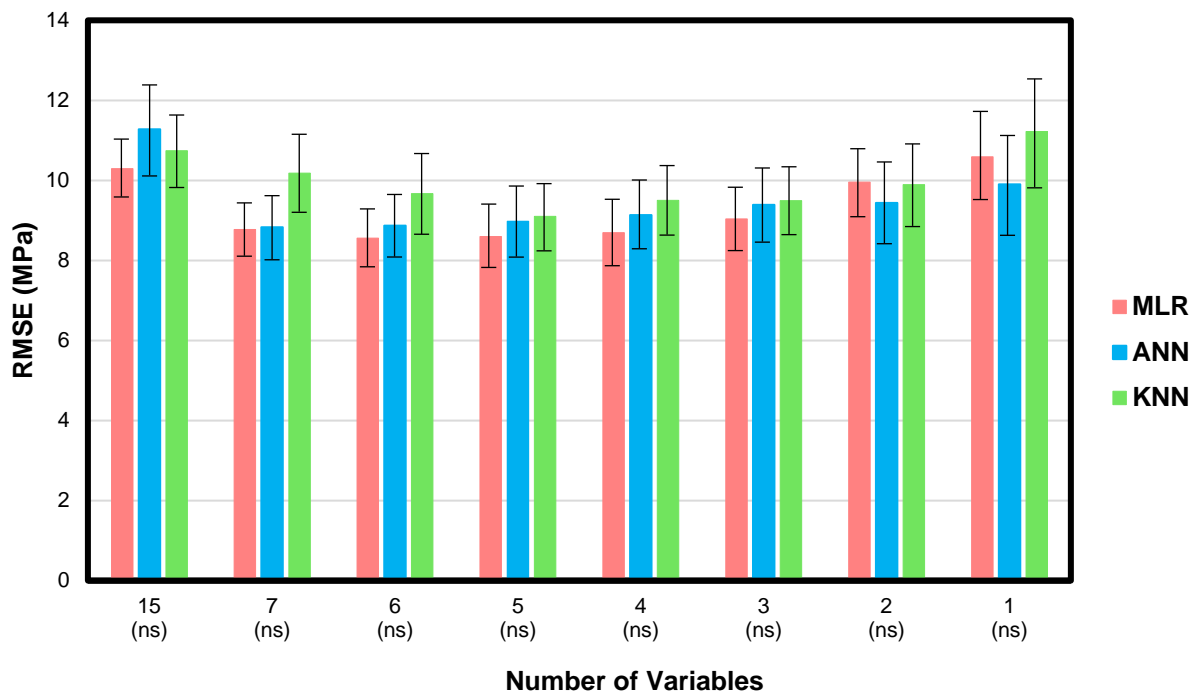


Figure 3.4. RMSE for MOR prediction through MLR, ANN, and KNN algorithms with 10-fold cross-validation and 5 repetitions; mean values and 95% confidence intervals (ns: non-significant differences between the three methods)

For the KNN-based models, the number of neighbor values employed were between 4 and 6. The inverse of the distance was used as distance weighting method. No improvement was observed in MOR prediction when using the KNN algorithm, with no statistically significant differences detected between the MLR and KNN results (Figure 3.4).

3.5. Conclusions

- 1 The variable with the lowest modulus of rupture (MOR) prediction error was knottiness. Despite the complexity required to obtain the knot area ratio (KAR) value, this method was unable to significantly decrease the error obtained when using the simpler method described in Annex A of European Standard EN 1309–3 (2018).
- 2 The prediction error of the best univariate model, based on knottiness, was clearly improvable through the incorporation of other variables. The model with 4 variables (knott, V_U , f_{LV} , and MOE_{EV}) was the most suitable, as adding more variables only decreased the error slightly and non-significantly.
- 3 Performing tests in different vibration modes proved to be better than when using a single vibration mode test, as the best model combined a transverse and a longitudinal variable.
- 4 The usage of a cross-validation method also proved to be a suitable strategy to avoid overfitting in multivariate models based on non-destructive testing (NDT) to determine bending strength in timber.
- 5 The nonlinear artificial neural network (ANN)– or k-nearest neighbors (KNN)–based models obtained similar results to those with multiple linear regression (MLR). No statistically significant differences were detected between these models in terms of MOR predictive capacity.

3.6. References

- Aira, J.R., Villanueva, J. L., Lafuente, E. (2019) Visual and machine grading of small diameter machined round *Pinus sylvestris* and *Pinus nigra* subsp. *salzmannii* wood from mature Spanish forests. Mater. Struct. 52(2): article no. 32.
- Alexander, D.L.J., Tropsha, A., Winkler, D.A. (2015) Beware of R²: Simple, unambiguous assessment of the prediction accuracy of QSAR and QSPR models. J. Chem Inf. Model. 55(7):1316–1322.

- Arriaga, F., Iñiguez-Gonzalez, G., Esteban, M., Divos, F. (2012) Vibration method for grading of large cross-section coniferous timber species. *Holzforschung* 66(3):381–387.
- Arriaga, F., Monton, J., Segues, E., Iñiguez-Gonzalez, G. (2014) Determination of the mechanical properties of radiata pine timber by means of longitudinal and transverse vibration methods. *Holzforschung* 68(3):299–305.
- ASTM Standard (2015) E1876–15 Standard Test Method for Dynamic Young's Modulus, Shear Modulus, and Poisson's Ratio by Impulse Excitation of Vibration. ASTM: West Conshohocken, PA, USA.
- Audacity Team (2015) Audacity®. Version 2.1.12. Audio editor and recorder. <http://audacityteam.org/>.
- Brunetti, M., Burato, P., Cremonini, C., Negro, F., Nocetti, M., Zanuttini, R. (2016) Visual and machine grading of larch (*Larix decidua* Mill.) structural timber from the Italian Alps. *Mater. Struct.* 49(7):2681–2688.
- Carballo, J., Hermoso, E., Fernández-Golfín, J.I. (2009) Mechanical properties of structural maritime pine sawn timber from Galicia (*Pinus pinaster* Ait. ssp. *atlantica*). *For. Syst.* 18(2):152–158.
- Conde García, M., Fernández-Golfín Seco, J.I., Hermoso Prieto, E. (2007) Mejora de la predicción de la resistencia y rigidez de la madera estructural con el método de ultrasonidos combinado con parámetros de clasificación visual. [*Improving the prediction of strength and rigidity of structural timber by combining ultrasound techniques with visual grading parameters*]. *Mater. Constr.* 57(288):49–59.
- Dahlen, J., Montes, C., Eberhardt, T.L., Auty, D. (2018) Probability models that relate nondestructive test methods to lumber design values of plantation loblolly pine. *Forestry* 91(3):295–306.
- European Standard (2012) EN 408:2010+A1:2012. Timber structures. Structural timber and glued laminated timber. Determination of some physical and mechanical properties. European Committee for Standardization (CEN): Brussels, Belgium.
- European Standard (2018) EN 1309–3:2018. Round and sawn timber – Methods of measurements – Part 3: Features and biological degradations. European Committee for Standardization (CEN): Brussels, Belgium.
- European Standard (2002a) EN 13183–1:2002. Moisture content of a piece of sawn timber. Part 1: Determination by oven dry method. European Committee for Standardization (CEN): Brussels, Belgium.
- European Standard (2002b) EN 13183–2:2002. Moisture content of a piece of sawn timber – Part 2: Estimation by electrical resistance method. European Committee for Standardization (CEN): Brussels, Belgium.
- Fathi, H., Nasir, V., Kazemirad, S. (2020) Prediction of the mechanical properties of wood using guided wave propagation and machine learning. *Constr. Build. Mater.* 262: article ID 120848.

- Faydi, Y., Brancheriau, L., Pot, G., Collet, R. (2017) Prediction of oak wood mechanical properties based on the statistical exploitation of vibrational response. *BioResources* 12(3):5913–5927.
- França, F.J.N., Seale, R.D., Shmulsky, R., França, T.S.F.A. (2019) Modeling mechanical properties of 2 by 4 and 2 by 6 southern pine lumber using longitudinal vibration and visual characteristics. *For. Prod. J.* 68(3):286–294.
- Frank, E., Hall, M.A., Witten, I.H. (2016) The WEKA workbench. Online Appendix for Data Mining: Practical Machine Learning Tools and Techniques. Morgan Kaufmann, (https://www.cs.waikato.ac.nz/ml/weka/Witten_et_al_2016_appendix.pdf), Accessed 9 Dec 2021
- García Esteban, L., García Fernández, F., De Palacios, P. (2009) MOE prediction in *Abies pinsapo* Boiss. timber: Application of an artificial neural network using non-destructive testing. *Comput. Struct.* 87(21–22):1360–1365.
- Grazide, C., Cointe, A., Coureau, J.L., Morel, S., Dumail, J.F. (2015) Wood heterogeneities and failure load of timber structural elements: A statistical approach. *Wood Sci. Technol.* 49(2):421–440.
- Halabe, U.B., Bidigalu, G.M., GangaRao, H.V.S., Ross, R.J. (1997) Nondestructive evaluation of green wood using stress wave and transverse vibration techniques. *Mater. Eval.* 55(9):1013–1018.
- Hashim, U.R., Hashim, S.Z.M., Muda, A.K. (2016) Performance evaluation of multivariate texture descriptor for classification of timber defect. *Optik* 127(15):6071–6080.
- Hassan, K.T.S., Horacek, P., Tippnera, J. (2013) Evaluation of stiffness and strength of Scots pine wood using resonance frequency and ultrasonic techniques. *BioResources* 8(2):1634–1645.
- Hautamäki, S., Kilpeläinen, H., Verkasalo, E. (2014) Factors and models for the bending properties of sawn timber from Finland and north-western Russia. Part II: Scots pine. *Baltic For.* 20(1):142–156.
- Íñiguez González, G., Arriaga Martítegui, F., Esteban Herrero, M., Argüelles Alvarez, R. (2007) Los métodos de vibración como herramienta no destructiva para la estimación de las propiedades resistentes de la madera aserrada estructural [*Vibration methods as non-destructive tool for structural properties assessment of sawn timber*]. *Inf. Constr.* 59(506):97–105.
- Lam, F., Barrett, J.D., Nakajima, S. (2005) Influence of knot area ratio on the bending strength of Canadian Douglas fir timber used in Japanese post and beam housing. *J. Wood Sci.* 51(1):18–25.
- Lever, J., Krzywinski, M., Altman, N. (2016) Model selection and overfitting. *Nat. Methods*. 13(9):703–704.
- Mansfield, S.D., Iliadis, L., Avramidis, S. (2007) Neural network prediction of bending strength and stiffness in western hemlock (*Tsuga heterophylla* Raf.). *Holzforschung* 61(6):707–716.

- Martins, C.E.J., Dias, A.M.P.G., Marques, A.F.S., Dias, A.M.A. (2017) Non-destructive methodologies for assessment of the mechanical properties of new utility poles. *BioResources* 12(2):2269–2283.
- Pommier, R., Breysse, D., Dumail, J.F. (2013) Non-destructive grading of green Maritime pine using the vibration method. *Eur. J. Wood Wood Prod.* 71(5):663–673.
- Tanaka, T., Tanaka, T., Nagao, H., Kato, H. (1996) A preliminary investigation on evaluation of strength of soft wood timbers by neural network. Proceeding of the 10th International Symposium on Nondestructive Testing of Wood, Lausanne, Switzerland.
- Tetko, I.V., Livingstone, D.J., Luik, A.I. (1995) Neural Network Studies. 1. Comparison of Overfitting and Overtraining. *J. Chem. Inf. Comput. Sci.* 35(5):826–833.
- Vega, A., Dieste, A., Guaita, M., Majada, J., Baño, V. (2012) Modelling of the mechanical properties of *Castanea sativa* Mill. structural timber by a combination of non-destructive variables and visual grading parameters. *Eur. J. Wood Wood Prod.* 70(6):839–844.
- Villasante, A., Iñiguez-Gonzalez, G., Puigdomenech, L. (2019) Comparison of various multivariate models to estimate structural properties by means of non-destructive techniques (NDTs) in *Pinus sylvestris* L. timber. *Holzforschung* 73(4):331–338.
- Walker, J. (1993) Primary Wood Processing: Principles and Practice. Chapman & Hall: London, UK.
- Weaver, W., Timoshenko, S., Young, D.H. (1990) Vibration problems in engineering. Wiley: New York, USA.
- Yang, B.Z., Seale, R.D., Shmulsky, R., Dahlen, J., Wang, X. (2017) Comparison of nondestructive testing methods for evaluating no. 2 southern pine lumber: Part B, modulus of rupture. *Wood Fiber Sci.* 49(2):134–145.
- Zhou, H., Smith, I. (1991) Factors influencing bending properties of white spruce lumber. *Wood Fiber Sci.* 23(4):483–500.

CAPÍTULO 4

Overtones

Villasante, A., Fernández-Serrano, Á., (2022) Dynamic modulus of elasticity in flexural vibration tests of *Pinus sylvestris* sawn timber obtained with fundamental resonant frequency and overtones. Holzforschung 76(6):485–492.
DOI: 10.1515/hf-2021-0190.

4. Dynamic modulus of elasticity in flexural vibration tests of *Pinus sylvestris* sawn timber obtained with fundamental resonant frequency and overtones

4.1. Abstract

The use of resonant frequency is presently one of the most used non-destructive testing (NDT) methods to predict the mechanical properties of sawn timber. In most cases, only the first vibration mode is used to estimate the static modulus of elasticity (MOEs). The use of other vibration modes (overtones) can improve the predictive capacity of this NDT. In this study, the dynamic modulus of elasticity (MOE_{dyn}) obtained from the fundamental flexural resonant frequency and overtones of 38 structural size samples ($2000 \times 100 \times 70$ mm 3) of *Pinus sylvestris* were analysed. The study was complemented with 16 small size samples ($1000 \times 20 \times 8.7$ mm 3) of the same species to know the shear effect in samples with a very high length-to-depth ratio. For the structural size samples, a 6% decrease in the MOE_{dyn} was detected each time the vibration mode increased. Using the second or third vibration mode offered lower errors in the prediction of the MOEs than the fundamental resonant frequency. The lowest MOEs prediction errors were obtained combining various vibration modes through power regression. This regression turned out to be a simple alternative to avoid the shear effect in the calculation of the MOE_{dyn} .

Keywords: NDT; power regression; resonant vibration mode; shear effect; Timoshenko equation of motion

4.2. Introduction

The use of vibration techniques to estimate the mechanical characteristics of sawn timber on the basis of the resonant frequency is one of the most widespread non-destructive testing (NDT) methods. Diverse authors have used the longitudinal resonant frequency to obtain the dynamic modulus of elasticity (MOE_{dyn}). This technique involves striking the end of the sample and processing the sound produced with fast Fourier transform (FFT). The stiffness of the sample can be estimated on the basis of the longitudinal resonant frequency, the length of the sample and its density. This is possible thanks to the relationship between the static modulus of elasticity (MOEs) and the longitudinal MOE_{dyn} (Arriaga *et al.* 2012; Íñiguez González *et al.* 2007).

Other authors have made use of the flexural resonant frequency. In this case, the timber is struck on its face or edge causing flexural vibration. Various authors have observed that better estimates of the MOEs are made with the flexural MOE_{dyn} than the longitudinal MOE_{dyn} (Hassan *et al.* 2013; Ilic 2001; Olsson *et al.* 2012).

Most of the studies that analysed sawn timber resonance only used the fundamental resonant frequency (Arriaga *et al.* 2014; Olsson *et al.* 2012; Wang *et al.* 2008). Although uncommon, some authors have also used overtones in their works. Brancherieu (2006) conducted a theoretical study on the shear effect in xylophone bars analysing five flexural vibration frequencies. Kubojima *et al.* (2006b) analysed five vibration modes in small clear specimens of various Japanese species and observed a clear decrease of the flexural MOE_{dyn} as the resonance mode number increased. This decrease was also detected in studies by Kubojima *et al.* (2006a) with defect-free samples and was attributed to the shear and rotary inertia effects in flexural vibrations. Yoshihara (2012) used four flexural vibration modes to simultaneously obtain the Young's modulus and the shear modulus in small clear specimens of spruce sawnwood. The author reported the difficulty of measuring high-order vibration modes due to the low amplitude of resonance frequencies above the fifth mode. The same author also observed that, in the low resonance mode of flexure numbers, the contribution of shear deflection is much less important than that of bending deflection. Brancherieu (2014) undertook a theoretical study in which flexural resonance frequencies were related with the MOEs and the shear modulus. The theoretical model developed was then compared with the experimental results obtained using a defect-free sample of *Dalbergia* sp. Qin *et al.* (2018) proposed use of the spectral response to quantify the dynamic bending modulus, estimating the MOEs from the mean MOE_{dyn} of fundamental, second and third flexural resonance mode frequencies. In their studies, they used small samples of *Pinus sylvestris* with diverse knots and found that the MOE_{dyn} was influenced by the volume of the knots but that their position had little impact.

Important differences have been observed in some studies between the theoretical frequencies of the different vibration modes calculated using the classic model of Bernoulli and those obtained experimentally. Olsson *et al.* (2012) attributed these differences to large inhomogeneity in wood samples. They quantified the inhomogeneity through the modulus of inhomogeneity variable obtained from the first six harmonics, although finally it was not possible to improve the predictive capacity offered by the fundamental resonant frequency. Pantelić *et al.* (2020) explained that the differences between theoretical and observed frequencies were due to Bernoulli's model only being valid for homogenous and isotropic materials, properties which wood does not share.

Some studies have considered overtones in roundwood. Chauhan and Walker (2006) based their research on the second harmonic. They reported the difficulty of obtaining in practice more than one or two overtones in longitudinal frequencies due to various energy loss mechanisms in wood. This concurs with the studies of Ouis (1999), who reported the difficulty of interpreting the spectra obtained in wood as a consequence of material inhomogeneity. Grabianowski *et al.* (2006) used second harmonics in their studies on roundwood. Their results concurred with those of Sobue *et al.* (2010), who found for longitudinal vibrations in wooden beams lower errors in the overtones than in the fundamental vibration.

In the case of the bending vibration of thin beams when the length-to-depth ratio is high, the shear can be ignored and the theoretical model of Bernoulli accepted. When the shear is non-negligible, use should be made of the Timoshenko equation of motion in free flexural vibration. To solve the Timoshenko equation, Brancherieu and Bailleres (2002) undertook a theoretical analysis of three different approaches (proposed by Goens–Hearmon, Rayleigh and Bordonné). Another alternative solution was proposed by Kubojima *et al.* (2020) in their development of a Timoshenko-based Goens–Hearmon regression method. With this method, they estimated Young's and shear moduli only with the bending vibration test.

The aim of the present study is to establish the differences between the flexural MOE_{dyn} on the basis of various vibration modes in a batch of structural size samples of sawn timber and a batch of samples with a very high length-to-depth ratio. The intention is to determine the predictive capacity of these MOE_{dyn} to estimate the MOEs. Grading *Pinus sylvestris* timber from the Montsec mountains (Spain) was not one of the objectives of this work.

4.3. Materials and methods

4.3.1. Structural size samples

A total of 38 structural size samples of *Pinus sylvestris* L. with 2 m length and 70 mm × 100 mm cross section were tested. The samples were randomly selected from stacks of ungraded timber obtained from trees in the Montsec mountains (Spain). The pieces were stored and allowed to dry naturally in the interior of a laboratory. Each month the weight of each sample was checked and its position in the pile changed to homogenize the drying process.

4.3.2. Vibration test and dynamic modulus of elasticity

Resonant frequencies were obtained using a RODE NT–USB (Rode Microphones, Australia) condenser microphone through a digital recording with Audacity® software (Audacity Team 2015). A resolution of 24 bits and a project sampling rate of 384 kHz were used. The sample was struck with an impulser consisting of a 26 mm diameter glass marble attached to a 230 mm long wooden handle. To ensure free vibration, the structural size samples were suspended from elastic cords situated 448 mm from the ends, positions corresponding to the fundamental resonant frequency nodes (ASTM Standard E1876–15 2015). Although this Standard indicates that the strike should be made halfway along the length of the sample it was observed that the frequencies corresponding to high-order modes of flatwise flexure were more clearly identified when the impact point was located on the face, and near its end (Figure 4.1). Each sample was struck twice and the spectrum that showed with greater clarity the first 10 vibration mode frequencies was used. Spectrum plots were made using a FFT with a rectangular window function. In some high-order vibration modes it was not possible to clearly identify a small percentage of frequencies (2.6% in the 7th vibration mode, 5.2% in the 8th vibration mode, 10.5% in the 9th vibration mode, and 29% in the 10th vibration mode). This was due to an overlap in the frequencies corresponding to different types of vibration (torsional, longitudinal or edgewise). With the frequencies of each of the first 10 vibration modes, the MOE_{dyn} were calculated through Equation (4.1) (Weaver *et al.* 1990):

$$\text{MOE}_{\text{dyn}} = \frac{48 \cdot \pi^2 \cdot \rho \cdot f_n^2 \cdot L^4}{m_n^4 \cdot h^2} \quad (4.1)$$

where ρ is the density of the sample; f_n is the flexural resonant frequency for vibration mode n ; L and h are the actual length and thickness of each sample, and m_n is a constant that depends on the vibration mode n : $m_1 = 4.73$; $m_2 = 7.853$; and $m_n = (n+0,5) \pi$ for $n > 2$. With the 10 flexural frequencies, the $\text{MOE}_{1\text{st}}$, $\text{MOE}_{2\text{nd}}$, $\text{MOE}_{3\text{rd}}$, $\text{MOE}_{4\text{th}}$, etc. were obtained. In total, 362 MOE_{dyn} were obtained.

The MOE_{dyn} as proposed by Kubojima *et al.* (2020) was also calculated. These authors obtained the MOE_{dyn} using the Goens–Hearmon regression method based on the Timoshenko theory of bending. In the present study, the first five vibration mode frequencies were used as a well as a shear factor of 1.18. This MOE_{dyn} was called MOE_{Kub} .

In addition, another MOE_{dyn} was obtained on the basis of power regression between vibration mode frequencies and vibration mode orders (Equation (4.2)). It was observed that this type of regression provided the best fit to the data, with R^2 above 0.99.

$$f_n = a \cdot n^b \quad (4.2)$$

In Equation (4.2), f_n is the flexural resonant frequency for vibration mode n , and a and b are the fitting function parameters. For each sample, the parameter a corresponds to the estimation of the first vibration mode frequency. This parameter was called the power frequency. The power modulus of elasticity (MOE_{pow}) was obtained by introducing this frequency into Equation (4.1).

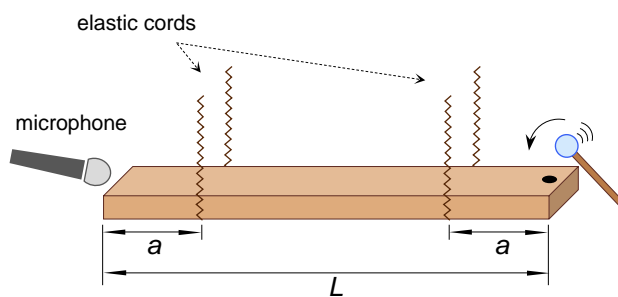


Figure 4.1. Outline of the flexural vibration test. For the structural size samples: $L = 2$ m, $a = 0.448$ m; for the small size samples: $L = 1$ m, $a = 0.224$ m. Black point •: the point where the sample was struck (It is located at the face, on its longitudinal axis, equidistant from its edges, near its end).

4.3.3. Static modulus of elasticity calculation

Immediately after the sound recording, a four-point bending test in flatwise direction was performed to obtain the global MOEs in accordance with European Standard 408:2010+A1 (2012). The static test was only conducted in flatwise direction so as to obtain a high length-to-depth ratio (26). A universal testing machine (Cohiner, Spain) was used. Deformation was measured using a displacement transducer which captured the deformation at the sample's mid-point. Following previous studies conducted with similar samples, the MOEs was derived using the stress-strain curve in the loading range between 0.5 kN and 2 kN. The regression between force and displacement presented a R^2 value equal or greater than 0.99 for all the samples. In line with European Standard 408:2010+A1 (2012), it was decided to ignore the shear effect when calculating the MOEs.

4.3.4. Small size samples

To further study the shear effect, the analyses were complemented using a set of 16 samples of *Pinus sylvestris*. The same sample size was used as that tested by Brancherieu (2014): 1 m long with a 20 mm × 8.7 mm section. These samples were only tested flatwise (static and dynamic tests), so as to obtain a very high length-to-depth ratio (115).

The drying process was the same as that outlined for the structural size samples, with a storage period of three years. No adjustments were made based on moisture content (MC) because all of the samples presented similar MC values and the dynamic and static tests for each sample were conducted within an interval of less than one hour.

The small size samples were not defect-free and contained knots of varying size and different growth ring orientations. The same test of vibration mode frequencies was performed as in the structural size samples, placing the elastic cords 224 mm from the ends in order to situate them on the fundamental resonant frequency nodes (ASTM Standard E1876–15 2015). Only the first 8 vibration mode frequencies were used due to the difficulty of clearly obtaining the high-order frequencies in this sample size. The MOE_{Kub} and MOE_{pow} were also obtained following the method described for the structural size samples. A three-point bending test was used to obtain the global MOEs. According to Brancherieu *et al.* (2002b), the 3-point bending test systematically underestimates the MOE due to the shear and indentation effects. The shear effect could be ignored because the small size samples had a length-to-depth ratio equal to 115 in the flatwise tests. The indentation effect could also be ignored because the force applied to the small size samples was small (100 N). In addition, a piece of plywood was placed between the samples and the 3 points of contact with the bending machine, one loading head and two supports (Spanish Standard UNE 56537 1979).

4.3.5. Statistical analyses

The statistical analysis was performed with R-software (The R Foundation, version 3.6.1, Vienna, Austria). Bartlett's test was applied to verify heteroscedasticity. If the requirements of heteroscedasticity were not met, an analysis of the differences among means was performed with the Kruskal–Wallis non-parametric test, performing the post hoc analysis using Dunn's test with Bonferroni adjustment. The significance level was 0.05.

4.4. Results and discussion

4.4.1. Structural size sample

The MOEs values, density and MC of the structural size samples are presented in Table 4.1. It can be observed that the differences in MC between the samples were small (less than 1%) due to the drying process that was applied. Figure 4.2 shows the experimental spectrum obtained in one of the structural size samples. The flexural flatwise frequencies were highlighted due to the area where the strike was made and the position of the microphone. In this sample, 12 flatwise vibration frequencies (the fundamental frequency and 11 overtones) could be clearly detected. Other vibration types (edgewise and longitudinal frequencies) can also be observed in the spectrum. However, these frequencies show lower amplitudes because the type of strike and the positioning of the support points resulted in less excitation associated with these vibration modes. The spectra of the samples were similar to that obtained in the 1000 mm × 20 mm × 8.7 mm sample in the work of Brancherieu (2014).

Table 4.1. Characteristics of the samples

Size	MOEs (MPa)			Density (kg · m ⁻³)			Moisture Content (%)		
	mean	SD	P _{5%}	mean	SD	P _{5%}	mean	SD	P _{5%}
Structural	7861	2177	5064	542	40.0	478	11.2	0.43	10.7
Small	8237	1289	6663	557	33.8	510	9.03	0.06	8.94

Table 4.2 shows the observed values for the flexural resonant frequencies, MOEs and MOE_{dyn} for the structural size samples. The MOEs of the set of structural size samples was 7861 MPa. This value is slightly lower than those obtained by other authors in studies with *Pinus sylvestris* (Arriaga *et al.* 2012; Hassan *et al.* 2013; Ranta–Maunus *et al.* 2011), where the values ranged between 9000 and 12000 MPa. These small differences are common in a material as heterogenous as structural size timber. The MOE_{dyn} corresponding to the 1st vibration mode was also slightly lower than the values obtained by other authors for *Pinus sylvestris* (Hassan *et al.* 2013), *Pinus radiata* (Arriaga *et al.* 2014) and *Picea abies* (Spycher *et al.* 2008), with values ranging between 10000 and

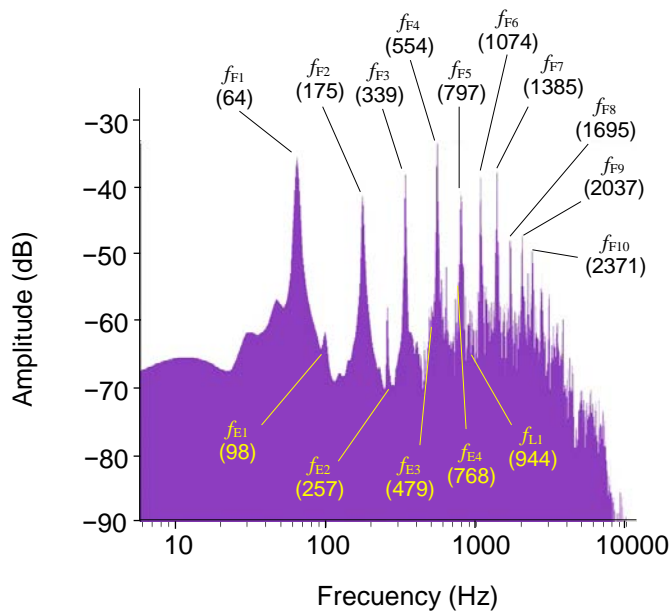


Figure 4.2. Example of a spectrum observed in one of the structural size samples. Shown in the upper part of the figure are the frequencies (in brackets) corresponding to the flatwise vibration (f_{F_n}). Also shown in the lower part of the figure are the frequencies corresponding to the edgewise vibration (f_{E_n}) and the longitudinal vibration (f_{L_n}).

12000 MPa. Considering exclusively the MOEs values obtained, the samples would correspond to class C16 of European Standard EN 338 (2016), and hence it was accepted that there were no abnormal stiffness values.

The MOE_{1st} was 7.7% higher than the MOEs. This overestimation is common in NDT (Arriaga *et al.* 2014; Hassan *et al.* 2013; Larsson *et al.* 1998; Spycher *et al.* 2008). Several authors have attributed this overestimation to wood being a viscoelastic material (Haines *et al.* 1996; Halabe *et al.* 1997).

Figure 4.3 shows the difference between the expected frequencies calculated on the basis of the fundamental resonant frequency following Bernoulli's model (Equation (4.3)) and the observed frequencies for one of the studied samples:

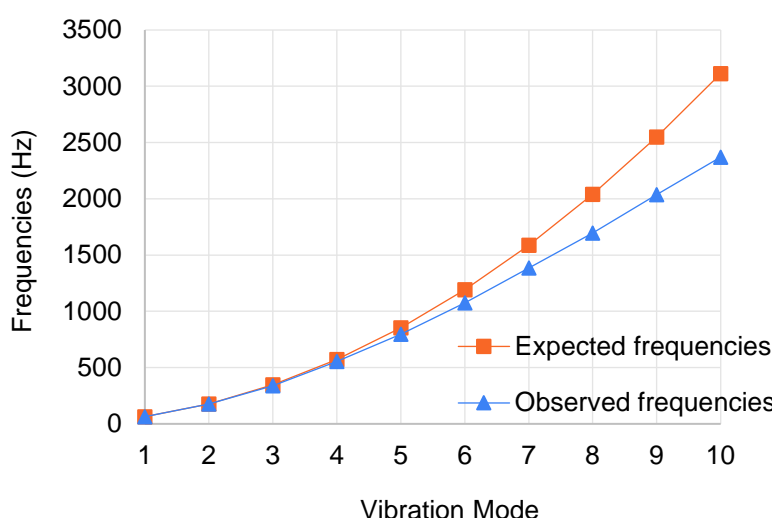
$$f_{n+1} = f_n \left(\frac{m_{n+1}}{m_n} \right)^2 \quad (4.3)$$

where f_n and f_{n+1} are the flexural resonant frequencies for vibration modes order n and $n+1$, and m_n is a constant that depends on the vibration mode order n : $m_1 = 4.73$; $m_2 = 7.853$; and $m_n = (n+0,5) \pi$ for $n > 2$.

Table 4.2. Mean, median and standard deviation of flexural resonant frequencies, MOE_{dyn} and MOEs for structural size samples

	Frequency (Hz)			MOE (MPa)		
	Mean	Median	Standard deviation	Mean	Median	Standard deviation
1st vibration mode	68.6	68	9.2	8471	7865	2281
2nd vibration mode	185.8	185	23.8	8151	7794	2042
3rd vibration mode	354.1	356	42.3	7702	7566	1832
4th vibration mode	565.0	559	65.7	7172	6866	1679
5th vibration mode	816.0	826	85.8	6700	6603	1448
6th vibration mode	1091.0	1087	106.7	6126	6061	1249
7th vibration mode	1380.0	1393	129.1	5560	5500	1118
8th vibration mode	1694.0	1706	155.9	5032	5039	999
9th vibration mode	2015.0	2022	172.2	4561	4490	873
10th vibration mode	2314.0	2367	196.8	4090	4126	813
MOE_{pow}	66.0	65	9.2	7856	7445	2214
MOE_{Kub}	—	—	—	8591	8267	2275
MOE_{s}	—	—	—	7861	7275	2177

In all the samples, the observed frequencies were lower than the expected frequencies according to the Bernoulli model. These results concur with those of Pantelić *et al.* (2020), who reported that the Bernoulli model was not applicable to wood as it is a heterogenous and isotropic material. Cho (2007) also obtained similar results, suggesting that the classic theory neglects rotational motions and shear deformations, and both of these effects cause the resonance frequencies to be lower than those predicted.

**Figure 4.3.** Example of expected frequencies (following the Bernoulli model) and observed frequencies for one of the studied structural size samples.

A comparison of the MOE_{dyn} and the MOEs in structural size samples is shown in Figure 4.4. A clear decrease can be observed in the relative errors of the MOE_{dyn} as the vibration mode order increases, in agreement with the results of Pantelić *et al.* (2020).

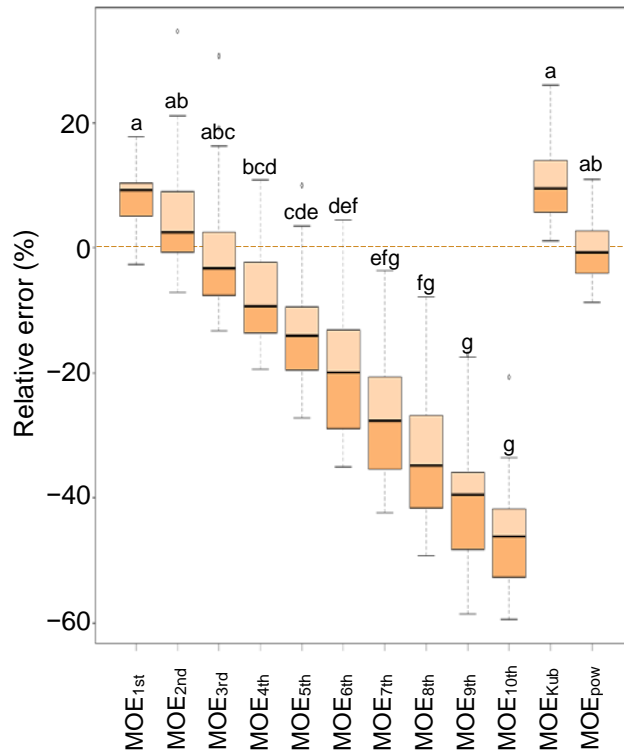


Figure 4.4 Relative error with respect to the MOEs in structural size samples. Values matched by the same letter do not differ significantly (Dunn's test with Bonferroni adjustment).

This decrease was favourable in the first two vibration modes in which the MOEs was overestimated. However, the effect was unfavourable from the third vibration mode as, in these modes, the MOEs is underestimated and the predictive value is increasingly defective. This decrease was relatively stable and remained around 6% between vibration mode n and n+1. Kubojima *et al.* (2006b) also detected a similar decrease in 300 mm × 25 mm × 5 mm samples, although in their study the reduction was around 3%. The shear effect explains this decrease. In the case of vibration mode 1, the length-to-depth ratio was equal to 28 and so the shear effect was small (Arriaga *et al.* 2014). As the vibration mode order increases the wavelength decreases and the beam becomes relatively deeper compared to the wavelength (Pantelić *et al.* 2020). In consequence, shear effects were more evident in high-order vibration modes. This explanation is in agreement with Yoshihara

(2012), who showed that, in the low-order modes of flexure, the contribution of shear deflection is relatively small with respect to that of the bending deflection.

Because overestimation of the MOEs on the basis of the MOE_{dyn} acts in the opposite direction to shear underestimation in higher-order vibration modes, it would be recommendable to use a MOE_{dyn} different to the fundamental frequency. In the set of structural size samples that were tested, equilibrium was found between the second and third vibration mode (the relative error went from +2.6% to -3.2%). These results concur with the studies of Chauhan and Walker (2006) and Grabianowski *et al.* (2006) in roundwood, who propose using the second vibration mode instead of the fundamental frequency. These results also concur with Qin *et al.* (2018), who estimated the MOEs from the MOE_{dyn} values of fundamental, second and third flexural resonance mode frequencies.

Table 4.3. Mean, median and standard deviation of flexural resonant frequencies, MOE_{dyn} and MOEs for small size samples

	Frequency (Hz)			MOE (MPa)		
	Mean	Median	Standard deviation	Mean	Median	Standard deviation
1st vibration mode	32.8	33.0	3.8	7593	7324	1943
2nd vibration mode	96.1	94.0	8.8	8503	8222	1508
3rd vibration mode	185.8	189.0	20.1	8291	7935	1764
4th vibration mode	318.0	324.5	24.1	8879	8590	1522
5th vibration mode	483.0	481.0	38.5	9196	8464	1730
6th vibration mode	670.6	663.5	35.4	9040	8658	1163
7th vibration mode	878.7	875.0	59.5	8770	8367	1363
8th vibration mode	1125.1	1122.0	66.6	8707	8321	1217
9th vibration mode	1396.5	1380.0	94.4	8612	7930	1395
10th vibration mode	1680.6	1699.5	107.8	8352	7862	1280
MOE_{pow}				7898	7663	1274
MOE_{Kub}				6297	6163	1099
MOE_{s}				8237	7867	1289

The MOE_{Kub} overestimated the MOEs by 9.5%, a similar value to the MOE_{1st} (+9.2%). The MOE_{Kub} was calculated on the basis of the values of the first 5 vibration modes. Despite the important shear effect in high-order modes of flexure, the Kubojima solution correctly corrected the Timoshenko equation. However, as a predictor of the MOEs it

presented no advantages over the MOE_{1st}, despite the difficulty of obtaining various vibration mode frequencies and the complexity of its calculation.

The MOE_{pow} was the MOE_{dyn} which presented the lowest relative error (+0.8%) with a relatively low scattering of values. Although it was obtained from various vibration modes, it was also able to take into account the shear effect. This was the MOE_{dyn} from which the best fitting MOEs predictions could be obtained.

4.4.2. Small size samples

The MOEs, density and MC values for the structural size samples are shown in Table 4.1. It is possible to observe that the differences in MC between the samples were only small (less than 0.2%); this was due to the long drying process associated with thin samples. Table 4.3 shows the values of the observed flexural resonant frequencies, MOEs and MOE_{dyn} for the small size samples. The box plot with the quartiles for the MOEs and MOE_{dyn} are shown in Figure 4.5. The decrease of the MOE_{dyn} of the structural size samples (Table 4.2) was not observed in this sample size. As no statistically significant differences were detected between the MOEs and any of the MOE_{dyn}, it can be accepted that the high length-to-depth ratio caused that the shear effect was negligible in all the vibration mode

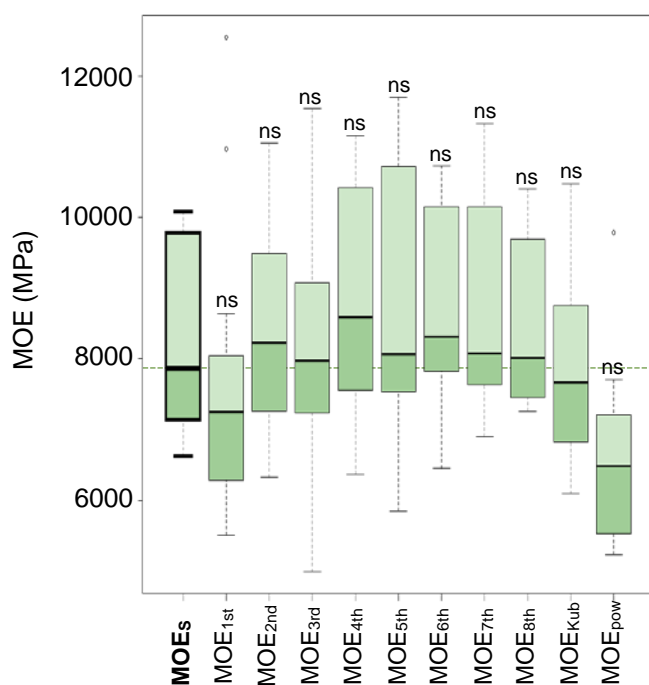


Figure 4.5. Static and dynamic MOE in small size samples (1000 mm × 20 mm × 8.7 mm). ns: values do not differ significantly from MOEs (Kruskal–Wallis test).

orders. In the small size samples all the vibration modes were good predictors of the global MOEs, so it would be recommendable to use the MOE_{dyn} obtained from the mean of various vibration modes in order to avoid experimental errors.

The predictive capacity of the MOE_{Kub} and the MOE_{pow} was also correct, though without any improvement on the MOE_{dyn} obtained from the vibration mode frequencies. Due to the greater complexity in obtaining these MOE, their use is not advisable when the shear effect is negligible.

4.5. Conclusions

As the vibration mode order increased in the structural size samples a constant decrease was generated (-6%) of the MOE_{dyn} calculated on the basis of the flexural resonant frequencies.

In the structural size samples, the MOE_{pow} calculated on the basis of power regression of the resonant frequencies of the harmonics was the MOE_{dyn} which presented the lowest prediction error of the MOEs. This method, which uses simultaneously the fundamental frequency and the overtones, was much easier to obtain than the methods proposed by Goens–Hearmon, Rayleigh or Bordonné to resolve the Timoshenko equation.

For the MOE_{dyn} calculated with only one frequency, the second and third vibration modes were those that presented the lowest prediction errors of the MOEs ($+2.6\%$ and -3.2% , respectively). In these cases, oversizing of the MOE_{dyn} was adequately compensated by undersizing generated by the overtones.

In small size samples with a very high length-to-depth ratio, no statistically significant differences were obtained between the MOE_{dyn} obtained from the fundamental frequency and overtones. In these samples, neither the MOE_{pow} nor MOE_{Kub} did not contribute any improvement. It would be recommendable to use a mean MOE_{dyn} value of various vibration modes for the prediction of the global MOEs in order to avoid experimental errors.

To identify with greater clarity the overtones of flexural flatwise frequencies it is recommendable to strike the sample at a point located at the face on its longitudinal axis, equidistant from its edges, near its end.

Author contributions

All the authors have accepted responsibility for the entire content of this submitted manuscript and approved submission.

Conflict of interest statement

The authors declare no conflicts of interest regarding this article

4.6. References

- Arriaga, F., Iñiguez-Gonzalez, G., Esteban, M., Divos, F. (2012) Vibration method for grading of large cross-section coniferous timber species. *Holzforschung* 66(3):381–387.
- Arriaga, F., Monton, J., Segues, E., Iñiguez-Gonzalez, G. (2014) Determination of the mechanical properties of radiata pine timber by means of longitudinal and transverse vibration methods. *Holzforschung* 68(3):299–305.
- ASTM Standard (2015) E1876–15 Standard Test Method for Dynamic Young's Modulus, Shear Modulus, and Poisson's Ratio by Impulse Excitation of Vibration. ASTM: West Conshohocken, PA, USA.
- Audacity Team (2015) Audacity®. Version 2.1.12. Audio editor and recorder. <http://audacityteam.org/>.
- Brancheriau, L., Bailleres, H. (2002) Natural vibration analysis of clear wooden beams: A theoretical review. *Wood Sci. Technol.* 36(4):347–365.
- Brancheriau, L., Bailleres H., Guitard, D. (2002) Comparison between modulus of elasticity values calculated using 3 and 4 point bending tests on wooden samples. *Wood Sci. Technol.* 36(5):367–383.
- Brancheriau, L. (2006) Influence of cross section dimensions on Timoshenko's shear factor – Application to wooden beams in free-free flexural vibration. *Ann. For. Sci.* 63(3):319–321.
- Brancheriau, L. (2014) An alternative solution for the determination of elastic parameters in free-free flexural vibration of a Timoshenko beam. *Wood Sci. Technol.* 48(6):1269–1279.
- Chauhan, S.S., Walker, J.C.F. (2006) Variations in acoustic velocity and density with age, and their interrelationships in radiata pine. *For. Ecol. Manage.* 229(1–3):388–394.
- Cho, C.L. (2007) Comparison of three methods for determining Young's modulus of wood. *Taiwan J. For. Sci.* 22(3):297–306.
- European Standard (2002) EN 13183–1:2002. Moisture content of a piece of sawn timber. Part 1: Determination by oven dry method. European Committee for Standardization (CEN): Brussels, Belgium.

European Standard (2012) EN 408:2010+A1:2012. Timber structures. Structural timber and glued laminated timber. Determination of some physical and mechanical properties. European Committee for Standardization (CEN): Brussels, Belgium.

European Standard (2016) EN 338:2016. Structural timber. Strength classes. European Committee for Standardization (CEN): Brussels, Belgium.

Grabianowski, M., Manley, B., Walker, J.C.F. (2006) Acoustic measurements on standing trees, logs and green lumber. *Wood Sci. Technol.* 40(3):205–216.

Haines, D.W., Leban, J.M., Herbé, C. (1996) Determination of Young's modulus for spruce, fir and isotropic materials by the resonance flexure method with comparisons to static flexure and other dynamic methods. *Wood Sci. Technol.* 30:253–263.

Halabe, U.B., Bidigalu, G.M., GangaRao, H.V.S., Ross, R.J. (1997) Nondestructive evaluation of green wood using stress wave and transverse vibration techniques. *Mater. Eval.* 55(9):1013–1018.

Hassan, K.T.S., Horacek, P., Tippnera, J. (2013) Evaluation of stiffness and strength of Scots pine wood using resonance frequency and ultrasonic techniques. *BioResources* 8(2):1634–1645.

Ilic, J. (2001) Relationship among the dynamic and static elastic properties of air-dry *Eucalyptus delegatensis* R. Baker. *Holz Als Roh-und Werkst.* 59(3):169–175.

Íñiguez González, G., Arriaga Martítegui, F., Esteban Herrero, M., Argüelles Alvarez, R. (2007) Los métodos de vibración como herramienta no destructiva para la estimación de las propiedades resistentes de la madera aserrada estructural [*Vibration methods as non-destructive tool for structural properties assessment of sawn timber*]. *Inf. Constr.* 59(506):97–105.

Kubojima, Y., Ohsaki, H., Kato, H., Tonosaki, M. (2006a) Fixed-fixed flexural vibration testing method of beams for timber guardrails. *J. Wood Sci.* 52(3):202–207.

Kubojima, Y., Sonoda, S., Kato, H., Harada, M. (2020) Effect of shear and rotatory inertia on the bending vibration method without weighing specimens. *J. Wood Sci.* 66(1):51.

Kubojima, Y., Tonosaki, M., Yoshihara, H. (2006b) Young's modulus obtained by flexural vibration test of a wooden beam with inhomogeneity of density. *J. Wood Sci.* 52(1):20–24.

Larsson, D., Ohlsson, S., Perstorper, M., Brundin, J. (1998) Mechanical properties of sawn timber from Norway spruce. *Holz Als Roh-Und Werkst.* 56(5):331–338.

Olsson, A., Oscarsson, J., Johansson, M., Källsner, B. (2012) Prediction of timber bending strength on basis of bending stiffness and material homogeneity assessed from dynamic excitation. *Wood Sci. Technol.* 46(4):667–683.

Ouis, D. (1999) Vibrational and acoustical experiments on logs of spruce. *Wood Sci. Technol.* 33(2):151–184.

Pantelić, F., Mijić, M., Šumarac Pavlović, D., Ridley-Ellis, D., Dudeš, D. (2020) Analysis of a wooden specimen's mechanical properties through acoustic measurements in the very near field. *J. Acoust. Soc. Am.* 147(4):EL320–EL325.

4. Overtones

- Qin, J., Liu, X., Van Den Abeele, K., and Cui, G. (2018) The study of wood knots using acoustic nondestructive testing methods. *Ultrasonics* 88:43–50.
- R Core Team (2019) R: A language and environment for statistical computing. Version 3.6.1. R Foundation for Statistical Computing, Vienna, Austria. <http://www.R-project.org/>.
- Ranta-Maunus, A., Denzler, J.K., Stapel, P. (2011) Strength of European timber. Part 2. Properties of spruce and pine tested in Gradewood project. VTT Technical Research Centre of Finland. VTT Working Papers, No. 179. <http://www.vtt.fi/inf/pdf/workingpapers/2011/W179.pdf>.
- Sobue, N., Fujita, M., Nakano, A., Suzuki, T. (2010) Identification of defect position in a wooden beam from the power spectrum of longitudinal vibration. *J. Wood Sci.* 56(2):112–117.
- Spanish Standard (1979) UNE 56–573–79. Características físico–mecánicas de la madera. Determinación de la resistencia a la flexión estática. [*Physical–mechanical characteristics of wood. Determination of static flexural strength*]. Asociación Española de Normalización, Madrid, Spain.
- Spycher, M., Schwarze, F.W.M.R., Steiger, R. (2008) Assessment of resonance wood quality by comparing its physical and histological properties. *Wood Sci. Technol.* 42(4):325–342.
- Wang, S.Y., Chen, J.H., Tsai, M.J., Lin, C.J., Yang, T.H. (2008) Grading of softwood lumber using non–destructive techniques. *J. Mater. Process. Tech.* 208(1–3):149–158.
- Weaver, W., Timoshenko, S., Young, D.H. (1990) *Vibration problems in engineering*. Wiley: New York, USA.
- Yoshihara, H. (2012) Examination of the specimen configuration and analysis method in the flexural and longitudinal vibration tests of solid wood and wood–based materials. *For. Prod. J.* 62(3):191–200.

CAPÍTULO 5

Edgewise and flatwise bending

Fernández-Serrano, Á., Villasante, A. Alterations to the bending mechanical properties of *Pinus sylvestris* L. timber according to test direction and knot position in the cross-section.

5. Alterations to the bending mechanical properties of *Pinus sylvestris* L. timber according to test direction and knot position in the cross-section

5.1. Abstract

Given the heterogeneity of the material, the behaviour of a timber beam may differ depending on which of its sides is subjected to tension and which one is subjected to compression. An analysis is undertaken in the present work of the behaviour in non-destructive bending tests on the four sides of 57 samples of *Pinus sylvestris* L. of structural size ($2000 \times 100 \times 70 \text{ mm}^3$). A study is additionally performed of the influence of the size and position of knots in the cross-section. The modulus of elasticity (MOE) in flatwise direction was found to be 3% higher than in edgewise direction. This difference could be attributable to the shear effect. While the introduction of knottiness variables did not improve MOE prediction, it did decrease the error in the prediction of the modulus of rupture (MOR). The margin knot area ratio corresponding to the outer eighth of the cross-section's width occupied by knots was the knottiness variable with the lowest error in MOR prediction.

Keywords: edgewise; flatwise; margin knot area ratio; MOE; MOR

5.2. Introduction

Various authors have investigated the mechanical properties of *Pinus sylvestris* L. timber through bending tests in order to know the modulus of elasticity (MOE) and the modulus of rupture (MOR) (Arriaga *et al.* 2012; Krzosek *et al.* 2021; Ranta–Maunus *et al.* 2011). Bending tests have been complemented with different non-destructive testing (NDT) techniques, including the vibration test (Arriaga *et al.* 2012; Hassan *et al.* 2013; Villasante *et al.* 2019). In this way, the stiffness and bending strength could be easily predicted.

Some studies on conifers have attempted to improve the prediction of mechanical properties made with NDT by adding different variables related to the features of sawn timber. Ranta–Maunus *et al.* (2011) in *Pinus sylvestris* L. and Simic *et al.* (2019) in *Picea sitchensis* studied the influence of density. Guntekin *et al.* (2013) in *Pinus brutia* and Martins *et al.* (2017) in *Pinus pinaster* studied the relationship between rate of growth

5. Edgewise and flatwise bending

and mechanical properties. Arriaga *et al.* (2007) studied the influence of wanes in *Pinus sylvestris* L., and Arriaga *et al.* (2014) the effect of the slope of grain in *Pinus radiata*.

Knottiness is one of the features with an important influence on the mechanical properties. This relationship has been studied in different works using *Pinus sylvestris* L. Conde García *et al.* (2007) used measurement of the relative diameter of the maximum knots on the face and on the edge. They verified that the inclusion of a knottiness variable improved MOE and MOR predictions made using models based exclusively on ultrasound speed. Hautamäki *et al.* (2014) found that MOR prediction from the MOE improved if the knot area ratio (KAR) was included in the model. Likewise, they found that MOE prediction on the basis of density improved when including KAR in the model. Arriaga *et al.* (2012) and Villasante *et al.* (2019) also used a similar measure of knottiness, the concentrated knot diameter ratio (CKDR). In both cases, the authors observed that adding the CKDR improved the prediction of MOR based on the longitudinal resonant frequency.

Some works have studied the influence of the position of knots along the piece. Baillères *et al.* (2012), in four-point bending tests using *Pinus radiata*, found that only the knots situated between the internal loading points had a significant contribution in the prediction of MOR. Wright *et al.* (2019), in tests with *Pinus taeda*, found that the best MOE prediction was obtained when including only the knots that were within 85% of the span and that the best MOR prediction was obtained with the knots located in 65% of the span.

In contrast, very few works have studied the influence of the position of knots in the cross-section (tension or compression zones). In these cases, the margin knot area ratio (MKAR) was used, which is included in BS 4978 (2017). The margin zone used was a quarter of the width in the upper and lower margins. Lam *et al.* (2005), in tests made with *Pseudotsuga menziesii*, found that the KAR and MKAR could be used to establish grades for Canadian Douglas fir timber. Algin (2019) performed a multivariate optimisation on machine graded scaffold boards from *Picea sitchensis*, including the KAR and MKAR simultaneously. In order to predict the mechanical characteristics of *Picea abies*, Lukacevic *et al.* (2015) constructed linear multivariate models that included some knot position measurements in the cross-section. Guindos and Guaita (2014) performed a theoretical simulation based on the characteristics of *Pinus sylvestris* L. timber to determine the influence of knot type and size, as well as its position in the cross-section. Their theoretical models indicated that the highest MOR decrease was due to the presence of margin knots (the knots most distant from the centre of the cross-section).

As wood is a heterogenous and anisotropic material, the choice of the tension side in the bending test can have a significant effect on the mechanical properties. This is important when comparisons are made of results obtained by machine grading performed with a continuous lumber tester with those obtained through conventional bending tests. In the first case the samples are normally bent flatwise, whereas in the second the bending is commonly performed in edgewise direction. For this reason, it is of fundamental importance to know the relationship between the results of the tests in the two directions. Despite this, only very few works have studied this relationship. Some authors have found a high correlation between the MOE values calculated via bending in edgewise and flatwise directions. These include Kim *et al.* (2010) in southern pine ($R^2 = 0.69$), Baillères *et al.* (2012) in *Pinus radiata* ($R^2 = 0.70$), Yang *et al.* (2015) in different conifers ($R^2 = 0.85$) and Pošta *et al.* (2016) in *Picea abies* ($R^2 = 0.88$). Baillères *et al.* (2012) obtained a weak relationship ($R^2 = 0.41$) for the multiple linear regression with the MOE in flatwise direction and knottiness to predict the MOR in edgewise direction.

The aims of the present study were (1) to analyse the mechanical properties obtained via edgewise and flatwise bending tests in samples of *Pinus sylvestris* L., and (2) to verify whether the variables that take into account knot position in the cross-section can improve prediction of the mechanical bending properties calculated in both directions. Grading of *Pinus sylvestris* L. timber from the Montsec mountains (Spain) was not an objective of this work.

5.3. Materials and methods

5.3.1. Materials

The study was carried out using 57 samples of *Pinus sylvestris* L. with a size of 70 x 100 x 2000 mm³ obtained from the province of Lleida (NE Spain). The pieces were selected randomly from a batch of unclassified timber at a local sawmill. Each sample was marked with a number. Each of the four sides was marked with a letter, A and C for the edges and B and D for the faces (Figure 5.1). The wood was stored for 10 months in the interior of a test laboratory until reaching constant weight (maximum difference of $\pm 0.1\%$ between weightings made with a time interval of 6 h) in accordance with EN 408:2011+A1 (2012).

5.3.2. Bending tests

The samples were subjected to a non-destructive four-point bending test using a 50-kN universal testing machine (Cohiner, Spain) to know the global MOE in accordance with EN 408:2011+A1 (2012). The test was performed four times, placing the loading heads on each of the four sides of the sample (Figure 5.1) to obtain four positional global MOE values (MOE_A , MOE_B , MOE_C , MOE_D). On the basis of these values, the mean MOE values in edgewise direction (MOE_{edge} , from MOE_A and MOE_C) and in flatwise direction (MOE_{flat} from MOE_B and MOE_D) were obtained. For this test, a linear displacement transducer with spring (AEP Transducers, Italy) was used situated on the lower part of the piece. The distance between supports (1800 mm) was the same for the tests in edgewise and flatwise direction, and so the length-to-depth ratio was 18 and 25.7, respectively. The MOE was calculated with Equation 5.1 (EN 408:2011+A1 2012) using the stress-strain curve in the loading area between 10% and 40% of the estimated ultimate bending strength. It was verified that the linear regression presented an R^2 value above 0.99 for all the samples.

$$MOE = \frac{3aL^2 - 4a^3}{2bh^3 \left(2\frac{\Delta w}{\Delta F} - \frac{6a}{5Gb} \right)} \quad (5.1)$$

where MOE is the modulus of elasticity, L is the distance between supports, a is the distance between the loading heads, b and h are the width and the depth of the sample, Δw is the increase in deformation, ΔF is the increase in force and G is the shear modulus. As allowed in EN 408:2011+A1 (2012), the shear effect was ignored taking a value G equal to infinity.

Test with other values of G were made in Equation 1 to analyse the influence of the shear effect on MOE_{edge} and MOE_{flat} . Firstly, 650 MPa was used as also permitted in EN 408:2011+A1 (2012). A value of G equal to the MOE divided by 16 was also considered (EN 338 2016). A value of G equal to the MOE divided by 17 was then used, as proposed by Brancherieu *et al.* (2002). Finally a value of G was calculated to make both MOE values (MOE_{edge} and MOE_{flat}) equal. These three values of G were obtained by iterative calculation.

The samples were also subjected to a destructive four-point bending test in edgewise direction to determine the MOR in accordance with EN 408:2011+A1 (2012). In this case, a different displacement transducer (Burster, Germany) was used situated on the mid-point of the side subjected to tension. The loading heads were always positioned on side A

(Figure 5.1) until rupture to obtain the MOR_A . In this test, another global MOE value was also obtained (MOE_{AR}). The MOE_A and MOE_{AR} values should be identical but may present slight differences as two different displacement transducers were used and the wood was repositioned between both bending tests (destructive and non-destructive). The MOE_{AR} was used as reference to analyse MOE variability according to the side on which the test was performed.

The final moisture content (MC) of each sample was measured immediately after the bending tests with the oven dry method at 103 °C in accordance with EN 13183–1 (2002). No adjustments were made based on MC because all of the samples presented similar MC values and all the tests for each sample were conducted within an interval of less than one hour.

5.3.3. Knottiness

Two different criteria were followed to measure knottiness (Appendix 1). In the first approach, the width of each knot was measured in the direction perpendicular to the length of the piece in accordance with Annex A of EN 1309–3 (2018). Two variables were obtained from this measurement, $knot_{tot}$ when the sum of all the knots of the sample was included, and $knot_{1/3}$ when only the knots situated in the central third of the sample were included. The second approach used (Figure 5.1) was based on the knot area ratio (KAR), that indicates the proportion of the complete cross-section occupied by knots (Walker 1993). The margin knot area ratio (MKAR), that indicates the proportion of the margin cross-section occupied by knots, was used to determine the influence of the position of the knots with respect to the direction of the load. The MKAR allowed variables of positional knottiness to be obtained.

The $MKAR_{1/4}$ (BS 4978 2017) was measured, using as margin the outer quarter of the cross-section's width. The $MKAR_{1/8}$ was also measured, using as margin the outer eighth of the cross-section's width. The MKAR (Figure 5.1) were measured taking into account the direction of the bending test (edgewise or flatwise). In addition, it was also taken into account if the margin area was subjected to tension or compression. In this way, a total of 12 different MKAR-based measures of positional knottiness were obtained (see Appendix 1).

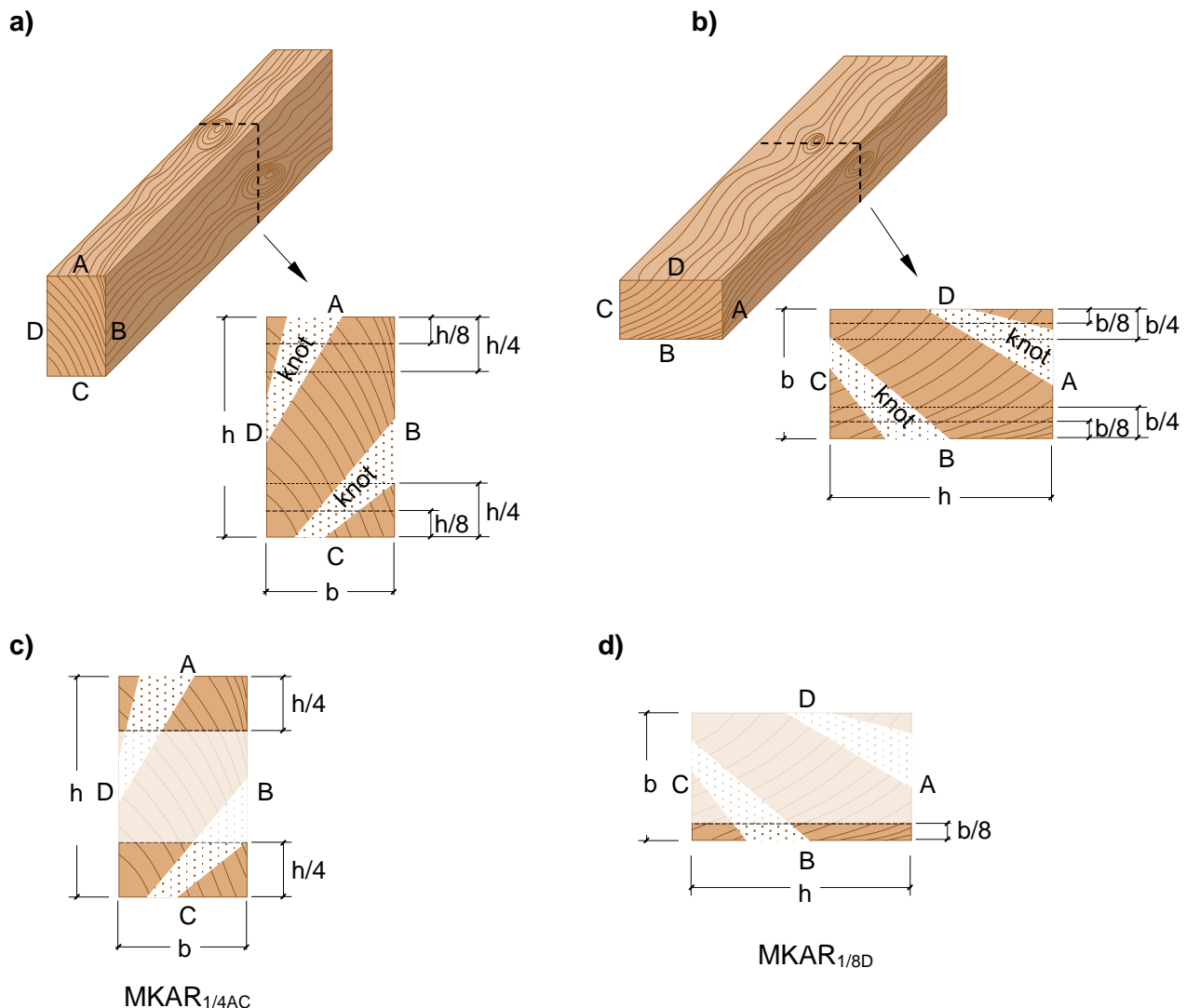


Figure 5.1: Knottiness measures based on the KAR: a) Cross-section, edgewise direction, b) Cross-section, flatwise direction, c) example of $\text{MKAR}_{1/4}$, proportion of the margin cross-section ($h/4$) occupied by knots when the sample was tested in edgewise direction (loading heads on A), d) example of $\text{MKAR}_{1/8}$, proportion of the margin cross-section of tension ($b/8$) occupied by knots when the sample was tested in flatwise direction (loading heads on D)

5.3.4. Statistical analyses

The prediction was studied through simple linear regression (SLR) of the MOE_{AR} and MOR_{A} on the basis of each of the 12 variables of knottiness (Appendix 1) and the four positional MOE (MOE_A , MOE_B , MOE_C , and MOE_D). This first calculation allowed selection of the knottiness variables with the best predictive capacity. Attempts were then made to improve the predictive capacity of the SLR models using multiple linear regression (MLR)

models of two variables. These models comprised a positional MOE and a knottiness variable.

The root-mean-square error (RMSE) was used instead of the coefficient of determination (R^2), commonly used in most previous studies, to assess the goodness-of-fit of the different models. This decision was adopted because it is more important to know the precision of the values generated by a model (RMSE) than to quantify the variability (R^2) of the predicted values (Alexander *et al.* 2015; Mansfield *et al.* 2007). Nonetheless, the R^2 value was also calculated to enable a comparison of the results obtained with those of other authors.

The models obtained from the whole dataset can be affected by overfitting because they are also fitted to the noise of the sample. For small datasets, the K-fold cross-validation can help avoid overfitting (Lever *et al.* 2016). In the present study, the 10-fold cross-validation method (Faydi *et al.* 2017; Hashim *et al.* 2016; Villasante *et al.* 2019) was used to calculate the RMSE of each model. The samples were randomly split into 10 groups of folds, using each group to validate the model generated with the remaining 9. This procedure was repeated 5 times to obtain 50 RMSE values for each model. WEKA 3.6 software (Waikato University 2014) was used to carry out this process. For the purposes of comparison with other studies, the 10-fold cross-validation was not applied in the calculation of R^2 .

The non-parametric Kruskal-Wallis test was used to compare the RMSE values of each model. If statistically significant differences between the RMSE were found, a post hoc analysis was carried out using Dunn's test with Bonferroni adjustment. The Kruskal-Wallis test and post hoc analysis were performed with R 3.6.1 software (R Core Team 2019). In all cases, the level of significance was 0.05.

5.4. Results and discussion

The MC, MOE, MOR and knottiness values observed in the samples are shown in Table 5.1. The differences in MC between samples were small. The mean MOE values obtained for the different sides ranged between 7600 and 7900 MPa. These values were slightly lower than those observed by other authors in *Pinus sylvestris* L. (Arriaga *et al.* 2012; Krzosek *et al.* 2021; Ranta-Maunus *et al.* 2011). This can be attributed to the fact that in the present study unclassified structural timber was used.

Table 5.1. Summary of the study variables

Variable	Units	Mean value	SD	CV (%)
MC	%	11.3	0.67	5.90
knot _{tot}	mm	283	166	58.7
knot _{1/3}	mm	78	61	78.2
KAR	mm ² · mm ⁻²	0.24	0.17	70.8
MKAR _{1/4A}	mm ² · mm ⁻²	0.27	0.25	92.6
MKAR _{1/4B}	mm ² · mm ⁻²	0.22	0.23	104.5
MKAR _{1/4C}	mm ² · mm ⁻²	0.23	0.26	113.0
MKAR _{1/4D}	mm ² · mm ⁻²	0.26	0.24	92.3
MKAR _{1/4AC}	mm ² · mm ⁻²	0.25	0.20	80.0
MKAR _{1/4BD}	mm ² · mm ⁻²	0.24	0.17	70.8
MKAR _{1/8A}	mm ² · mm ⁻²	0.28	0.26	92.9
MKAR _{1/8B}	mm ² · mm ⁻²	0.21	0.23	109.5
MKAR _{1/8C}	mm ² · mm ⁻²	0.23	0.27	117.4
MKAR _{1/8D}	mm ² · mm ⁻²	0.27	0.26	96.3
MKAR _{1/8AC}	mm ² · mm ⁻²	0.26	0.20	76.9
MKAR _{1/8BD}	mm ² · mm ⁻²	0.24	0.18	75.0
MOE _A	MPa	7701	1838	23.9
MOE _B	MPa	7879	2038	25.9
MOE _C	MPa	7647	1829	23.9
MOE _D	MPa	7869	1998	25.4
MOE _{edge}	MPa	7674	1829	23.8
MOE _{flat}	MPa	7874	2011	25.5
MOEAR	MPa	7717	1849	24.0
MORA	MPa	40.0	15.6	39.0

MC: moisture content; knot_{tot}: knots measured in accordance with EN 1309-3; knot_{1/3}: as the previous but just for the central third; KAR: knot area ratio; MKAR_{1/4*i*}, MKAR_{1/8*i*}: margin knot area ratio, the margin is the outer quarter or eighth of the cross-section subjected to tension when the loading heads are situated on side *i* (A, B, C, or D). When *i* is AC the sample was tested in edgewise direction and both margins, tension and compression had been considered. When *i* is BD, as the previous but in flatwise direction; MOE_{*i*}: global modulus of elasticity, loading heads on side *i* (A, B, C, or D); MOE_{edge}: global MOE in edgewise direction, mean value of MOE_A and MOE_C; MOE_{flat}: global MOE in flatwise direction, mean value of MOE_B and MOE_D; MOEAR: global MOE obtained in the destructive bending test. MORA: modulus of rupture in edgewise direction, loading heads situated on side A

In the case of the MOR a mean value of 40.0 MPa was obtained, similar to that obtained in other studies with *Pinus sylvestris* L. in Spain (Arriaga *et al.* 2012; Villasante *et al.* 2019). As for knottiness, a mean KAR value of 0.24 was obtained with high coefficient of variation (CV) values. This high variability between samples was a consequence of the

random selection of unclassified samples. Similar KAR values were observed by Hautamäki *et al.* (2014) in *Pinus sylvestris* L. (from 0.17 to 0.29), Hautamäki *et al.* (2013) in *Picea abies* (from 0.17 to 0.21) and Steffen *et al.* (1997) in *Picea abies* (from 0.17 to 0.24). For the different MKAR-related variables, values of around 0.25 were also obtained with a very high variability.

5.4.1. Comparison of MOE_{flat} and MOE_{edge}

The MOE_{flat} value was 2.6% higher than the MOE_{edge} value (Table 5.2). This difference can be attributed to the shear effect. When the deformation is measured over the entire length of the beam (global MOE), deformations due to shear are included in the total measured deformation (Boström 1999). In consequence, for both MOE_{flat} and MOE_{edge}, in reality an apparent value was obtained that underestimated the true MOE value. The shear effect increases as the length-to-depth ratio decreases (Timoshenko 1938), which explains how MOE_{flat} was higher than MOE_{edge} (length-to-depth ratio of 25.7 and 18, respectively). The shear effect is especially important in wood because the MOE/G ratio is particularly high in comparison with an isotropic elastic material (Brancherieu *et al.* 2002). These results coincide with those of Kim *et al.* (2010) who, in three pine species of Korea, also found that MOE_{flat} was higher than MOE_{edge} (between 1.3% and 6.1%). These authors used a length-to-depth ratio in flatwise direction between 23% and 45% higher than in edgewise direction. This length-to-depth ratio value was similar to that of the present study (25.7%), which explains the similar relationships between the MOE values. However, Boström (1994) and Steffen *et al.* (1997) obtained the opposite result in *Picea abies*, with MOE_{flat} between 20% and 40% lower than MOE_{edge}. This discrepancy can be put down to two reasons. Firstly, these authors used different spans for the different bending directions, and so the length-to-depth ratio in flatwise direction was up to 30% lower than in edgewise direction. With this arrangement, the shear effect caused an increase in the underestimation of the MOE in flatwise direction. Secondly, these authors used a four-point bending test in edgewise direction and a three-point bending test in flatwise direction. Brancherieu *et al.* (2002) found that a three-point bending test underestimates by about 19% the MOE value in relation to a four-point loading test.

The differences detected between MOE_{flat} and MOE_{edge} should be taken into account when the pieces are classified by bending tests in flatwise direction and are subsequently installed in the structure in edgewise direction. Currently, classification is commonly made on the basis of flatwise direction tests because less loading is required to deform the pieces, as is the case of continuous lumber testers.

5. Edgewise and flatwise bending

The MOE_{edge} and MOE_{flat} results with the different tested G values are shown in Table 5.2. When the shear effect is ignored ($G = \infty$) higher differences between both MOE are found. The value of 650 MPa proposed in EN 408:2011+A1 (2012) decreased the differences, but does not seem to be an appropriate value as it is a generic value for any MOE value and any species of softwood. Lower differences between MOE_{edge} and MOE_{flat} were observed with a G value equal to the MOE divided by 16 (EN 338 2016) and divided by 17 (Brancherieu *et al.* 2002). The differences between MOE_{edge} and MOE_{flat} disappeared for a G value equal to the MOE divided by 18.2. All indications are that the differences between the MOE_{edge} and MOE_{flat} values were due to shear effect differences caused by modifications to the length-to-depth ratio.

Table 5.2. MOE_{flat} y MOE_{edge} according to different G values

G (MPa)	MOE_{edge} (MPa)	MOE_{flat} (MPa)	Increase of MOE_{flat} with respect to MOE_{edge}
$\infty^{(1)}$	7674	7874	+ 2.61%
650 ⁽¹⁾	7946	8012	+ 0.83%
503 ⁽²⁾	8028	8053	+ 0.31%
474 ⁽³⁾	8051	8065	+ 0.17%
444 ⁽⁴⁾	8078	8078	0

G : shear modulus; MOE_{flat} , MOE_{edge} : global modulus of elasticity in edgewise and flatwise direction, respectively

⁽¹⁾proposed by European Standard EN 408:2011+A1 (2012)

⁽²⁾proposed by European Standard EN 338 (2016)

⁽³⁾proposed by Brancherieu *et al.* (2002)

⁽⁴⁾value of G that makes both MOE values equal

⁽²⁾⁽³⁾⁽⁴⁾ G values obtained by iterative calculation

5.4.2. Selection of knottiness variables for MOE and MOR prediction

The predictive capacity of mechanical characteristics on the basis of knottiness variables is shown in Table 5.3. In the MOE_{AR} prediction, the lowest RMSE value was obtained with $\text{knot}_{1/3}$ and knot_{tot} , the two knot variables based on EN 1309–3 (2018). These knot measures achieved better predictions than the local measures associated to KAR. The explanation for this is that the MOE values the global behaviour of the piece. The $\text{knot}_{1/3}$

variable obtained the lowest RMSE value because the highest bending moment values in the four-point bending test are given in the central third of the piece.

As for the MOR_A , the lowest RMSE values were obtained with $MKAR_{1/8AC}$. This shows that the knots situated in the tension and compressions margins are those which have the highest influence on rupture because this is where the highest bending stress values are found.

Table 5.3 Simple Linear Regression based on knottiness to predict MOE_{AR} and MOR_A .

	MOE_{AR}		MOR_A	
	RMSE (MPa)	R^2	RMSE (MPa)	R^2
knot _{tot}	1538	0.30	10.59	0.51
knot _{1/3}	1458	0.37	11.59	0.45
KAR	1671	0.16	10.81	0.51
$MKAR_{1/4A}$	1783	0.04	11.45	0.45
$MKAR_{1/4B}$	1728	0.08	13.39	0.23
$MKAR_{1/4C}$	1700	0.11	13.75	0.20
$MKAR_{1/4D}$	1744	0.11	13.39	0.26
$MKAR_{1/4AC}$	1706	0.12	10.61	0.53
$MKAR_{1/4BD}$	1644	0.18	11.22	0.48
$MKAR_{1/8A}$	1803	0.01	12.04	0.39
$MKAR_{1/8B}$	1711	0.11	13.28	0.24
$MKAR_{1/8C}$	1677	0.15	13.23	0.26
$MKAR_{1/8D}$	1757	0.11	14.02	0.20
$MKAR_{1/8AC}$	1714	0.11	10.09	0.57
$MKAR_{1/8BD}$	1618	0.21	11.80	0.42

RMSE calculated with the mean value of the 50 RMSE values (10-fold cross-validation, 5 repetitions). R^2 calculated with the whole dataset. MOE_{AR} : global MOE obtained in the destructive bending test. MOR_A : modulus of rupture in edgewise direction, loading heads situated on side A; knot_{tot}: knots measured in accordance with EN 1309-3; knot_{1/3}: as the previous but just for the central third; KAR: knot area ratio; $MKAR_{1/4i}$, $MKAR_{1/8i}$: margin knot area ratio, the margin is the outer quarter or eighth of the cross-section subjected to tension when the loading heads are situated on side i (A, B, C, or D). When i is AC the sample was tested in edgewise direction and both margins, tension and compression had been considered. When i is BD, as the previous but in flatwise direction

The R^2 values obtained in the prediction of the MOR_A on the basis of knottiness variables were higher than those obtained in the MOE_{AR} prediction (Table 5.3), which concurs with the observations of other authors in *Pinus sylvestris* L. (Conde García *et al.*

2007; Šilinskas *et al.* 2020) and in other pine species (Conde García *et al.* 2007; França *et al.* 2019; Wright *et al.* 2019). Only in one study was the opposite trend observed (Hautamäki *et al.* 2013, 2014).

5.4.3. Linear Regression to predict the MOE

Table 5.4 shows the predictive capacity of the MOE_{AR} (reference MOE) obtained on the basis of the four positional MOE (MOE_A , MOE_B , MOE_C , MOE_D). With respect to the differences between the four sides, MOE_A was the best MOE_{AR} predictor, which was expected as, although the sample was repositioned, the loading heads were positioned on the same side. MOE_B and MOE_D , both carried out in flatwise direction, obtained the worst prediction result, almost doubling the RMSE obtained with MOE_A . The explanation for this difference is that the test taken as reference (MOE_{AR}) corresponds to the edgewise direction.

Table 5.4. RMSE of the linear regression to predict MOE_{AR}

Variable	RMSE ⁽¹⁾ (MPa)	$\Delta \text{RMSE}^{(2)}$ (%)
$1.00001 \times \text{MOE}_A + 15.39$	194.0 ^a	+0.2
$1.00364 \times \text{MOE}_A + 0.17577 \times \text{knot}_{1/3} - 26.23$	197.3 ^a	+1.9
$1.01683 \times \text{MOE}_A + 0.32321 \times \text{knot}_{\text{tot}} - 205.70$	193.7 ^a	-
$0.8904 \times \text{MOE}_B + 701.68$	341.2 ^{bcd}	+76.1
$0.85951 \times \text{MOE}_B - 1.76229 \times \text{knot}_{1/3} + 1082.51$	331.7 ^{bcd}	+71.2
$0.87864 \times \text{MOE}_B - 0.26483 \times \text{knot}_{\text{tot}} + 869.52$	342.4 ^{bcd}	+76.8
$0.99975 \times \text{MOE}_C + 72.26$	270.2 ^{bc}	+39.5
$0.99310 \times \text{MOE}_C - 0.32417 \times \text{knot}_{1/3} + 148.32$	274.5 ^{bc}	+41.7
$1.01940 \times \text{MOE}_C + 0.37190 \times \text{knot}_{\text{tot}} - 183.37$	268.7 ^b	+38.7
$0.90585 \times \text{MOE}_D + 588.90$	368.7 ^d	+90.3
$0.87478 \times \text{MOE}_D - 1.72791 \times \text{knot}_{1/3} + 967.97$	360.5 ^{cd}	+86.1
$0.88466 \times \text{MOE}_D - 0.47838 \times \text{knot}_{\text{tot}} + 891.16$	362.4 ^{cd}	+87.1

MOE in MPa, knot_{1/3}, and knot_{tot} in mm

(^{a b c}) The same letter indicates there are no statistically significant differences (Kruskal–Wallis test, post hoc Dunn's test with Bonferroni adjustment)

⁽¹⁾Mean value of the 50 RMSE values (10-fold cross-validation, 5 repetitions)

⁽²⁾RMSE increase with respect to the model with the lowest error

MOE_{AR} : global MOE obtained in the destructive bending test. knot_{tot}: knots

measured in accordance with EN 1309-3; knot_{1/3}: as the previous but just for the central third; MOE_i : global modulus of elasticity, loading heads on side *i* (A, B, C, or D)

It was also observed that adding a knottiness variable to any of the positional MOE did not improve MOE_{AR} prediction, and so the multivariable models offered no advantage. França *et al.* (2020) in southern pine and Wright *et al.* (2019) in *Pinus taeda* also found that introducing a knottiness variable in an MLR together with the dynamic MOE did not improve the prediction of the static MOE.

5.4.4. Linear Regression to predict the MOR

Table 5.5 shows the predictive capacity of the MOR obtained on the basis of the four positional MOE and the knottiness variables. No statistically significant differences were found between the MOR predictions made through SLR on the basis of any of the four positional MOE.

Table 5.5. Linear regression to predict the MOR_A

Model	RMSE ⁽¹⁾ (MPa)	ΔRMSE ⁽²⁾ (%)	R ²
0,00561×MOE _A -3,21	11.71 ^c	+48.8	0.44
0,00383×MOE _A -45,6×MKAR _{1/8AC} +22,2	7.93 ^{ab}	+0.8	0.75
0,00322×MOE _A -0,0461×knot _{tot} +28,3	10.09 ^{bc}	+28.2	0.60
0,00491×MOE _B +1,37	11.99 ^c	+52.4	0.41
0,00337×MOE _B -39,8×MKAR _{1/8BD} +23,1	10.41 ^c	+32.3	0.57
0,00277×MOE _B -0,0480×knot _{tot} +31,8	10.13 ^c	+28.7	0.60
0,00571×MOE _C -3,62	11.61 ^c	+47.5	0.45
0,00391×MOE _C -45,3×MKAR _{1/8AC} +21,7	7.87 ^a	-	0.75
0,00331×MOE _C -0,0455×knot _{tot} +27,6	10.01 ^{abc}	+27.2	0.61
0,00494×MOE _D +1,19	12.08 ^c	+53.5	0.40
0,00340×MOE _D -40,8×MKAR _{1/8BD} +23,1	10.38 ^c	+31.9	0.57
0,00277×MOE _D -0,0488×knot _{tot} +32,0	10.11 ^c	+28.5	0.59

MOE in MPa, MKAR in mm²·mm⁻², knot_{tot} in mm

^(a b c) The same letter indicates there are no statistically significant differences (Kruskal–Wallis test, post hoc Dunn's test with Bonferroni adjustment)

⁽¹⁾Mean value of the 50 RMSE values (10-fold cross-validation, 5 repetitions) ⁽²⁾RMSE increase with respect to the model with the lowest error. knot_{tot}: knots measured in accordance with EN 1309-3; MKAR_{1/8AC}: margin knot area ratio, the margins are the outer eightths of the width when the sample was tested in edgewise direction; MKAR_{1/8BD}: as the previous but in flatwise direction; MOE_i: global modulus of elasticity, loading heads on side *i* (A, B, C, or D); MOR_A: modulus of rupture in edgewise direction, loading heads situated on side A

Inclusion in the model of the knot_{tot} variable did give improvements to the prediction but these were not statistically significant. The situation changed when including MKAR_{1/8} in the model as a knottiness variable. When adding this variable, the two tests performed in edgewise direction predicted MOR with a statistically significant lower RMSE (around 48%) than that of the tests in flatwise direction. The R² value also improved, with an increase of 0.30. However, this reduction in the error was clearly lower in flatwise direction.

This trend concurred with that observed by other authors in *Pinus sylvestris* L. who also obtained improvements in MOR prediction on the basis of the MOE when introducing a knottiness variable in the model. None of the studies used positional variables of knottiness similar to the MKAR_{1/8} used in the present study. Hautamaki *et al.* (2014) observed an RMSE reduction of 3% and an R² increase of 0.05. Villasante *et al.* (2019) obtained an RMSE reduction of 6% and an R² increase of 0.07. Arriaga *et al.* (2012) and Conde García *et al.* (2007) observed increases of 0.04 and 0.16, respectively, in the R² value. França *et al.* (2020, 2019) in southern pine and Wright *et al.* (2019) in *Pinus taeda* obtained an R² increase of between 0.05 and 0.17. In these studies, the R² increase when including a knottiness variable in the MOR prediction (between 0.04 and 0.17) was some distance from the 0.31 increase obtained in the present study. This result shows the advantage of using the positional knottiness variable MKAR_{1/8} in the MOR prediction.

5.5. Conclusions

The MOE calculated in flatwise direction was higher than the MOE calculated in edgewise direction. The difference between the two values could be explained by the shear effect.

A ratio of 18 between the MOE and the shear modulus was obtained. This value is close to the ratio of 17 proposed by Brancherieu *et al.* (2002), the relationship found in previous works that best explained the differences between the flatwise and edgewise directions.

Knottiness measured in accordance with Annex A of EN 1309–3 (2018) was the best MOE predictor. The positional measures of knottiness which take into account the position of knots in the cross-section were the most useful for MOR prediction. Of these positional measures, MKAR_{1/8} produced the lowest error in MOR prediction.

No differences were found in MOR prediction in edgewise direction on the basis of the four positional MOE (MOE_A, MOE_B, MOE_C, and MOE_D). However, when including the

positional variable MKAR_{1/8} in the prediction, the MOE obtained in edgewise direction presented statistically significantly lower RMSE values than the MOE in flatwise direction.

The RMSE value in MOR prediction on the basis of the MOE decreased by 32.3% when the positional knottiness variable MKAR_{1/8} was added.

The differences between MOE_{edge} and MOE_{flat} should be taken into account when the wood is classified with a bending test in one direction and is installed in the structure in another direction.

5.6. References

- Alexander, D.L.J., Tropsha, A., Winkler, D.A. (2015) Beware of R²: Simple, Unambiguous Assessment of the Prediction Accuracy of QSAR and QSPR Models. *J. Chem. Inf. Model.* 55(7):1316–1322.
- Algin, Z. (2019) Multivariate performance optimisation of scaffold boards with selected softwood defects. *Constr. Build. Mater.* 220:667–678.
- Arriaga, F., Esteban, M., Argüelles, R., Bobadilla, I., Íñiguez-González, G. (2007) The effect of wanes on the bending strength of solid timber beams. *Mater. Constr.* 57(288):61–76.
- Arriaga, F., Íñiguez-Gonzalez, G., Esteban, M., Divos, F. (2012) Vibration method for grading of large cross-section coniferous timber species. *Holzforschung* 66(3):381–387.
- Arriaga, F., Monton, J., Segues, E., Íñiguez-Gonzalez, G. (2014) Determination of the mechanical properties of radiata pine timber by means of longitudinal and transverse vibration methods. *Holzforschung* 68(3):299–305.
- Baillères, H., Hopewell, G., Boughton, G., Brancherieu, L. (2012) Strength and stiffness assessment technologies for improving grading effectiveness of radiata pine wood. *BioResources* 7(1):1264–1282.
- Boström, L. (1994) Machine strength grading. Comparison of four different systems. Swedish National Testing and Research Institute. SP Report 1994:49.
- Boström, L. (1999) Determination of the modulus of elasticity in bending of structural timber – Comparison of two methods. *Holz Als Roh–und Werkst.* 57(2):145–149.
- Brancherieu, L., Bailleres H., Guitard, D. (2002) Comparison between modulus of elasticity values calculated using 3 and 4 point bending tests on wooden samples. *Wood Sci. Technol.* 36(5):367–383.
- British Standard (2017) BS 4978:2017. Visual strength grading of softwood. Specification. British Standards Institution: London, UK.

5. Edgewise and flatwise bending

- Conde García, M., Fernández-Golfín Seco, J.I., Hermoso Prieto, E. (2007) Mejora de la predicción de la resistencia y rigidez de la madera estructural con el método de ultrasonidos combinado con parámetros de clasificación visual. [*Improving the prediction of strength and rigidity of structural timber by combining ultrasound techniques with visual grading parameters*]. Mater. Constr. 57(288):49–59.
- European Standard (2002) EN 13183–1:2002. Moisture content of a piece of sawn timber. Part 1: Determination by oven dry method. European Committee for Standardization (CEN): Brussels, Belgium.
- European Standard (2012) EN 408:2010+A1:2012. Timber structures. Structural timber and glued laminated timber. Determination of some physical and mechanical properties. European Committee for Standardization (CEN): Brussels, Belgium.
- European Standard (2016) EN 338:2016. Structural timber. Strength classes. European Committee for Standardization (CEN): Brussels, Belgium.
- European Standard (2018) EN 1309–3:2018. Round and sawn timber – Methods of measurements – Part 3: Features and biological degradations. European Committee for Standardization (CEN): Brussels, Belgium.
- Faydi, Y., Brancherieu, L., Pot, G., Collet, R. (2017) Prediction of oak wood mechanical properties based on the statistical exploitation of vibrational response. BioResources 12(3):5913–5927.
- Fernández-Serrano, Á., Villasante, A. (2022) Modulus of Rupture Prediction in *Pinus sylvestris* with Multivariate Models Constructed with Resonance, Ultrasound, and Wood Heterogeneity Variables. BioResources 17(1):1106–1119.
- França, F.J.N., França, T.S.F.A., Seale, R.D., Shmulsky, R. (2020) Use of longitudinal vibration and visual characteristics to predict mechanical properties of No. 2 southern pine 2x8 and 2x10 lumber. Wood Fiber Sci. 52(3):280–291.
- França, F.J.N., Seale, R.D., Shmulsky, R., França, T.S.F.A. (2019) Modeling mechanical properties of 2 by 4 and 2 by 6 southern pine lumber using longitudinal vibration and visual characteristics. For. Prod. J. 68(3):286–294.
- Guindos, P., Guaita, M. (2014) The analytical influence of all types of knots on bending. Wood Sci. Technol. 48(3):533–552.
- Guntekin, E., Emiroglu, Z., Yilmaz, T. (2013) Prediction of bending properties for Turkish Red Pine (*Pinus brutia* Ten.) Lumber using stress wave method. BioResources 8(1):231–237.
- Hashim, U.R., Hashim, S.Z.M., Muda, A.K. (2016) Performance evaluation of multivariate texture descriptor for classification of timber defect. Optik 127(15):6071–6080.
- Hassan, K.T.S., Horacek, P., Tippnera, J. (2013) Evaluation of stiffness and strength of Scots pine wood using resonance frequency and ultrasonic techniques. BioResources 8(2):1634–1645.
- Hautamäki, S., Kilpeläinen, H., Verkasalo, E. (2013) Factors and models for the bending properties of sawn timber from Finland and north-western Russia. Part I: Norway spruce. Baltic For. 19(1):106–119.

- Hautamäki, S., Kilpeläinen, H., Verkasalo, E. (2014) Factors and models for the bending properties of sawn timber from Finland and north-western Russia. Part II: Scots pine. *Baltic For.* 20(1):142–156.
- Kim, K.-M., Shim, K.-B., Lum, C. (2010). Predicting tensile and compressive moduli of structural lumber. *Wood Fiber Sci.* 43(1):83–89.
- Krzosek, S., Grześkiewicz, M., Burawska-Kupniewska, I., Mańkowski, P., Wieruszewski, M. (2021) Mechanical properties of polish-grown *Pinus sylvestris* L. structural sawn timber from the butt, middle and top logs. *Wood Res.* 66(2):231–242.
- Lam, F., Barrett, J.D., Nakajima, S. (2005) Influence of knot area ratio on the bending strength of Canadian Douglas fir timber used in Japanese post and beam housing. *J. Wood Sci.* 51(1):18–25.
- Lever, J., Krzywinski, M., Altman, N. (2016) Model selection and overfitting. *Nat. Methods.* 13(9):703–704.
- Lukacevic, M., Füssl, J., Eberhardsteiner, J. (2015) Discussion of common and new indicating properties for the strength grading of wooden boards. *Wood Sci. Technol.* 49(3):551–576.
- Mansfield, S.D., Iliadis, L., Avramidis, S. (2007) Neural network prediction of bending strength and stiffness in western hemlock (*Tsuga heterophylla* Raf.). *Holzforschung* 61(6):707–716.
- Martins, C.E.J., Dias, A.M.P.G., Marques, A.F.S., Dias, A.M.A. (2017) Non-destructive methodologies for assessment of the mechanical properties of new utility poles. *BioResources* 12(2):2269–2283.
- Pošta, J., Ptáček, P., Jára, R., Terebesyová, M., Kuklík, P., Dolejš, J. (2016) Correlations and differences between methods for non-destructive evaluation of timber elements. *Wood Res.* 61(1):129–140.
- R Core Team (2019) R: A language and environment for statistical computing. Version 3.6.1. R Foundation for Statistical Computing, Vienna, Austria. <http://www.R-project.org/>.
- Ranta-Maunus, A., Denzler, J.K., Stapel, P. (2011) Strength of European timber. Part 2. Properties of spruce and pine tested in Gradewood project. VTT Technical Research Centre of Finland. VTT Working Papers, No. 179. <http://www.vtt.fi/inf/pdf/workingpapers/2011/W179.pdf>.
- Šilinskas, B., Varnagiryte-Kabašinskiene, I., Aleinikovas, M., Beniušiene, L., Aleinikoviene, J., Škema, M. (2020) Scots pine and norway spruce wood properties at sites with different stand densities. *Forests* 11(5):1–15.
- Simic, K., Gendvilas, V., O'Reilly, C., Harte, A.M. (2019) Predicting structural timber grade-determining properties using acoustic and density measurements on young Sitka spruce trees and logs. *Holzforschung* 73(2):139–149.
- Steffen, A., Johansson, C.J., Wormuth, E.W. (1997) Study of the relationship between flatwise and edgewise moduli of elasticity of sawn timber as a means to improve mechanical strength grading technology. *Holz Als Roh- und Werkst.* 55(4):245–253.

5. Edgewise and flatwise bending

Timoshenko, S. (1938) Strength of materials. D. Van Mostrand Company, Inc.: New York, USA.

Villasante, A., Iñiguez-Gonzalez, G., Puigdomenech, L. (2019) Comparison of various multivariate models to estimate structural properties by means of non-destructive techniques (NDTs) in *Pinus sylvestris* L. timber. Holzforschung 73(4):331–338.

Waikato University (2014) WEKA software. Version 3.6.12. Waikato University, Hamilton, New Zealand. <https://www.cs.waikato.ac.nz/ml/weka/>.

Walker, J. (1993) Primary Wood Processing: Principles and Practice. Chapman & Hall: London, UK.

Wright, S., Dahlen, J., Montes, C., Eberhardt, T.L. (2019) Quantifying knots by image analysis and modeling their effects on the mechanical properties of loblolly pine lumber. Eur. J. Wood Wood Prod. 77(5):903–917.

Yang, B.Z., Seale, R.D., Shmulsky, R., Dahlen, J., Wang, X. (2017) Comparison of nondestructive testing methods for evaluating no. 2 southern pine lumber: Part B, modulus of rupture. Wood Fiber Sci. 49(2):134–145.

APPENDIX 1: Knottiness and MOE variables. Description

Variable	Meaning
knot_{tot}	Sum of the cross dimensions of all the knots of the sample, in accordance with EN 1309-3
knot_{1/3}	As above, but only the knots found in the central third of the sample
KAR	Knot Area Ratio, the proportion of the cross-section occupied by the knots
MKAR_{1/4AC}	The proportion of the margin cross section (outer quarters: $h/4$) occupied by the knots when the sample is tested in edgewise direction (loading heads situated on sides A or C)
MKAR_{1/4BD}	The proportion of the margin cross section (outer quarters: $b/4$) occupied by the knots when the sample is tested in flatwise direction (loading heads situated on sides B or D)
MKAR_{1/4<i>i</i>}	The proportion of the margin cross section occupied by the knots. Margin: outer quarter subjected to tension when the loading heads are situated on side <i>i</i> (MKAR _{1/4A} , MKAR _{1/4B} , MKAR _{1/4C} , MKAR _{1/4D} for A, B, C, and D, respectively)
MKAR_{1/8AC}	The proportion of the margin cross section (outer eighth: $h/8$) occupied by the knots when the sample is tested in edgewise direction (loading heads situated on sides A or C)
MKAR_{1/8BD}	The proportion of the margin cross section (outer eighth : $b/8$) occupied by the knots when the sample is tested in flatwise direction (loading heads situated on sides B or D)
MKAR_{1/8<i>i</i>}	The proportion of the margin cross section occupied by the knots. Margin: outer eighth subjected to tension when the loading heads are situated on side <i>i</i> (MKAR _{1/8A} , MKAR _{1/8B} , MKAR _{1/8C} , MKAR _{1/8D} for A,B, C, and D, respectively)
MOE_i	Global MOE. Loading heads situated on side <i>i</i> (<i>i</i> = A, B, C, or D)
MOE_{edge}	Global MOE in edgewise direction, mean value of MOE _A and MOE _C
MOE_{edge}	Global MOE in flatwise direction, mean value of MOE _B and MOE _D
MOE_{AR}	Global MOE obtained in the destructive bending test. Loading heads situated on side A. Edgewise direction
MOR_A	MOR in edgewise direction. Loading heads situated on side A

CAPÍTULO 6

Discusión global de los resultados

6. Discusión global de los resultados

6.1. Análisis estadístico

La validación cruzada resultó una buena estrategia para evitar el sobreajuste en los modelos multivariable (Lever *et al.* 2016). Se pudo observar que, cuando no se tomó ninguna precaución frente al sobreajuste, al ir añadiendo variables a un modelo de predicción, el RMSE fue disminuyendo. En cambio, cuando se utilizó la validación cruzada, a partir de un determinado número de variables, al añadir una nueva, el RMSE aumentaba. La validación cruzada fue utilizada en algunos trabajos previos para estudiar las propiedades mecánicas de la madera (Faydi *et al.* 2017; Villasante *et al.* 2019).

No se encontraron diferencias significativas entre las predicciones del MOEs y el MOR realizadas con modelos multivariable complejos, como las redes neuronales o el método de los k vecinos más próximos, y las realizadas con regresiones lineales múltiples. Algunos autores observaron un comportamiento parecido al comparar las redes neuronales con las regresiones lineales (Tanaka *et al.* 1996; Villasante *et al.* 2019). En otros casos, sin embargo, sí se observaron mejoras. García Esteban *et al.* (2009) comprobaron que la predicción del MOEs realizada con modelos basados en redes neuronales mejoraba sensiblemente el valor de R^2 obtenido con una regresión lineal múltiple, aunque este último resultó anormalmente bajo. Fathi *et al.* (2020) y Mansfield *et al.* (2007) encontraron que la predicción del MOR mediante redes neuronales mejoraba la realizada con un regresión lineal múltiple, aunque en ambos casos trabajaron con piezas pequeñas libres de defectos, por lo que es difícil la comparación con el presente trabajo.

6.2. Propiedades mecánicas

El valor del MOE estático (MOEs) encontrado en las piezas estudiadas (7701 MPa) fue inferior a los observados en la mayoría de los estudios previos realizados con *Pinus sylvestris* L. (Arriaga *et al.* 2012; Hassan *et al.* 2013; Ranta-Maunus *et al.* 2011) que se encontraron entre 9000 MPa y 12000 MPa. Aunque entre los objetivos de la presente tesis no se encontraba el clasificar las muestras estudiadas, puede decirse que, si se atendiera únicamente al valor del MOEs, se encontrarían en la clase C16 de la European Standard EN 338 (2016), por lo que puede considerarse que los valores obtenidos no fueron anómalos. Estos valores bajos pueden ser debidos a que el estudio se realizó con madera sin clasificar.

En cuanto al MOR, el valor obtenido (40 MPa) fue similar al que se encontró en otros estudios realizados con *Pinus sylvestris* L. (Arriaga *et al.* 2012; Villasante *et al.* 2019) o con otras especies de pino (Arriaga *et al.* 2012; Íñiguez González *et al.* 2007; Yang *et al.* 2017) con valores entre 35 MPa y 45 MPa.

6.3. Predicción del MOEs

6.3.1. Ensayos de vibración

El MOE dinámico (MOE_{dyn}) calculado a partir de técnicas de vibración ofreció buenos resultados en la predicción del MOEs mediante regresión lineal simple. El MOE_{EV} , obtenido a partir de la frecuencia fundamental de resonancia en la vibración de canto, fue la variable con un valor más bajo del RMSE, presentando una diferencia estadísticamente significativa respecto a las otras variables. Este resultado pudo explicarse porque ambos ensayos, el de vibración de canto y el de flexión estática, se realizaron con la pieza en la misma posición. Después del MOE_{EV} , las variables con un menor valor del RMSE fueron los MOE_{dyn} obtenidos en la vibración de cara y longitudinal, MOE_{FV} y MOE_{LV} respectivamente, significativamente menores que los del resto de variables. Diferentes autores también observaron que el MOE_{dyn} obtenido en la vibración de canto predecía el MOEs mejor que los obtenidos en las otras direcciones (Arriaga *et al.* 2014; Cho 2007; Ilic 2001).

Los MOE_{dyn} obtenidos a partir de técnicas de vibración sobreestimaron el MOEs (entre un 13 % y un 15 %), algo que coincidió con los resultados de otros trabajos (Arriaga *et al.* 2014; Hassan *et al.* 2013; Larsson *et al.* 1998; Spycher *et al.* 2008). Esto podría explicarse porque el ensayo de vibración transversal tiene una duración mucho más corta que el ensayo estático de flexión, lo que provoca que la madera tenga una respuesta diferente en ambos debido a su comportamiento viscoelástico (Cho 2007; Halabe *et al.* 1997).

De acuerdo con Pantelić *et al.* (2020), el modelo de Bernoulli en el que se basa el cálculo del MOE_{dyn} tiene limitaciones para ser aplicado a la madera por tratarse de una material heterogéneo y anisótropo. Dicho modelo no tiene en cuenta el movimiento rotacional y la deformación por cortante (Cho 2007), algo que tiene especial incidencia en la madera, al tratarse de un material con una relación $MOEs/G$ particularmente alta en comparación con un material isotrópico (Brancherieu *et al.* 2002). Estas particularidades de la madera provocaron que las frecuencias de resonancia observadas en todos los armónicos fueran inferiores a las teóricas predichas por el modelo de Bernoulli en todas las piezas

analizadas. Además, la diferencia se fue haciendo mayor a medida que aumentaba el orden de vibración. Así, el valor del MOE_{dyn} fue disminuyendo aproximadamente un 6 % a medida que se iba aumentando un armónico. Kubojima *et al.* (2006) y Yoshihara (2012) observaron una tendencia parecida. Este fenómeno se pudo aprovechar para corregir la sobreestimación del MOEs, utilizando el segundo o el tercer armónico para calcular el MOE_{dyn} en lugar de la frecuencia fundamental. Otros autores propusieron una estrategia similar, como Chauhan and Walker (2006) y Grabianowski *et al.* (2006) que utilizaron el segundo armónico, o Qin *et al.* (2018) que utilizaron el segundo y el tercer armónico.

Este comportamiento de las frecuencias observadas, alejándose de las teóricas obtenidas con el modelo de Bernoulli, se debe al hecho de que las frecuencias van aumentando con el orden de vibración y, por lo tanto, las longitudes de onda van disminuyendo. Esto provoca que la relación entre el canto en flexión de la pieza (la dimensión de la sección transversal que se sitúa en posición vertical) y la longitud de onda sea cada vez mayor y, en consecuencia, la influencia de la deformación por cortante también aumente a medida que se incrementa el orden de vibración (Pantelić *et al.* 2020). El modelo de Bernoulli para calcular el MOE_{dyn} a partir de la frecuencia de vibración atribuye toda la deformación a la flexión, por lo que ofrece buenos resultados solo en el caso de que la deformación por cortante pueda ser despreciada.

Algunos autores (Arriaga *et al.* 2014) propusieron que el efecto del cortante podía obviarse en el cálculo del MOE_{dyn} cuando la relación entre el canto en flexión y la longitud es igual o superior 15. No obstante, en las piezas de tamaño estructural analizadas en esta tesis, con una relación igual a 20, se observó que eso era cierto solo para los primeros armónicos. En cambio, para las piezas pequeñas con una relación igual a 115 se pudo comprobar que no existían diferencias estadísticamente significativas entre el MOEs y el MOE_{dyn} calculado con cualquiera de los primeros 8 armónicos. A la luz de estos datos, por lo tanto, parece que la relación entre el canto de flexión y la longitud a partir de la cual se puede despreciar el efecto del cortante debe ser un valor comprendido entre 20 y 115.

Se comprobó que una regresión potencial a partir de las frecuencias observadas para cada pieza podía salvar el problema planteado por la influencia de la deformación por cortante. El MOE dinámico calculado a partir de dicha regresión (MOE_{pow}) resultó ser el que ofrecía la mejor predicción del MOEs, además de obtenerse mediante un método muy sencillo.

6.3.2. Ensayos de flexión estática

En la flexión estática se obtuvo el MOEs de canto (MOE_{edge}) y el de cara (MOE_{flat}). En el primer caso los cabezales de carga se situaron sobre la parte más estrecha de la sección transversal y en el segundo, sobre la más ancha. De este modo, la relación entre el canto en flexión y la longitud fue igual a 18 para el MOEs de canto y de 25,7 para el de cara. En ambos casos se despreció la influencia del cortante, considerando un valor de G igual a infinito. Los resultados mostraron que el MOE_{flat} era mayor que el MOE_{edge} , un resultado similar al obtenido por Kim *et al.* (2010), lo que podría explicarse, precisamente, porque se atribuyó toda la deformación a la flexión, al no haber tenido en cuenta la deformación provocada por el cortante (Boström 1999). La influencia del cortante aumenta a medida que disminuye la relación entre el canto en flexión y la longitud (Timoshenko 1938), por lo que es más importante en el ensayo de canto que en el de cara. Las diferencias entre el MOE_{flat} y el MOE_{edge} se anularon al considerar un valor de G igual al MOEs dividido por 18,2. Esta relación es similar al valor de 17 propuesto por Brancherieu *et al.* (2002). Estos resultados parecen indicar que la influencia del cortante es apreciable incluso cuando la longitud entre apoyos es igual a 25 veces el canto en flexión.

6.3.3. Influencia de las singularidades de la madera en el MOEs

Se encontró una relación débil entre las diferentes singularidades estudiadas y el MOEs. Esta tendencia coincide con lo observado por otros autores (Larsson *et al.* 1998; Mania *et al.* 2020; Ranta-Maunus *et al.* 2011). La inclusión de las singularidades en modelos multivariable tampoco mejoró la predicción del MOEs obtenida a partir del MOE_{EV} . Otros estudios previos también mostraron que las singularidades no mejoraban las predicciones realizadas con el MOE_{dyn} (Arriaga *et al.* 2014; Faydi *et al.* 2017; França *et al.* 2020; Wright *et al.* 2019). Este comportamiento puede explicarse por dos factores. En primer lugar la predicción del MOE_{EV} obtuvo un coeficiente de determinación muy alto ($R^2 = 0,97$) y un error muy bajo ($\text{RMSE} = 333 \text{ MPa}$). En segundo lugar, el MOEs depende del comportamiento global de la pieza y no de los efectos locales que pueden provocar las singularidades.

6.4. Predicción del MOR

6.4.1. Ensayos de vibración

Las predicciones del MOR a partir de los diferentes MOE_{dyn} presentaron unas correlaciones débiles, con valores de R^2 en torno a 0,40, y unos errores que pueden calificarse como elevados, con valores de RMSE en torno a 12 MPa. Este resultado coincide con lo observado por otros autores (Arriaga *et al.* 2014; França *et al.* 2019; Pommier *et al.* 2013). No se encontraron diferencias estadísticamente significativas entre las predicciones del MOR mediante los tres MOE_{dyn} (MOE_{EV} , MOE_{FV} , MOE_{LV}). Al contrario de lo que ocurre con el MOE, el MOR no depende tanto del comportamiento global de la pieza como de la influencia local de defectos o singularidades. Es por este motivo que el MOE_{dyn} presenta una correlación débil con el MOR.

6.4.2. Influencia de las singularidades de la madera en el MOR

De las diferentes singularidades estudiadas, las bolsas de resina, el azulado, la desviación de la fibra, las gemas y el coeficiente de crecimiento mostraron una relación débil con el MOR. Su inclusión en modelos multivariable no mejoró la predicción realizada a partir de los diferentes MOE_{dyn} . La nudosidad, en cambio, medida a través de diferentes procedimientos, resultó ser un buen predictor del MOR, con un valor de RMSE similar al encontrado con el MOE_{dyn} . Los resultados mostraron que la nudosidad predice mejor el MOR que el MOEs, algo que ha sido descrito en diferentes estudios (Conde García *et al.* 2007; França *et al.* 2019; Šilinskas *et al.* 2020; Wright *et al.* 2019).

La predicción del MOR a partir del MOEs mejoró con la inclusión de variables de nudosidad en modelos multivariable, al disminuir significativamente el valor del RMSE, una tendencia similar a la encontrada por otros autores (Arriaga *et al.* 2012; Conde García *et al.* 2007; Hautamäki *et al.* 2014; Villasante *et al.* 2019). Cuando se incluyeron las variables de nudosidad posicional basadas en el KAR (BS 4978 2017), se observó un valor del RMSE significativamente menor que cuando se incluyeron las variables de nudosidad global basadas en la EN 1309–3 (2018). La variable $MKAR_{1/8}$, que valora los nudos en los bordes de tracción y compresión de la sección transversal, fue la que obtuvo un mejor resultado al incluirla en un modelo multivariable junto al MOE. Esto significa que el MOR depende del efecto local de los nudos, más que de la cantidad total de los mismos. Así, los nudos situados en los bordes superior e inferior de la sección transversal, que se

corresponden con las zonas donde los esfuerzos de tracción y compresión son mayores, tienen una mayor influencia.

Además, al incluir la variable MKAR_{1/8} junto al MOEs en el modelo de predicción del MOR, se pudo observar que el RMSE era significativamente menor si se utilizaba el MOEs de canto que si se utilizaba el MOEs de cara. Por lo tanto, la posición de la pieza en el ensayo de flexión influye en el resultado del MOR. No se han encontrado trabajos previos que describieran esta diferencia, ni que utilizaran la variable MKAR_{1/8} para valorar los nudos.

6.5. Referencias

- Arriaga, F., Iniguez-Gonzalez, G., Esteban, M., Divos, F. (2012) Vibration method for grading of large cross-section coniferous timber species. Holzforschung 66(3):381–387.
- Arriaga, F., Monton, J., Segues, E., Iniguez-Gonzalez, G. (2014) Determination of the mechanical properties of radiata pine timber by means of longitudinal and transverse vibration methods. Holzforschung 68(3):299–305.
- Boström, L. (1999) Determination of the modulus of elasticity in bending of structural timber – Comparison of two methods. Holz Als Roh–Und Werkst. 57(2):145–149.
- Brancheriau, L., Bailleres, H., Guitard, D. (2002) Comparison between modulus of elasticity values calculated using 3 and 4 point bending tests on wooden samples. Wood Sci. Technol. 36(5):367–383.
- British Standard (2017) BS 4978:2017. Visual strength grading of softwood. Specification. British Standards Institution: Londres, Reino Unido.
- Chauhan, S.S., Walker, J.C.F. (2006) Variations in acoustic velocity and density with age, and their interrelationships in radiata pine. For. Ecol. Manage. 229(1–3):388–394.
- Cho, C.-L. (2007) Comparison of three methods for determining Young's modulus of wood. Taiwan J. For. Sci. 22(3):297–306.
- Conde García, M., Fernández-Golfín Seco, J.I., Hermoso Prieto, E. (2007) Mejora de la predicción de la resistencia y rigidez de la madera estructural con el método de ultrasonidos combinado con parámetros de clasificación visual. Mater. Constr. 57(288):49–59.
- European Standard (2016) EN 338:2016. Structural timber. Strength classes European Committee for Standardization (CEN).
- European Standard (2018) EN 1309-3:2018. Round and sawn timber - Methods of measurements - Part 3: Features and biological degradations European Committee for Standardization (CEN).

- Fathi, H., Nasir, V., Kazemirad, S. (2020) Prediction of the mechanical properties of wood using guided wave propagation and machine learning. *Constr. Build. Mater.* 262:article ID 120848.
- Faydi, Y., Brancherieu, L., Pot, G., Collet, R. (2017) Prediction of oak wood mechanical properties based on the statistical exploitation of vibrational response. *BioResources* 12(3):5913–5927.
- França, F.J.N., França, T.S.F.A., Seale, R.D., Shmulsky, R. (2020) Use of longitudinal vibration and visual characteristics to predict mechanical properties of No. 2 southern pine 2x8 and 2x10 lumber. *Wood Fiber Sci.* 52(3):280–291.
- França, F.J.N., Seale, R.D., Shmulsky, R., França, T.S.F.A. (2019) Modeling mechanical properties of 2 by 4 and 2 by 6 southern pine lumber using longitudinal vibration and visual characteristics. *For. Prod. J.* 68(3):286–294.
- García Esteban, L., García Fernández, F., de Palacios, P. (2009) MOE prediction in *Abies pinsapo* Boiss. timber: Application of an artificial neural network using non-destructive testing. *Comput. Struct.* 87(21–22):1360–1365.
- Grabianowski, M., Manley, B., Walker, J.C.F. (2006) Acoustic measurements on standing trees, logs and green lumber. *Wood Sci. Technol.* 40(3):205–216.
- Halabe, U.B., Bidigal, G.M., GangaRao, H.V.S., Ross, R.J. (1997) Nondestructive evaluation of green wood using stress wave and transverse vibration techniques. *Mater. Eval.* 55(9):1013–1018.
- Hassan, K.T.S., Horacek, P., Tippner, J. (2013) Evaluation of stiffness and strength of Scots pine wood using resonance frequency and ultrasonic techniques. *BioResources* 8(2):1634–1645.
- Hautamäki, S., Kilpeläinen, H., Verkasalo, E. (2014) Factors and models for the bending properties of sawn timber from Finland and north-western Russia. Part II: Scots pine. *Balt. For.* 20(1):142–156.
- Ilic, J. (2001) Relationship among the dynamic and static elastic properties of air-dry *Eucalyptus delegatensis* R. Baker. *Holz Als Roh- Und Werkst.* 59(3):169–175.
- Íñiguez González, G., Arriaga Martítegui, F., Esteban Herrero, M., Argüelles Alvarez, R. (2007) Los métodos de vibración como herramienta no destructiva para la estimación de las propiedades resistentes de la madera aserrada estructural. *Inf. Constr.* 59(506):97–105.
- Kim, K.-M., Shim, K.-B., Lum, C. (2010) Predicting tensile and compressive moduli of structural lumber. *Wood Fiber* 43(1):83–89.
- Kubojima, Y., Tonosaki, M., Yoshihara, H. (2006) Young's modulus obtained by flexural vibration test of a wooden beam with inhomogeneity of density. *J. Wood Sci.* 52(1):20–24.
- Larsson, D., Ohlsson, S., Perstorper, M., Brundin, J. (1998) Mechanical properties of sawn timber from Norway spruce. *Holz Als Roh–Und Werkst.* 56(5):331–338.

7. Discusión global

- Lever, J., Krzywinski, M., Altman, N. (2016) Model selection and overfitting. *Nat. Methods* 13(9):703–704.
- Mania, P., Siuda, F., Roszyk, E. (2020) Effect of slope grain on mechanical properties of different wood species. *Materials* 13:1503.
- Mansfield, S.D., Iliadis, L., Avramidis, S. (2007) Neural network prediction of bending strength and stiffness in western hemlock (*Tsuga heterophylla* Raf.). *Holzforschung* 61(6):707–716.
- Pantelić, F., Mijić, M., Šumarac Pavlović, D., Ridley-Ellis, D., Dudeš, D. (2020) Analysis of a wooden specimen's mechanical properties through acoustic measurements in the very near field. *J. Acoust. Soc. Am.* 147(4):EL320–EL325.
- Pommier, R., Breysse, D., Dumail, J.F. (2013) Non-destructive grading of green Maritime pine using the vibration method. *Eur. J. Wood Wood Prod.* 71(5):663–673.
- Qin, J., Liu, X., Van Den Abeele, K., Cui, G. (2018) The study of wood knots using acoustic nondestructive testing methods. *Ultrasonics* 88:43–50.
- Ranta-Maunus, A., Denzler, J.K., Stapel, P. (2011) Strength of European timber. Part 2. Properties of spruce and pine tested in Gradewood project. VTT Technical Research Centre of Finland. VTT Working Papers, No. 179. <http://www.vtt.fi/inf/pdf/workingpapers/2011/W179.pdf>.
- Šilinskas, B., Varnagiryte-Kabašinskiene, I., Aleinikovas, M., Beniušiene, L., Aleinikoviene, J., Škema, M. (2020) Scots pine and norway spruce wood properties at sites with different stand densities. *Forests* 11(5):1–15.
- Spycher, M., Schwarze, F.W.M.R., Steiger, R. (2008) Assessment of resonance wood quality by comparing its physical and histological properties. *Wood Sci. Technol.* 42(4):325–342.
- Tanaka, T., Tanaka, T., Nagao, H., Kato, H. (1996) A preliminary investigation on evaluation of strength of soft wood timbers by neural network. Proceeding of the 10th International Symposium on Nondestructive Testing of Wood, Lausana, Suiza.
- Timoshenko, S. (1938) Strength of materials D. Van Mostrand Company, Inc.: Nueva York, EE. UU.
- Villasante, A., Iniguez-Gonzalez, G., Puigdomenech, L. (2019) Comparison of various multivariate models to estimate structural properties by means of non-destructive techniques (NDTs) in *Pinus sylvestris* L. timber. *Holzforschung* 73(4):331–338.
- Wright, S., Dahlen, J., Montes, C., Eberhardt, T.L. (2019) Quantifying knots by image analysis and modeling their effects on the mechanical properties of loblolly pine lumber. *Eur. J. Wood Wood Prod.* 77(5):903–917.
- Yang, B.Z., Seale, R.D., Shmulsky, R., Dahlen, J., Wang, X. (2017) Comparison of nondestructive testing methods for evaluating no. 2 southern pine lumber: Part B, modulus of rupture. *Wood Fiber Sci.* 49(2):134–145.

Yoshihara, H. (2012) Examination of the specimen configuration and analysis method in the flexural and longitudinal vibration tests of solid wood and wood-based materials. *For. Prod. J.* 62(3):191–200.

CAPÍTULO 7

Conclusiones

7. Conclusiones

7.1. Procedimiento de ensayo y análisis estadístico

En los ensayos de vibración transversal es habitual que el golpe de excitación se realice en el punto medio de la longitud de la pieza. Este punto de golpeo es adecuado para encontrar la frecuencia fundamental de resonancia. No obstante, se pudo constatar que si el golpe se producía cerca de una de las testas, resultó mucho más fácil identificar las frecuencias correspondientes a los armónicos.

La comparación de la capacidad predictiva de los diferentes modelos mediante el test de Kruskal–Wallis permitió descartar algunos que aportaban una mejora aparente en el RMSE, pero sin que hubiera diferencias estadísticamente significativas.

La validación cruzada mediante carpetas se mostró como un procedimiento eficaz para reducir el efecto del sobreajuste en los modelos multivariable. Añadir muchas variables a un modelo, como se hizo en la predicción del MOR y del MOE, puede causar la falsa impresión de que mejora la predicción si no se toman precauciones respecto al sobreajuste. A medida que aumenta el número de variables, puede parecer que se está mejorando la predicción, porque disminuye el error. Sin embargo, aplicando la validación cruzada se pudo comprobar que, a partir de un determinado número de variables, añadir otras nuevas al modelo aumentaba el error.

Los modelos multivariable confeccionados con algoritmos no lineales (KNN y ANN) no mejoraron la predicción realizada con modelos lineales multivariable.

7.2. Ensayos de vibración para predecir el MOR y el MOE

Los ensayos no destructivos basados en técnicas de vibración resultaron más adecuados para predecir el MOE que el MOR.

Utilizar modelos que combinan frecuencias de resonancia obtenidas en ensayos de vibración realizados en diferentes direcciones (transversal de canto, transversal de cara y longitudinal) no aportó mejoras en la predicción de las propiedades mecánicas de la madera.

Los ensayos de ultrasonidos obtuvieron mayores errores que los de vibración, tanto en la predicción del MOE como en la del MOR.

7.3. Modelos univariable y multivariable para predecir el MOR y el MOE

De las variables obtenidas con técnicas de vibración, el MOE_{dyn} obtenido a partir de la frecuencia de resonancia correspondiente a la vibración transversal de canto (MOE_{EV}) fue el que obtuvo el menor RMSE en la predicción del MOE. Este resultado pudo explicarse porque ambos ensayos (estático y dinámico) se realizaron en la misma dirección.

Los modelos multivariable no pudieron mejorar la predicción del MOE realizada con una única variable que, por otra parte, ya ofrecía un valor de RMSE muy bajo. La predicción del MOR, en cambio, sí se pudo mejorar con un modelo lineal multivariable. A pesar de esta mejora, el valor del RMSE en la predicción del MOR resultó elevado.

7.4. La influencia de las singularidades en la predicción del MOR y el MOE

Combinar las frecuencias de resonancia con las singularidades de la madera resultó una buena estrategia para reducir el error de predicción del MOR. Las variables de desviación de la fibra y de nudosidad resultaron las que más contribuyeron a reducir el valor del RMSE en las predicciones multivariable.

Dentro de las variables que describen la nudosidad, la variable $\text{MKAR}_{1/8}$ definida en este estudio, fue la que proporcionó una mejor predicción del MOR, por encima de KAR y $\text{MKAR}_{1/4}$ que son de uso frecuente en los trabajos previos. En el caso del MOE, en cambio, se obtuvieron mejores predicciones con las medidas de nudos basadas en la norma europea que con las medidas basadas en el KAR.

Al predecir el MOR a partir del MOE obtenido en el ensayo de flexión cargando en cualquiera de las dos caras o los dos cantos no se encontraron diferencias significativas. Sin embargo, al añadir una variable de nudosidad posicional al modelo sí que aparecieron diferencias significativas entre la predicción obtenida de cara y la obtenida de canto.

7.5. Efecto del cortante en el MOE

La frecuencia fundamental de resonancia en la vibración transversal sobreestimó el MOE debido al comportamiento viscoelástico de la madera. Sin embargo, a medida que aumenta el modo de vibración la influencia del cortante es mayor, por lo que la frecuencia observada fue alejándose progresivamente por debajo de la teórica esperada, provocando la subestimación del MOE. En el tercer armónico ambos efectos se compensaron, por lo que resultó una frecuencia más adecuada que la fundamental para predecir el MOE. El tercer armónico se pudo identificar con facilidad en el espectro, por lo que su utilización es

sencilla. La subestimación del MOE debida al cortante fue especialmente importante a partir del quinto armónico.

En la predicción del MOE a partir de las frecuencias de resonancia, la regresión potencial de las frecuencias de varios armónicos resultó el método con un menor error de predicción. Además resultó un método más sencillo que los propuestos en los trabajos previos consultados.

También se pudo observar que el ensayo de flexión estática subestima el valor del MOE al no tener en cuenta la deformación causada por el cortante. Ese efecto fue mayor cuando el ensayo se realizó cargando sobre el canto que cuando se cargó sobre la cara. Se observó que tomando un valor de G igual a una dieciochoava parte del MOE se anulaba la diferencia entre ambos valores del MOE, el de cara y el de canto.

La comparación de los valores de MOE obtenidos en el ensayo de flexión estática de cara y de canto podría ser un procedimiento prometedor para estimar de forma simultánea el valor de G y del MOE.